OFFICE OF NAVAL RESEARCH

Contract N7onr-35810

NR-360-003

Technical Report No. 22

FINAL REPORT ON

YIELD LOADS OF SLABS WITH REINFORCED CUTOUTS

by

P. R. Hodge, Jr.

GRADUATE DIVISION OF APPLIED MATHEMATICS

BROWN UNIVERSITY

PROVIDENCE, R. I.

B11-22/137

September, 1953

FINAL REPORT ON YIELD LOADS OF SLABS WITH REINFORCED CUTOUTS[0.1]

by P. G. Hodge, Jr.[0.2]

0.1 The results presented in this paper were obtained in the course of research conducted as a Consultant to Contract N7onr-35810 between the Office of Naval Research and Brown University.

0.2 Assistant Professor of Mathematics, University of California, Los Angeles.

PREFACE

During the past two years the author has been associated with Contract N7onr-35810 between the Office of Naval Research and Brown University, first as Visiting Professor of Applied Mathematics at Brown University, and later as consultant. During that time, problems of uniform slabs with cutouts and reinforced cutouts have been studied. The following report is a survey of those results which have been obtained by the theory of limit analysis. Some additional results involving complete solutions [4, 8][0.3] are not included. However, all other results obtained are either included in detail here, or specific reference is made to a previous report. With these exceptions, then, the present survey supersedes the "B.11" reports [1-9] listed in the references.

This survey report is being issued at this time primarily because the contract supporting it is about to expire, rather than because the subject may be regarded as fully understood. For this reason, many of the results presented are admittedly incomplete. However, it has seemed worthwhile to indicate possible lines for future attack, rather than to limit the report to entirely solved problems.

The author would like to take this opportunity to express his appreciation to E. Levin and R. K. Froyd, graduate students at the University of California, Los Angeles, for

---

0.3 Numbers in parentheses refer to the references collected at the end of the report.

their assistance throughout the past year and a half. In addition to results for which they are directly responsible [5, 6, 9], they have helped considerably with many of the concepts and calculations throughout the report. The author also wishes to thank the staff at the Graduate Division of Applied Mathematics, in particular Professors W. Prager, H. J. Weiss, and P. S. Symonds for their many useful suggestions and helpful criticisms throughout the past two years.

Philip G. Hodge, Jr.
Los Angeles
May, 1953

Table of Contents

INTRODUCTION

The problems to be discussed in this report are best exemplified by an example. Let us consider first a thin plane slab of thickness h, made of a homogeneous material, and loaded in its plane by uniform tensions of magnitude $2k\lambda hT_x$, $2k\lambda hT_y$ per unit length applied along the boundary of the slab (Fig. 0.1a). As λ is slowly increased from zero, there will be some critical value λ_1^{**} for which the slab will be no longer serviceable.

We shall return to a more precise formulation of λ_1^{**} shortly. First, however, let us consider a second slab identical with the first except that it contains a centered cutout (Fig. 0.1b). If this slab is also loaded with tensions $2k\lambda hT_x$, $2k\lambda hT_y$ and λ is slowly increased from zero, the critical load λ_2^{**} will, in general, be less than λ_1^{**} , since material which formerly carried part of the load has been cut out. Finally, if thin reinforcing rings are welded to either side of the slab (Fig. 0.1c) the critical load λ_3^{**} will be increased over the unreinforced slab.

The design problem implicit in the preceding paragraph is two-fold. First, to design the reinforcing rings so that the slab with the reinforced cutout has the same critical load as the original whole slab (obviously one cannot, in general, reinforce the slab to more than original full strength). Second, if design to full strength is impracticable, to determine the actual strength of the final reinforced cutout slab.

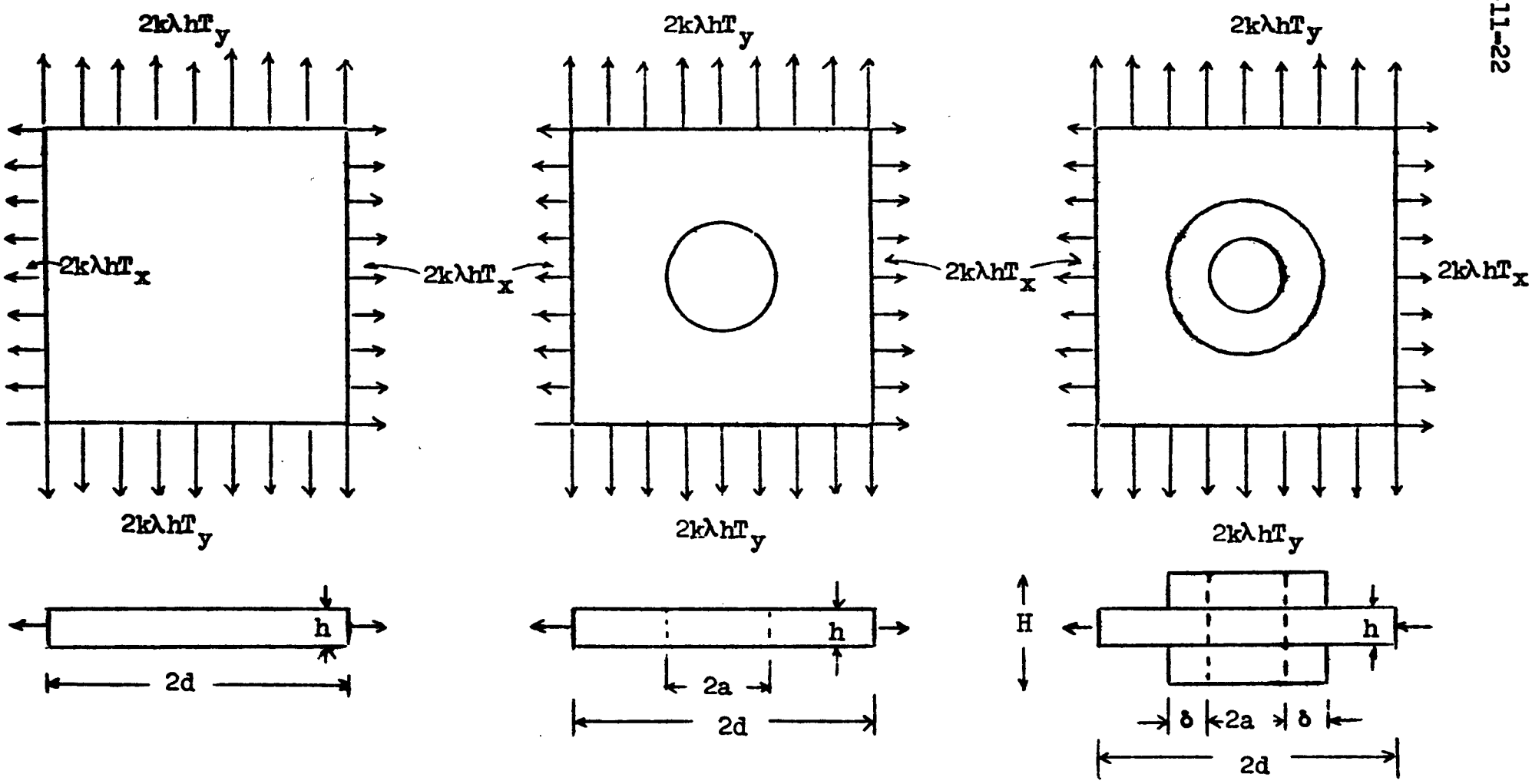

(a)
Without cutout

(b)
With unreinforced cutout

(c)
With reinforced cutout

Fig. 0.1
Plane slabs under uniform loading.

In order to approach these problems, it is first necessary to obtain a more precise idea of the critical load λ^{**}. To this end, let us consider more closely the behavior of the unreinforced slab in Fig. 0.1b. As λ is increased from zero, the material will first be everywhere elastic. The relation between the applied load and any particular displacement will be linear, and if the load is removed the slab will return to its original undeformed state. This will continue until λ reaches a value λ^* , at which point the slab will become plastic at the most highly stressed portions A (Fig. 0.2a). Further

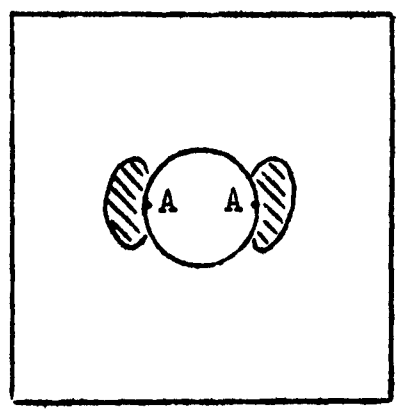

(Contained plastic deformation)

Fig. 0.2a

Partially plastic slabs.

increases of the load will no longer be related linearly to displacements, and an unloading would produce residual stresses and strains.

For certain applications, it may be that this nonlinear behavior with residual stresses and strains, would render the slab no longer useful. However, the deformations at this point are still small, and there is no tendency for them to increase rapidly. Therefore, it may be that further increases in

load are acceptable. In this case, regions of plastic material will begin to form about the points A (shaded regions in Fig. 0.2a, 0.2b), and possibly to start at other points. However,

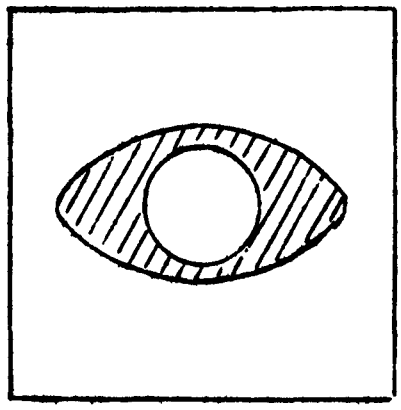

(Contained plastic deformation)

Fig. 0.2b
Partially plastic slabs.

there will still be a constraining framework of elastic material, so that the slab can stand further increases in load. As λ is further increased, these plastic regions will grow, until for some critical value λ^{**} , the elastic framework is no longer able to constrain the plastic flow (Fig. 0.2c); even if

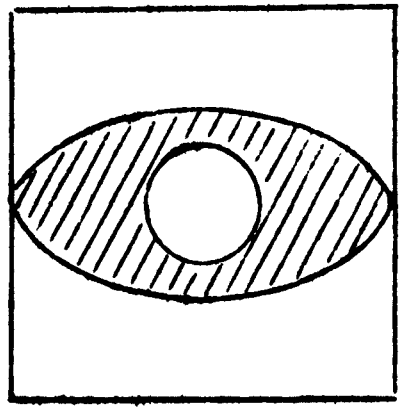

(Unrestricted plastic flow)

Fig. 0.2c
Partially plastic slabs.

the material in the elastic regions were replaced by rigid material the overall deformations of the slab could still increase to large values. If the material is perfectly plastic, the plastic regions can support no further load, so that the slab as a whole may deform indefinitely. For a strain-hardening material somewhat greater loads can be supported, but a relatively large increase in deformation will accompany a comparatively small increase in load. Typical load displacement curves for both types of material are shown in Fig. 0.3.

Throughout this report, we shall assume that the material is perfectly plastic and incompressible.[0.4] For such a material we can specify the requirements of a "complete" solution of the problem corresponding to any value of the slowly increasing load. Assuming the slab to be in a state of plane stress, such a solution will consist of determining three stress components σ_x, σ_y, τ_{xy} and three velocity components v_x, v_y, v_z all as functions of x and y. The stress components must everywhere satisfy the yield inequality

$$F(\sigma_x, \sigma_y, \tau_{xy}) \leq 0 \qquad (0.1)$$

where F is a given function for the material, and the equilibrium equations

$$\frac{\partial \sigma_x}{\partial x} + \frac{\partial \tau_{xy}}{\partial y} = 0 \ , \ \frac{\partial \tau_{xy}}{\partial x} + \frac{\partial \sigma_y}{\partial y} = 0. \qquad (0.2)$$

0.4 This last restriction is not vital to the general conclusions, but considerably simplifies the mathematical presentation.

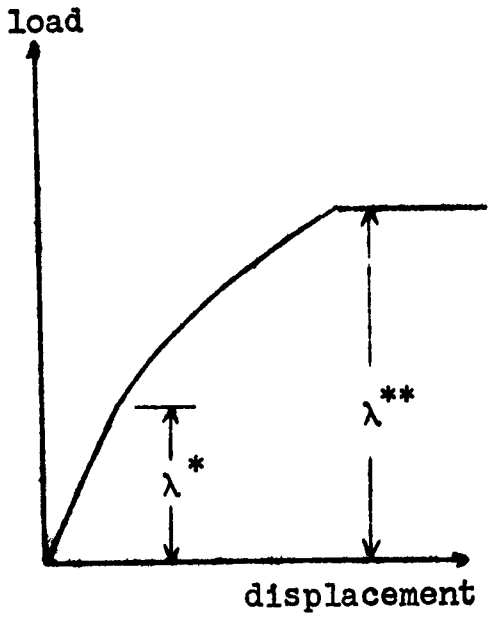

(Perfectly plastic material)

(a)

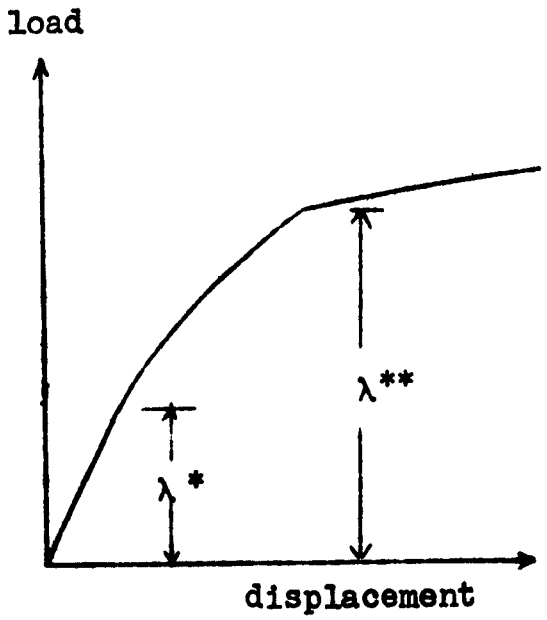

(Strain-hardening material)

(b)

Fig. 0.3

Load displacement curves.

The velocity components must satisfy the condition of incompressibility

$$\frac{\partial v_x}{\partial x} + \frac{\partial v_y}{\partial y} + \frac{\partial v_z}{\partial z} = 0. \tag{0.3}$$

Where the strict inequality holds in 0.1, the material is said to be elastic and must satisfy Hooke's law:

$$E\,\frac{\partial v_x}{\partial x} = \dot{\sigma}_x - 1/2\,\dot{\sigma}_y\,,\quad E\,\frac{\partial v_y}{\partial y} = \dot{\sigma}_y - 1/2\,\dot{\sigma}_x\,,$$
$$G\left(\frac{\partial v_x}{\partial y} + \frac{\partial v_y}{\partial x}\right) = \dot{\tau}_{xy}\,. \tag{0.4}$$

Together with Eqs. 0.2 and 0.3 this provides the necessary six equations. Where the equality holds in 0.1 the material is said to be plastic, and must satisfy the plastic potential stress strain law

$$\frac{\partial F/\partial \sigma_x}{E(\partial v_x/\partial x) - (\dot{\sigma}_x - \frac{1}{2}\dot{\sigma}_y)} = \frac{\partial F/\partial \sigma_y}{E(\partial v_y/\partial y) - (\dot{\sigma}_y - \frac{1}{2}\dot{\sigma}_x)}$$
$$= \frac{\partial F/\partial \tau_{xy}}{G(\partial v_x/\partial y + \partial v_y/\partial x) - \dot{\tau}_{xy}}\,. \tag{0.5}$$

Equations 0.1, 0.2, 0.3 and 0.5 provide the necessary six equations in the plastic case. In addition, the stress components must be in equilibrium with the applied loads, and certain continuity conditions must be satisfied in the interior of the slab. These latter conditions determine the position of the boundary between the elastic and plastic regions.

A cursory examination of Eqs. 0.1 through 0.5 indicates that the problem of finding a complete solution is

extremely difficult, since not only must we solve six equations in as many unknowns, but some of the equations are non-linear, and a free boundary must be determined. The only known solutions are in cases where symmetry or other restrictions reduce the number of independent and dependent variables. An example of such a solution is given in (4). In general, however, Eqs. 0.1 through 0.5 have defied solution, to date.

Although the determination of a complete solution appears impossible, we can use recent theorems by Drucker, Greenberg, and Prager [10, 11] to determine something about the critical load λ^{**} . A precise formulation of these theorems will be given in the first chapter. However, the basic ideas behind them may be stated as follows. In addition to considering λ^{**} as the <u>maximum</u> load which the slab can withstand without yielding indefinitely, we may also consider it as the <u>minimum</u> load for which increased deformation becomes possible with no increase in load. Using this viewpoint, it can then be shown that by considering essentially only those equations which contain stresses alone we can obtain a lower bound on the collapse load, while considering only the equations which contain velocities we can obtain an upper bound. If the two bounds are equal, we have the actual value of the collapse load, but even if this is not the case we may be able to obtain bounds sufficiently accurate for engineering purposes.

The body of this report will be concerned with the application of the theorems of Drucker, Greenberg, and Prager to the problem of analysis and design of slabs with both

unreinforced and reinforced cutouts. In Chapter I, we shall state the theorems precisely and indicate the precautions which must be used in applying the results to actual situations. Also we shall show that for a symmetric cutout it is necessary to examine only uniaxial and uniform biaxial loadings to deduce certain results concerning any type of uniform loading. Finally, we shall discuss certain relationships between the reinforced and unreinforced cutouts.

In Chapter II we shall be concerned with problems of narrow reinforcing rings which may be reasonably approximated by curved beams. Various shaped cutouts and types of reinforcements will be considered. Chapters III and IV are concerned with different methods of finding upper and lower bounds, respectively, for slabs with unreinforced cutouts, while Chapter V gives examples of these techniques as applied to various shaped slabs and cutouts. Finally in Chapter VI we consider slabs with reinforced cutouts and compare some of the results with experimental data.

I. BASIC CONCEPTS

1. Mathematical Model. In connection with some of the results which will be presented in later chapters, the question may well be raised as to whether the assumptions made are "realistic." The subject of what constitutes a realistic assumption is a most important one, yet one which is often neglected in the arguments generated pro and con when a new theory is presented.

The first point which must be emphasized is that no mathematical theory can be entirely realistic. Consider for example the uncut slab in Fig. 0.1a, and compare an actual slab being stressed in a testing machine (in uniform tension, say). This actual slab is not a perfect rectangle, since there will inevitably be minor cuts and irregularities along the edges; by the same token the faces are not perfect planes. The applied load can be only approximately uniform. Any mathematical analysis must moreover assume knowledge concerning the physical properties of importance, in particular in this case concerning the yield stress function and the post-yield behavior of the metal. It is well known, however, both that these properties are highly complex and that they may vary appreciably for specimens cut from different points of a structure, because of unavoidable differences in treatment during the manufacturing process.

Since it is practically impossible and in fact undesirable because of the tremendously complicated nature of the analysis, we do not even attempt to give a completely realistic mathematical account. Instead, we begin our

mathematical analysis by postulating a mathematical model. For the example considered in Fig. 0.1a, the mathematical model consists of a perfectly rectangular slab with perfectly plane faces acted upon only by perfectly uniform forces applied precisely at the edges. In general, a mathematical model singles out those features of the physical problem which are considered important by the investigator, replaces them by corresponding mathematical idealizations, and ignores all features considered unessential. Once the mathematical model has been chosen, one operates on it according to the laws of mathematics, in order to predict the results of certain experiments. These experiments are also carried out for the original physical problem, and the two results are compared. If this comparison is satisfactory for the purpose for which the results are intended, and of course for a sufficient variety of tests, the mathematical model is deemed satisfactory.

Suppose, however, that the comparison of results is unsatisfactory. Even in this case, the model may be used to advantage in any of several methods. It may be that although the results are not satisfactory in all generality, they are useful in a more limited context. Thus, a mathematical model of a metal which specifies a linear relation between stress and strain is inadequate for very large stresses, but highly satisfactory for sufficiently small ones.

Alternatively, the experience gained in formulating and comparing the model may suggest ways of specifying a better model and may suggest the mathematical techniques

necessary to work with the more complex model. And finally, the crude model may, when supplemented by suitably chosen experimental results, enable one to make better predications than the experiments alone could lead to.

With the preceding discussion [1.1] as background, we shall formulate appropriate mathematical models for slabs with cutouts in the following chapters. However, there are certain general features which are common to all cases. First, that part of the slab which is not covered by the reinforcement (and which we shall refer to as the base slab) is assumed to be in a state of plane stress. The reinforcement together with that part of the slab covered by the reinforcement will be called the hub. The state of stress within the hub will be differently specified for different applications, but in all cases the tractions transmitted to the hub from the base slab will be assumed to be uniformly distributed over the total thickness of the hub. Observe that this assumption may depart rather far from reality if the reinforcements are thick compared to the slab.

Finally, it will be assumed that the material of base slab and hub is perfectly plastic, incompressible, and satisfies Tresca's yield condition [13] of maximum shearing stress:

$$F(\sigma_x, \sigma_y, \tau_{xy}) = \max [|\sigma_1|, |\sigma_2|, |\sigma_1 - \sigma_2|] - 2k \leq 0 \quad (1.1)$$

1.1 For a more complete treatment of the subject of mathematical models, see, for instance, Ref. 12, Sec. 1.1.

where σ_1 and σ_2 are the principle stresses in the slab. A perfectly plastic material is one which behaves elastically for stresses less than the yield stress, flows indefinitely under constant yield stress, and cannot support stresses greater than the yield stress. The stress-strain curve for such a material is given in Fig. 1.1a while Fig. 1.1b shows a graphical representation of Tresca's yield condition. In Fig. 1.1b, states of elastic stress are represented by points within the hexagon ABCDEF, and the material cannot support stresses represented by points outside of the hexagon. Points on the hexagon represent plastic states of stress: A is uniaxial tension, B is equal biaxial tension, G is pure shear, etc.

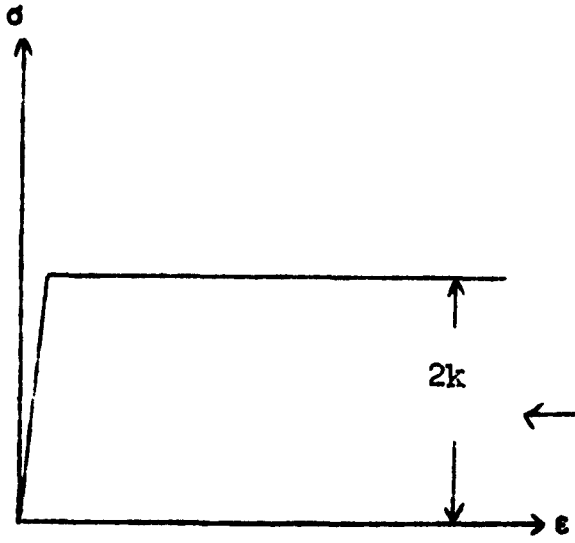

Fig. 1.1a
Stress-strain diagram

Fig. 1.1b
Yield condition

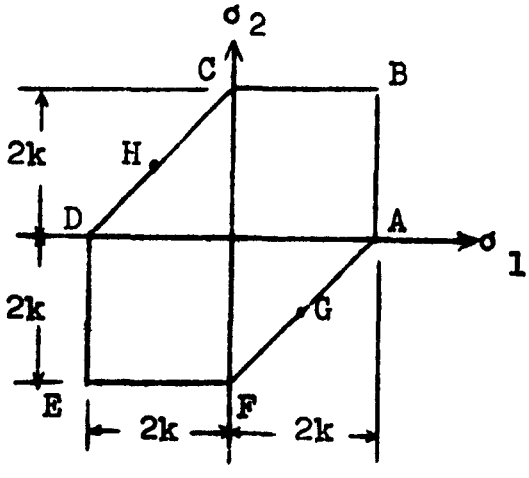

Fig. 1.1
Perfectly plastic material

2. The Drucker-Greenberg-Prager Theorems. As previously stated, the basic concept behind the theorems of Drucker, Greenberg, and Prager is to determine the smallest load for which an increase in deformation can occur with no increase in applied load. This load will be referred to as the yield load and the structure will be considered safe if the acting load is less than the yield load. Subject only to the additional qualification that loads up to this value can be considered to be applied to the undeformed boundary, certain significant results have been obtained. It is beyond the scope of the present report to reproduce the proofs of these theorems;[2.1] we shall merely state the results insofar as they apply to the problems under consideration.

First, then, let us consider a stress field (i.e., a set of three functions σ_x, σ_y, τ_{xy}) which satisfy the equations of equilibrium (Eqs. 0.1) and the Tresca yield restriction (1.1). If any such stress field is called statically admissible, then the first theorem may be stated as follows:

> Theorem 1. The yield load is the largest load for which there exists a statically admissible stress field.

It follows from Thm. 1 that any load for which a statically admissible stress field can be found must represent a lower bound for the yield load. Further, it should be noted that no explicit requirements of continuity were made. Of

---

2.1 Both theorems were originally proved for a Prandtl-Reuss material in plane strain [10]. Complete proofs for these cases are also given in [14], Secs. 33 and 39. They have

course, equilibrium implies that the tractions across any element must be continuous, but it will frequently be useful to consider stress fields across which the remaining stress component (the interior component of stress [14, p. 155]) exhibits a finite jump.

The second limit analysis theorem is concerned with velocity fields which satisfy the equation of incompressibility (Eq. 0.3). Let such a velocity field be considered as producing purely plastic strain rates, and define a stress field by the stress-strain law (Eqs. 0.5 with the stress rates equal to zero). The resulting internal rate of dissipation of energy has been shown [1] to be given at each point by

$$D = 2k \max | \dot{\varepsilon} | \tag{2.1}$$

where $\max | \dot{\varepsilon} |$ denotes the absolutely largest principal component of plastic strain rate. The total internal energy is defined by

$$\mathcal{D}_i = \int_V D \, dv = 2k \int_V \max | \dot{\varepsilon} | \, dv. \tag{2.2}$$

Also, if $\vec{v}$ represents the vector velocities of points on the boundary, and $\vec{F}$ the applied force on the boundary, the external rate of dissipation of energy is given by

$$\mathcal{D}_e = \int_S \vec{F} \cdot \vec{v} \, ds. \tag{2.3}$$

2.1(Cont'd). also been proved for the general perfectly plastic solid [11]. A detailed account for the case of a material satisfying Tresca's yield condition may be found in [1]. Also, see [1] for a more thorough discussion as applied to states of plane stress.

With these preliminaries, an incompressible velocity field will be called kinematically admissible if the internal rate of dissipation of energy does not exceed the external rate:

$$\mathcal{D}_i \leq \mathcal{D}_e. \tag{2.4}$$

The second theorem then reads as follows.

Theorem 2. The yield load is the smallest load for which it is possible to find a kinematically admissible velocity field.

It follows from Thm. 2 that any load for which it is possible to find a kinematically admissible velocity field is an upper bound on the yield load. Further, it follows from Thms. 1 and 2 together that the yield load is the unique load for which it is possible to find both a statically admissible stress field and a kinematically admissible velocity field. It will be observed that in this case also no explicit requirements of continuity were stated. It follows from the incompressibility of the material that the normal component of velocity must be continuous across any surface, but the tangential component may exhibit a finite jump. The appropriate internal energy dissipation may be evaluated by a limiting process. This procedure will be illustrated in Chapter III.

3. Arbitrary uniform edge loads. For the main part of this report we shall be considering loadings of the type given in Figs. 0.1, i.e., a uniform tensile load of magnitude $2k\lambda hT_x$ per unit length on the sides normal to the x axis, and a uniform tensile load of magnitude $2k\lambda hT_y$ on the remaining sides.

If we consider first Fig. 0.1a, and take $\lambda = 1$, it is evident that for the uncut slab the resulting stress field will be constant:

$$\sigma_x = 2k\, T_x, \quad \sigma_y = 2k\, T_y, \quad \tau_{xy} = 0. \tag{3.1}$$

Since the principle directions are those of the coordinate axes, it follows from 1.1 that the stress field 3.1 will be statically admissible only if

$$\max [\, | T_x |, | T_y |, | T_x - T_y | \,] \leq 1 \tag{3.2}$$

Therefore, if we consider a load space with coordinates T_x, T_y, the load point must lie in the hexagon ABCDEF (Fig. 3.1). This hexagon will be called the domain of safe loads.

Let us next consider the same slab with a cutout (Fig. 0.1b). Obviously the domain of safe loads in this case will be some region R wholly contained in the hexagon ABCDEF. For reasons which will be elaborated on in the next section, we are not as interested in the actual region R as we are in the largest hexagon A'B'C'D'E'F' similar and similarly placed to ABCDEF which is contained in R. In other words, we seek the largest number λ such that if T_x, T_y is a safe load for the uncut slab, then the loads λT_x, λT_y are safe for the slab with cutout. Such a value λ will be termed the cutout factor.

With this definition of a cutout factor, we can show that for a slab which is symmetric with respect to the x and y axes, only a few different types of loading need be considered in order to establish a lower bound on λ. To this end, suppose that a statically admissible stress field S_1 can be

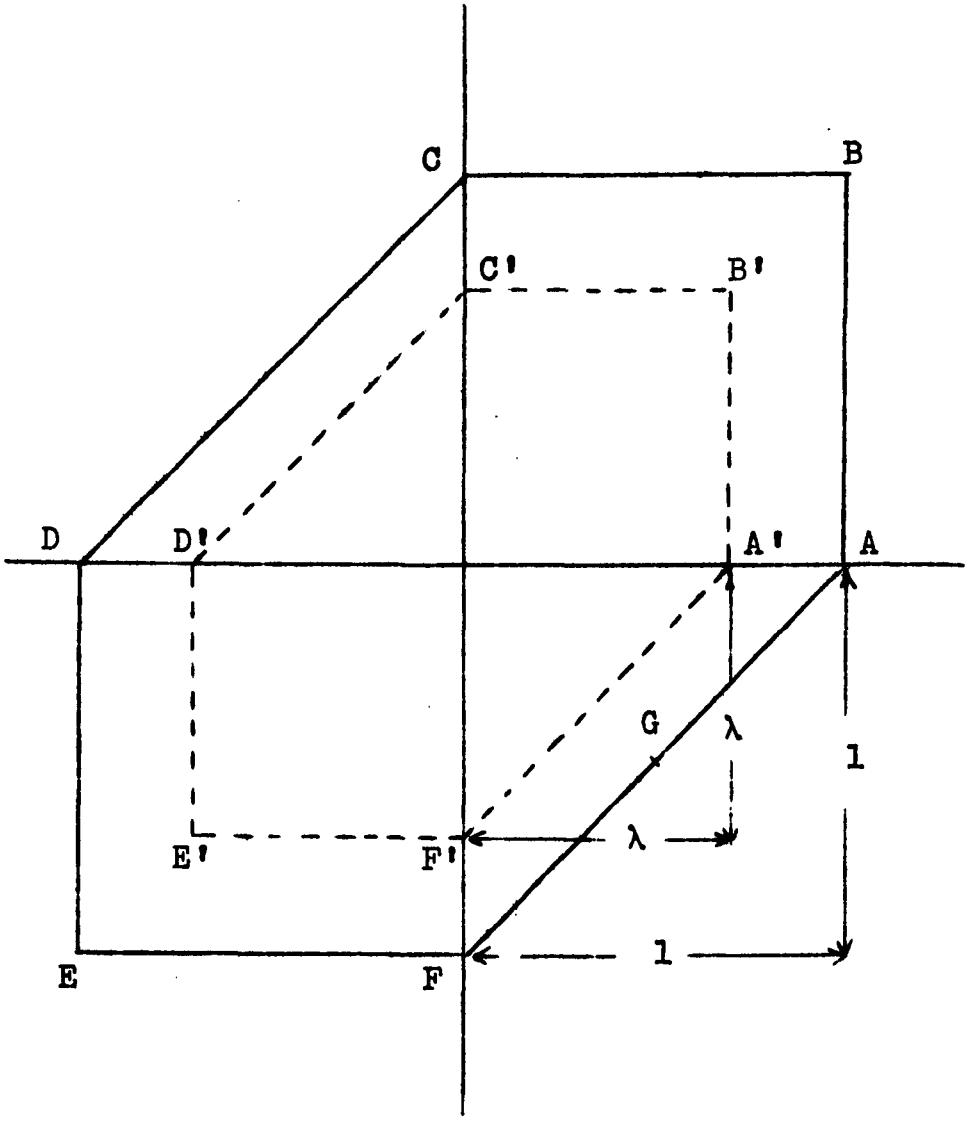

Fig. 3.1

Domain of safe loads.

——— slab without cutout
- - - - - - slab with cutout

constructed for the uniaxial tension load (λ_o, 0), that a statically admissible field S_2 can be constructed for the uniaxial tension load (0, λ_o), and that a statically admissible stress field S_3 can be found for equal biaxial tensions (λ_o, λ_o). It can then be shown that a statically admissible stress field can be constructed for any load point lying in the hexagon determined by λ_o. If, in addition, the slab is symmetric with respect to the line y = x, then the existence of S_2 can be deduced from S_1. The proof of this result follows from the convexity of the load domain and the yield surface. Details may be found in [2] , [7], or [10].

For a reinforced slab, the same results are generally valid. In particular, if the slab is to be reinforced to full strength, the dimensions of the reinforcement must be such that $\lambda = 1$.

4. Relations between reinforced and unreinforced cutouts. For certain types of application, it is desirable to design a reinforcement for a cutout which will restore the slab to full strength, independently of the base slab dimensions. The only method of guaranteeing this, is to choose a constant stress field in the base slab, since such a stress field will satisfy the boundary conditions along any parallel boundary. Thus, the determination of a statically admissible stress field in the base slab is trivial, and it remains only to consider the hub.

If the hub is of constant thickness H, then it may itself be considered as a plane slab. When loads $2khT_x$, $2khT_y$ per unit length are applied to the base slab, the same tractions will be submitted to the hub, so that the stress on the hub boundary is $2k(h/H)T_x$, $2k(h/H)T_y$. Therefore, the analysis of the reinforced cutout slab is reduced to an analysis of a plane unreinforced slab.

It is basically for this reason that, in analyzing an unreinforced slab we are more interested in obtaining the largest possible load hexagon (Fig. 3.1) rather than the actual domain of safe loads. For, once the value of λ has been determined for a slab of given dimensions and cutout, the thickness H of a hub of the same dimensions and cutout necessary to restore a slab of thickness h to full strength, independently of the dimensions of the base slab is

$$H = h/\lambda \, . \qquad (4.1)$$

The principles underlying the above remarks remain valid even if the surfaces of the hub are not plane. In this case, of course, other means must be used to analyze the hub, but if this can be done, Eq. 4.1 is still valid, provided that the reinforcement is so designed that h/H = const.

II. NARROW REINFORCEMENTS

5. General theory. Consider a cutout of arbitrary shape in a slab of thickness h, reinforced by arbitrary narrow reinforcing rings (Fig. 5.1). It is desired to find a lower bound for the cutout factor of such a slab, valid for any type of uniform loading and independent of the dimensions of the base slab.

In view of the results of Secs. 3 and 4, the analysis of this problem can be reduced to the consideration of the hub alone, loaded under uniform uniaxial or equal biaxial tensions. In the present section we make the stipulation that the dimensions of a hub are such that it may be reasonably approximated by a closed curved beam and that shear in the beam may be neglected. Of course, such an assumption can be incorporated into the mathematical model of the problem for any dimensions. However, the results predicted are likely to be reasonable only if the reinforcement is reasonably narrow, and if the thickness ratio of hub to slab is not so great as to seriously affect the carrying capacity of the hub.

Let the hub be referred to polar coordinates Γ, θ with origin at the center of symmetry, if any - otherwise at some interior point. Let the inner radius of the hub be denoted by

$$\Gamma = a(\theta) \tag{5.1}$$

and the radial thickness by $\delta(\theta)$ so that the outer radius is

$$\Gamma = a(\theta) + \delta(\theta) \tag{5.2}$$

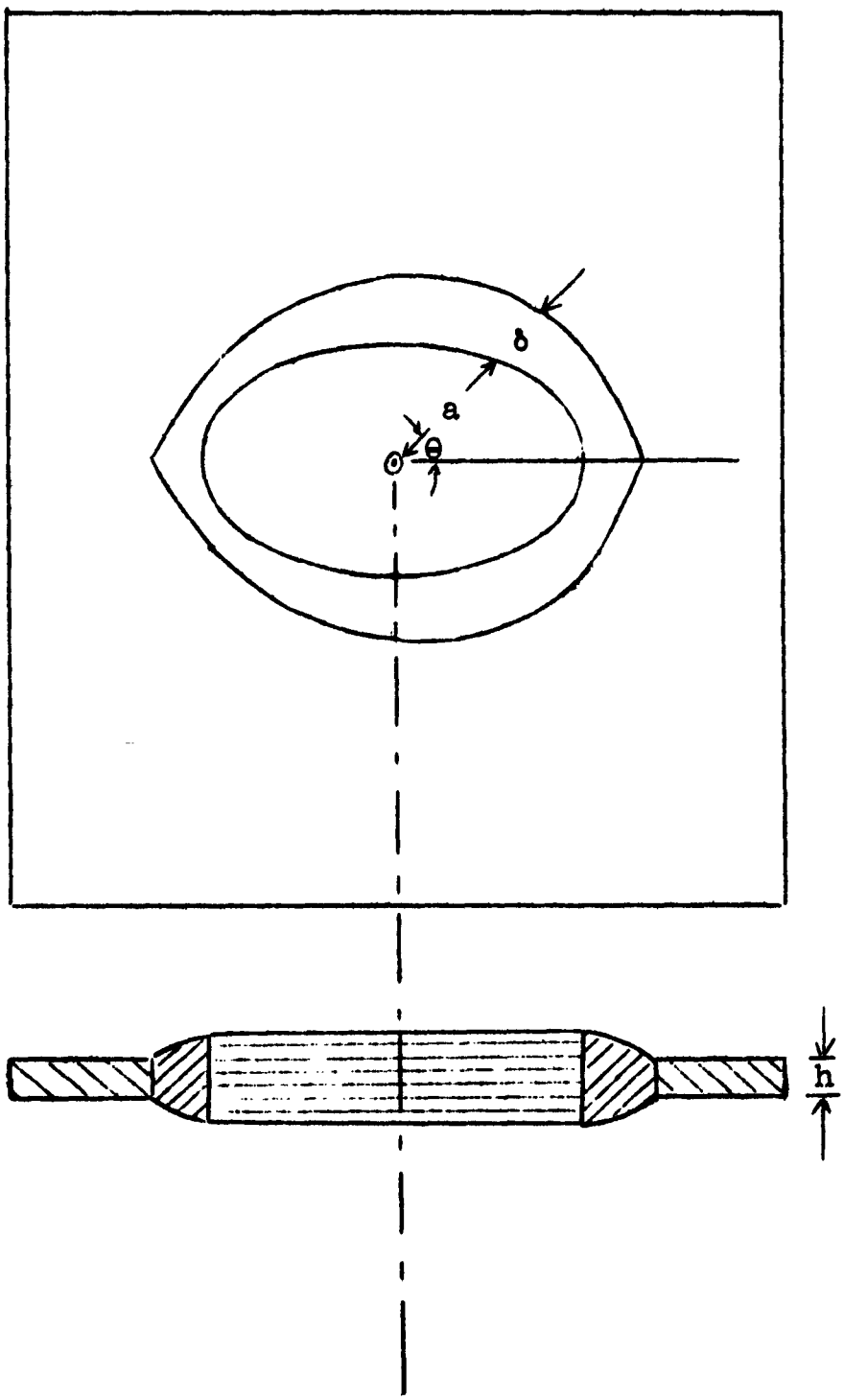

Fig. 5.1

Slab with narrow hub.

The height of the hub at any point is then given by

$$H = H(r,\theta) \tag{5.3}$$

We shall restrict our consideration to hubs whose inner and outer boundaries are sufficiently near to circular, so that a "cross-section" of the hub may reasonably be considered as a section θ = const. (Fig. 5.2a). Within the framework of beam theory, the stresses across any such section may be replaced by the stress resultants. Since shear is to be neglected, at each section θ we have an axial force $N(\theta)$ and a bending moment $M(\theta)$. Let these moments be taken about an arbitrary value $r = b(\theta)$.

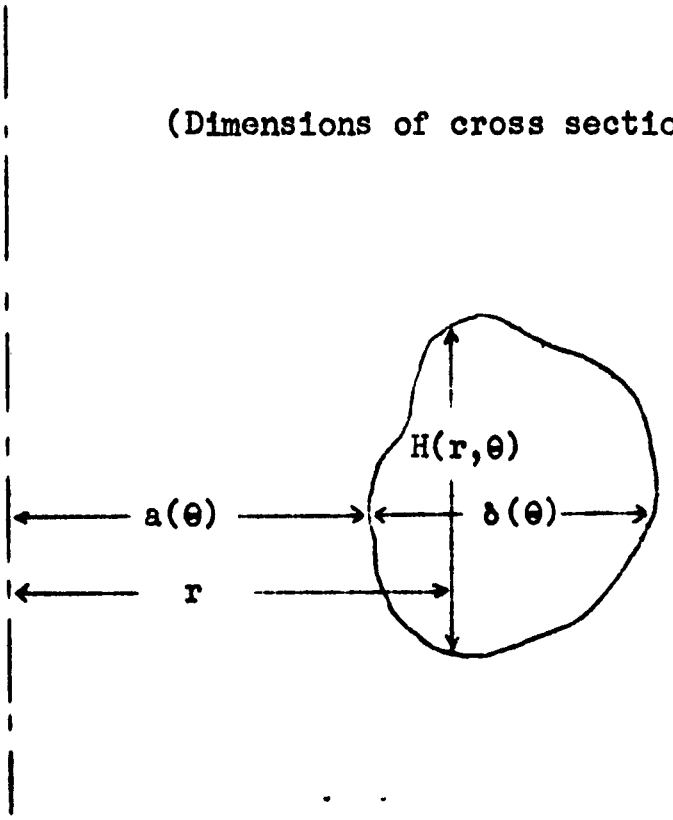

Fig. 5.2a

Cross section of hub.

The resultants N and M must be derived from the axial stress σ exerted across the section. Since this stress cannot be greater than the yield stress, the resultants will be subject to certain inequalities. To determine these inequalities, consider the case where the section is stressed to capacity. Thus, in Fig. 5.2b, suppose the hub section to be stressed to the yield limit in tension for $\Gamma > \eta$ and in compression for $\Gamma > \eta$. If the yield stress is denoted by 2k, the resultant force and moment are

$$N(\theta) = \int \sigma \, dA = 2k \left[\int_{a}^{b+\eta} -H \, d\Gamma + \int_{b+\eta}^{a+\delta} +H \, d\Gamma \right], \qquad (5.4a)$$

(Fully plastic cross section)

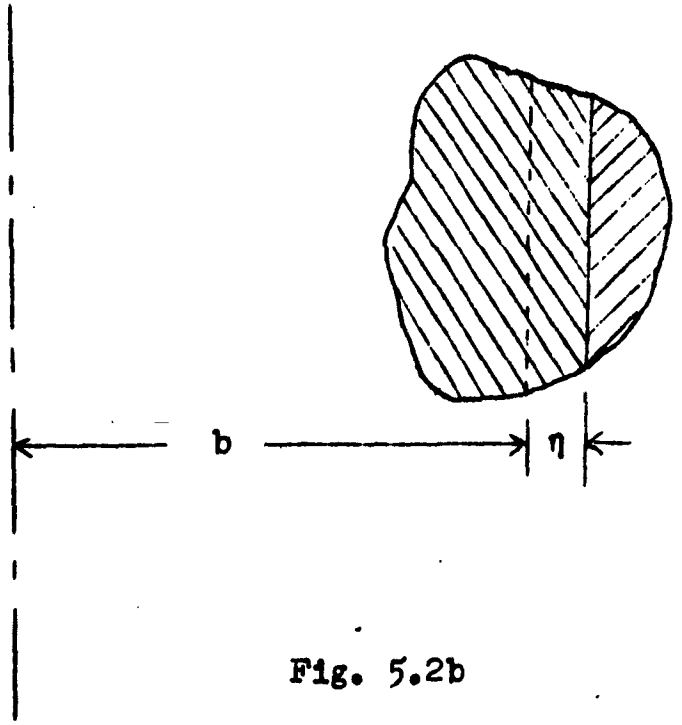

Fig. 5.2b

Cross section of hub.

$$M(\theta) = \int \sigma(b - r)dA = 2k\left[\int_a^{b+\eta} -(b-r)Hdr + \int_{b+\eta}^{a+\delta} (b-r)Hdr\right]. \qquad (5.4b)$$

Equations 5.4 define N and M in terms of a parameter η which may take on any value between a-b and a+δ-b. Similarly, if the regions in tension and compression are reversed, one obtains the equations

$$N(\theta) = 2k\left[\int_a^{b+\eta} Hdr + \int_{b+\eta}^{a+\delta} -Hdr\right], \qquad (5.5a)$$

$$M(\theta) = 2k\left[\int_a^{b+\eta} (b-r)Hdr + \int_{b+\eta}^{a+\delta} -(b-r)Hdr\right]. \qquad (5.5b)$$

If these curves are sketched in on N, M plane, the resulting closed curve is called an interaction curve. Stress resultants corresponding to safe stresses must lie within this closed curve.

The closed hub represents a structure with one degree of indeterminancy, so that the forces and moments at any point may be expressed in terms of the applied loads and a single redundant. Let this latter be the moment at section $\theta = 0$. For simplicity of exposition, we shall assume that the hub is symmetric with respect to the x and y axes, although the results are easily extended. Equilibrium of the first quadrant in the y direction then demands that

$$N(0) = 2k\lambda hT_y(a_o + \delta_o) \qquad (5.6)$$

where a_o and δ_o are the values at $\theta = 0$ of a and δ, respectively.

Next, let us consider equilibrium of an arbitrary segment of the hub, OABCD (Fig. 5.3). For convenience we may replace the uniform loads on BC and CD by equipollent concentrated forces

$$F_x = 2k\lambda h T_x (a + \delta) \sin\theta,$$

$$F_y = 2k\lambda h T_y [(a_o + \delta_o) - (a + \delta)\cos\theta] \qquad (5.7)$$

acting at the midpoints of BC and CD, respectively. Equilibrium in the direction of $N(\theta)$ then yields

$$N(\theta) = F_x \sin\theta - F_y \cos\theta + N(0)\cos\theta$$

$$= 2k\lambda h(a + \delta)[T_x \sin^2\theta + T_y \cos^2\theta], \qquad (5.8a)$$

while moment equilibrium about $r = b$ furnishes

$$M(\theta) = M(0) - (b_o - b\cos\theta) N(0)$$

$$+ F_x (b - \tfrac{a+\delta}{2}) \sin\theta + F_y [\tfrac{a_o + \delta_o + (a+\delta)\cos\theta}{2} - b\cos\theta]$$

$$= M(0) + 2k\lambda h(a+\delta)(b - \tfrac{a+\delta}{2})(T_x \sin^2\theta + T_y \cos^2\theta)$$

$$- 2k\lambda h T_y (a_o + \delta_o)(b_o - \tfrac{a_o + \delta_o}{2}).$$

(5.8b)

The analysis problem now consists of the following. Eliminate η between Eqs. 5.4 and between Eqs. 5.5 to find the interaction curve, and express the fact that the point with coordinates N, M must lie within this curve by means of inequalities.

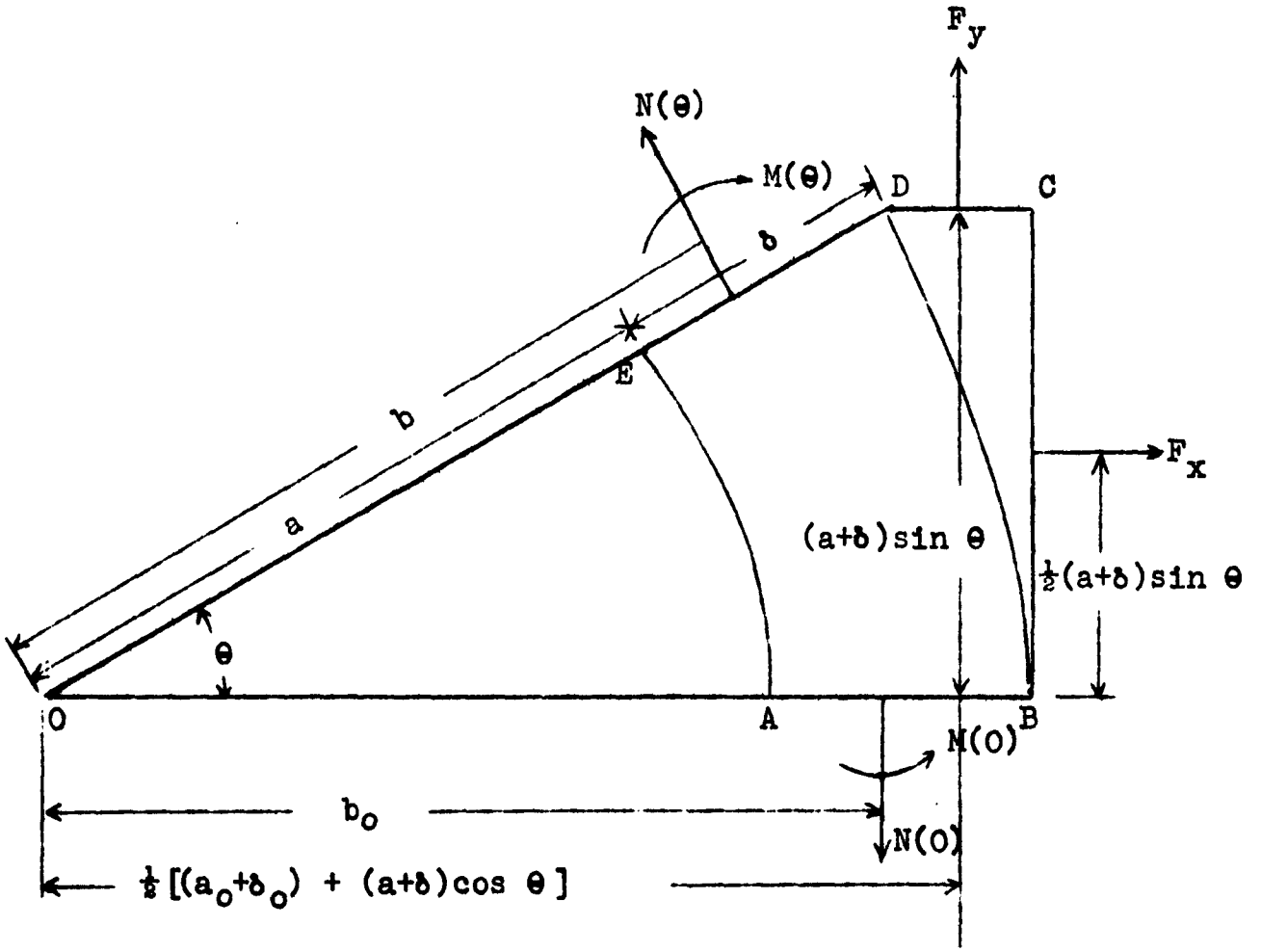

Fig. 5.3

Equilibrium of hub segment.

Substitute Eqs. 5.8 into these inequalities to obtain inequalities involving $M(0), \theta, \lambda$ and known quantities. $M(0)$ is now chosen so that λ will be a maximum subject to the condition that these inequalities be satisfied for all $0 \leq \theta \leq \frac{\pi}{2}$. Several examples of how this is done, together with the application of these results to design will be given in the remaining sections of this chap

6. Cylindrical ring reinforcements [2, 7]. If the height $H(\theta)$ of the hub is a constant it is convenient to choose b to be the center of the section:

$$b = a + 1/2\,\delta \tag{6.1}$$

Integrating Eqs. 5.4 and 5.5 we then obtain

$$N = -2kH\eta, \quad M = -2kH\left(\frac{\delta^2}{4} - \eta^2\right), \tag{6.2a}$$

$$N = 2kH\eta, \quad M = +2kH\left(\frac{\delta^2}{4} - \eta^2\right), \tag{6.2b}$$

respectively. After eliminating η, Eqs. 6.2 can be combined to give the interaction curve in the form (Fig. 6.1)

$$8\,k\,H\,|\,M\,| + N^2 = (2kH\delta)^2. \tag{6.3}$$

Therefore, safe stress resultants must satisfy

$$8\,k\,H\,|\,M\,| + N^2 \leq (2kH\delta)^2 \tag{6.4}$$

As a first example, let us consider a circular cutout with a circular reinforcement, so that a and δ are each constant [2]. In the case of biaxial tension, $T_x = T_y = 1$ Eqs. 5.8 reduce to

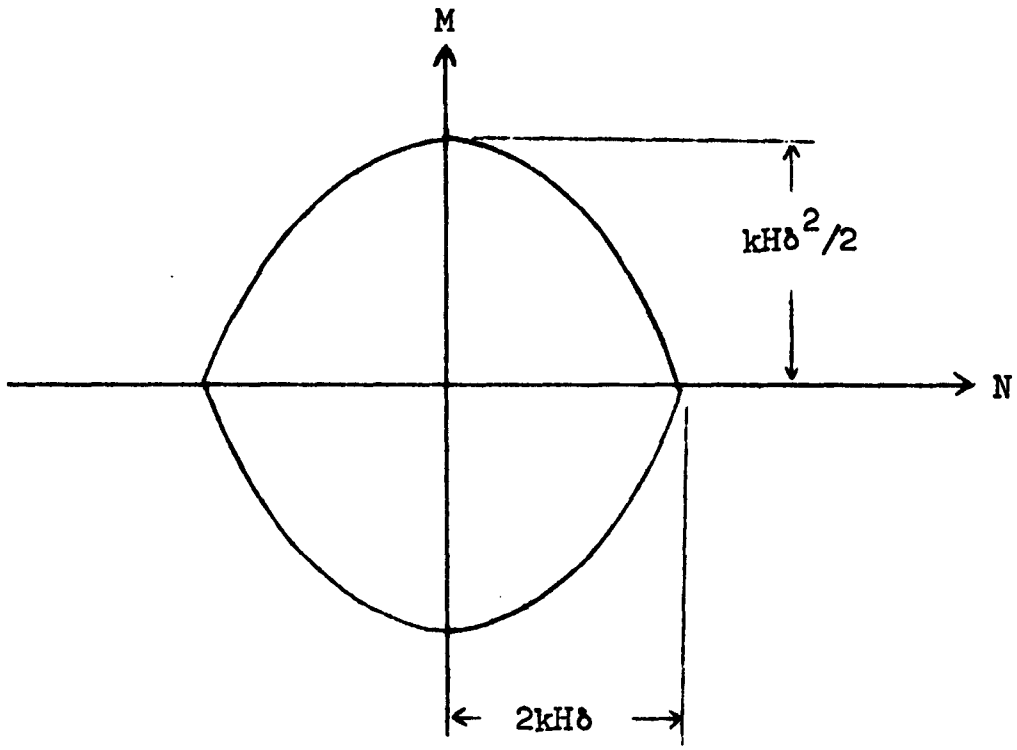

Fig. 6.1
Domain of safe stress resultants for cylindrical hub.

$$N(\Theta) = 2k\lambda h(a_o + \delta_o),\ M(\Theta) = M(0). \qquad (6.5)$$

Obviously the best choice of M(0) is zero, so that inequality 6.4 becomes

$$2k\lambda h\ (a_o + \delta_o) < 2kH\delta_o. \qquad (6.6)$$

For given dimensions a_o, δ_o, H the maximum cutout factor for equal biaxial loading is thus

$$\lambda = \frac{H\delta_o}{h(a_o + \delta_o)}, \qquad (6.7)$$

with, of course, the stipulation that $\lambda \leq 1$.

For uniaxial loading the result is not quite so trivial. In this case, $T_x = 1$, $T_y = 0$ so that Eqs. 5.8 reduce to

$$N(\Theta) = 2k\lambda h\ (a_o + \delta_o)\ \sin^2 \Theta$$

$$M(\Theta) = M(0) + k\lambda h\ a_o\ (a_o + \delta_o)\ \sin^2 \Theta$$

Substituting these values into 6.4 we obtain

$$8kH\ |\ M(0) + k\lambda h\ a_o\ (a_o + \delta_o)\ \sin^2 \Theta\ |$$

$$+ 4\ k^2\ \lambda^2\ h^2 (a_o + \delta_o)^2\ \sin^4 \Theta \leq (2kH\delta_o)^2. \quad (6.8)$$

The left-hand side of 6.8, considered as a function of $\sin^2 \Theta$, obviously achieves its maximum value at one or both of the end-points $\sin^2 \Theta = 0$ or $\sin^2 \Theta = 1$. Therefore, 6.8 will be satisfied for all $0 \leq \Theta \leq \frac{\pi}{2}$ if and only if

$$8kH[\ M(0) + k\lambda h a_o\ (a_o + \delta_o)\ ]\ + 4\ k^2\ \lambda^2\ h^2\ (a_o + \delta_o)^2 \leq (2kH\delta_o)^2,$$

$$8kH\ [-M(0) - k\lambda h a_o (a_o + \delta_o)\ ] + 4\ k^2\ \lambda^2\ h^2\ (a_o + \delta_o)^2 \leq (2kH\delta_o)^2,$$

$$8kH\ M(0) \leq (2kH\delta_o)^2$$

$$-8kH\ M(0) \leq (2kH\delta_o)^2 \quad (6.9)$$

Inequalities 6.9 are conveniently treated by a semi-graphical approach in [2]. However, in view of the more complex examples to follow, in this report, it is instructive to solve them by a formal mathematical procedure. To this end, we first solve 6.9 for 8kH M(0), obtaining

$$-(2kH\delta_o)^2 - 8\lambda k^2\ Hha_o(a_o + \delta_o) + 4\ k^2\ \lambda^2\ h^2(a_o + \delta_o)^2 \leq M(0)$$

$$\leq (2kH\delta_o)^2 - 8\lambda k^2\ \ Hha_o(a_o + \delta_o) - 4\ k^2\ \lambda^2\ h^2(a_o + \delta_o)^2, \quad (6.10a)$$

$$-(2kH\delta_o)^2 \leq 8kH\, M_o \leq (2kH\delta_o)^2. \qquad (6.10b)$$

Now, since M(0) is a redundant moment, we are not only free to choose it as we wish, but we don't really care what it is. Therefore, the only requirement we make of Inequalities 6.10 is that the system of inequalities is not incompatible, but actually possesses a solution. A necessary and sufficient condition that this be the case is that the left-hand side of each continued Inequality 6.10 be less than the right-hand side. The resulting four inequalities are all independent of M(0) and may be written

$$2\lambda^2 h^2(a_o + \delta_o)^2 \leq 2(H\delta_o)^2, \qquad (6.11a)$$

$$-2(h\delta_o)^2 - 2\lambda Hha_o(a_o + \delta_o) + \lambda^2 h^2 (a_o + \delta_o)^2 \leq 0, \qquad (6.11b)$$

$$-2(h\delta_o)^2 + 2\lambda Hha_o(a_o + \delta_o) + \lambda^2 h^2 (a_o + \delta_o)^2 \leq 0, \qquad (6.11c)$$

$$-(H\delta_o)^2 \leq (H\delta_o)^2. \qquad (6.11d)$$

Inequality 6.11d is an identity, and since λ is positive, 6.11b will be satisfied whenever 6.11c is. Therefore, λ is the largest number which satisfies 6.11a and 6.11c. Which of these inequalities provides the dominating restriction depends upon the ratio δ_o/a_o. It is readily verified that

$$\lambda = \frac{H\delta_o}{h(a_o + \delta_o)} \quad \text{if } \frac{\delta_o}{a_o} \geq 2,$$

$$\lambda = H\,\frac{\sqrt{a_o^2 + 2\delta_o^2} - a_o}{h(a_o + \delta_o)} \quad \text{if } \frac{\delta_o}{a_o} \leq 2. \qquad (6.12)$$

Obviously, if λ satisfies 6.12, it also satisfies 6.7. Therefore, it follows from the results of Sec. 3 that λ as given by 6.12 is the cutout factor for a slab with a circular cutout reinforced by annular rings of constant height.

In particular, if we want to design a reinforcement to restore the slab to full strength, we may set $\lambda = 1$ in Eqs. 6.12 and solve for the necessary thickness H:

$$H = h\left(1 + \frac{a_o}{\delta_o}\right), \text{ if } \frac{\delta_o}{a_o} \geq 2,$$

$$H = h\,\frac{a_o + \delta_o}{\sqrt{a_o^2 + 2\,\delta_o^2} - a_o}, \text{ if } \frac{\delta_o}{a_o} \leq 2. \tag{6.13}$$

Fig. 6.2 solid curve, shows H/h as a function of $\frac{\delta_o}{a_o}$.

As a second example, consider a square hole reinforced by a square reinforcement. The hub to be analyzed is then bounded by two similarly situated squares of half side a_o and $a_o + \delta_o$. The equations of the inner and outer boundaries in the first quadrant are given by

$$a = a_o \sec\theta, \quad \delta = \delta_o \sec\theta \text{ for } 0 \leq \theta \leq \pi/4, \tag{6.14a}$$

$$a = a_o \csc\theta, \quad \delta = \delta_o \csc\theta \text{ for } \pi/4 \leq \theta \leq \pi/2. \tag{6.14b}$$

Consider first the case of biaxial tension. Due to symmetry it is here sufficient to consider only the first octant, $0 \leq \theta \leq \pi/4$. Substituting 6.14a into 5.8, and taking $T_x = T_y = 1$, we obtain

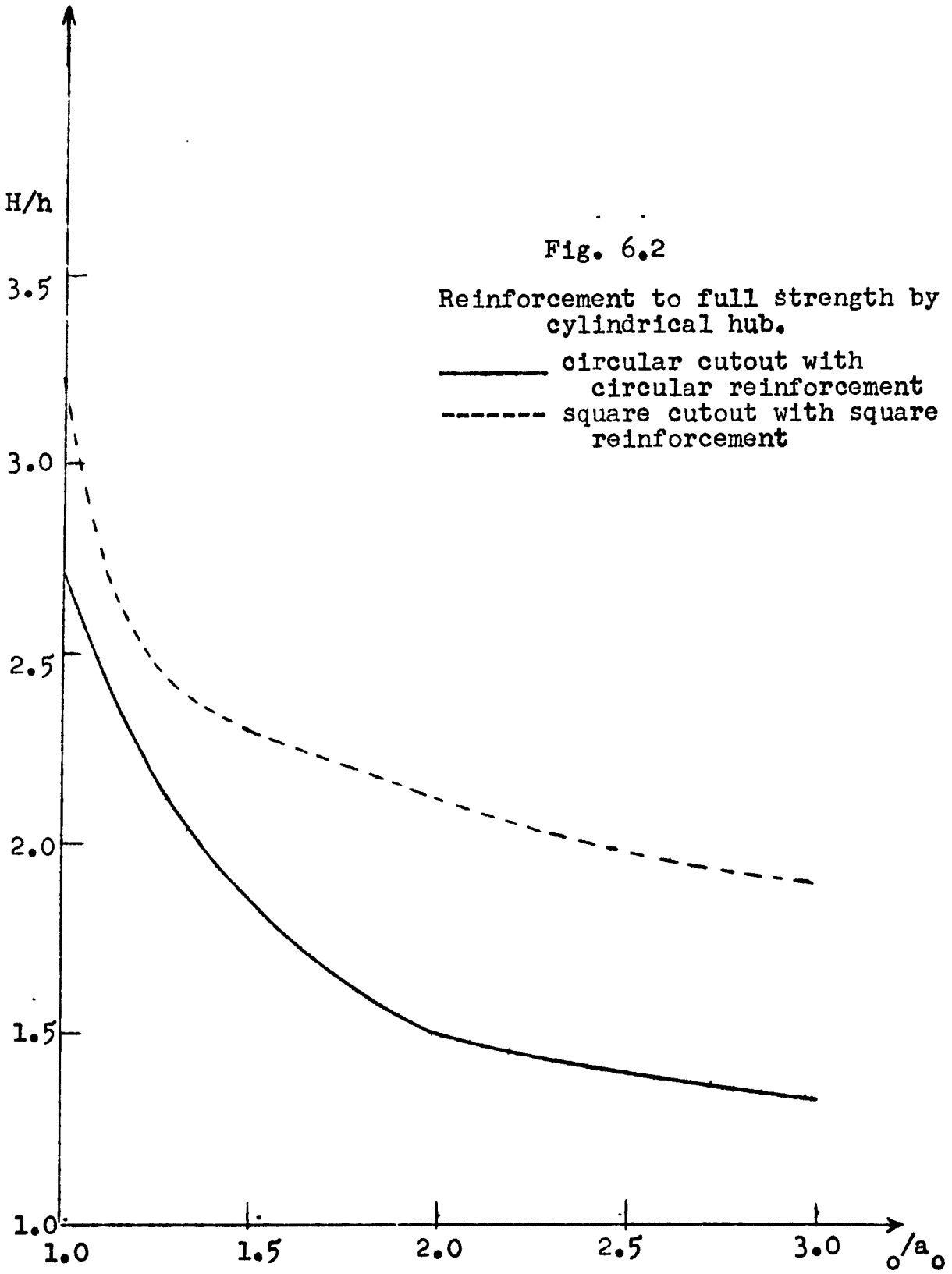

Fig. 6.2

Reinforcement to full strength by cylindrical hub.

_____ circular cutout with circular reinforcement

------- square cutout with square reinforcement

$$N = 2k\lambda h\ (a_o + \delta_o)\ \sec\theta,$$
$$M = M(0) + k\lambda h a_o\ (a_o + \delta_o)\ \tan^2\theta. \qquad (6.15)$$

The substitution of Eqs. 6.15 into the yield inequality furnishes an expression which is linear in $\tan^2\theta$. Therefore, the extreme values must come at the endpoints 0 and $\pi/4$ of the interval of consideration. Further, it is obvious from 6.15 that both M and N are increasing functions of θ. Therefore, the yield condition 6.4 will be satisfied for all values of θ if and only if

$$8kH\ M(\pi/4) + [\ N(\pi/4)\ ]^2 \leq (2k\lambda\delta)^2,$$
$$-8kH\ M(0) + [\ N(0)\ ]^2 \leq (2k\lambda\delta)^2.$$

In view of Eqs. 6.15, these inequalities may be written

$$-(H\delta)^2 + \lambda^2 h^2\ (a_o + \delta_o)^2 \leq 2H\ M(0)/k,$$
$$\leq (H\delta)^2 - 2kHha_o\lambda\ (a_o + \delta_o) - 2\lambda^2 h^2\ (a_o + \delta_o)^2.$$

A necessary and sufficient condition that there exist an M(0) such that the above inequality is true is that the left-hand member be less than the right-hand. Solving the resulting inequality for λ we obtain finally

$$\lambda \leq \frac{H}{3h}\ \frac{-a_o + \sqrt{a_o^2 + 2\delta_o^2}}{a_o + \delta_o}. \qquad (6.15)$$

Under uniaxial tension, we must consider both the first and second octants. For $0 \leq \theta \leq \pi/4$, we find that the extreme values may occur at either end of the interval, and hence are lead to

$$2\,H\,|\,M(0)\,|/k \le H^2\,\delta_o^2, \tag{6.17a}$$

$$2\,H\,|\,M(0)/k + \lambda h a_o(a_o + \delta_o)\,| + 2\,\lambda^2 h^2 (a_o + \delta_o)^2 \le H^2\,\delta_o^2. \tag{6.17b}$$

In the second octant M is constant and N is an increasing linear function of sin θ which leads to the two inequalities

$$2H\,[\,-Mo/k - \lambda h a_o(a_o + \delta_o)\,] \le H^2\,\delta_o^2,$$

$$2H\,[\,Mo/k + \lambda h a_o(a_o + \delta_o)\,] + \lambda^2 h^2\,(a_o + \delta_o)^2 \le H^2\,\delta_o^2. \tag{6.17c}$$

Solving each of the six inequalities 6.17 for 2H M(0)/k we see that Eqs. 6.17c are each automatically satisfied by one of the other inequalities. The remaining four inequalities obtained by eliminating M(0) will all be satisfied if

$$\left.\begin{aligned} \lambda &\le \frac{H}{h}\,\frac{\delta_o}{\sqrt{2}(a_o + \delta_o)}, \text{ if } \frac{\delta_o}{a_2} \ge \sqrt{2} \\ \lambda &\le \frac{H}{h}\,\frac{-a_o + \sqrt{a_o^2 + 4\,\delta_o^2}}{2\,(a_o + \delta_o)}, \text{ if } \frac{\delta_o}{a_o} \le \sqrt{2} \end{aligned}\right\} \tag{6.18}$$

Since any λ satisfying 6.18 also satisfies 6.16, it follows that 6.18 is a lower bound on the yield load for any type of loading. In particular, the height necessary to restore full strength under these conditions is obtained by setting $\lambda = 1$ in Eq. 6.18 and solving for H (Fig. 6.2, dashed curve).

$$\left.\begin{aligned} H &= \sqrt{2}\, h\left(1 + \frac{a_o}{\delta_o}\right), \text{ if } \frac{\delta_o}{a_o} \geq \sqrt{2} \\ H &= 2h\, \frac{a_o + \delta_o}{\sqrt{a_o^2 + 4\,\delta_o} - a_o}, \text{ if } \frac{\delta_o}{a_o} \leq \sqrt{2} \end{aligned}\right\} \qquad (6.19)$$

7. Bevelled ring reinforcement for a circular hole [6]. As an example of a non-cylindrical reinforcement, let us consider the bevelled reinforcement shown in Fig. 7.1. Since the section of the hub ABCC'B'A' does not possess any vertical

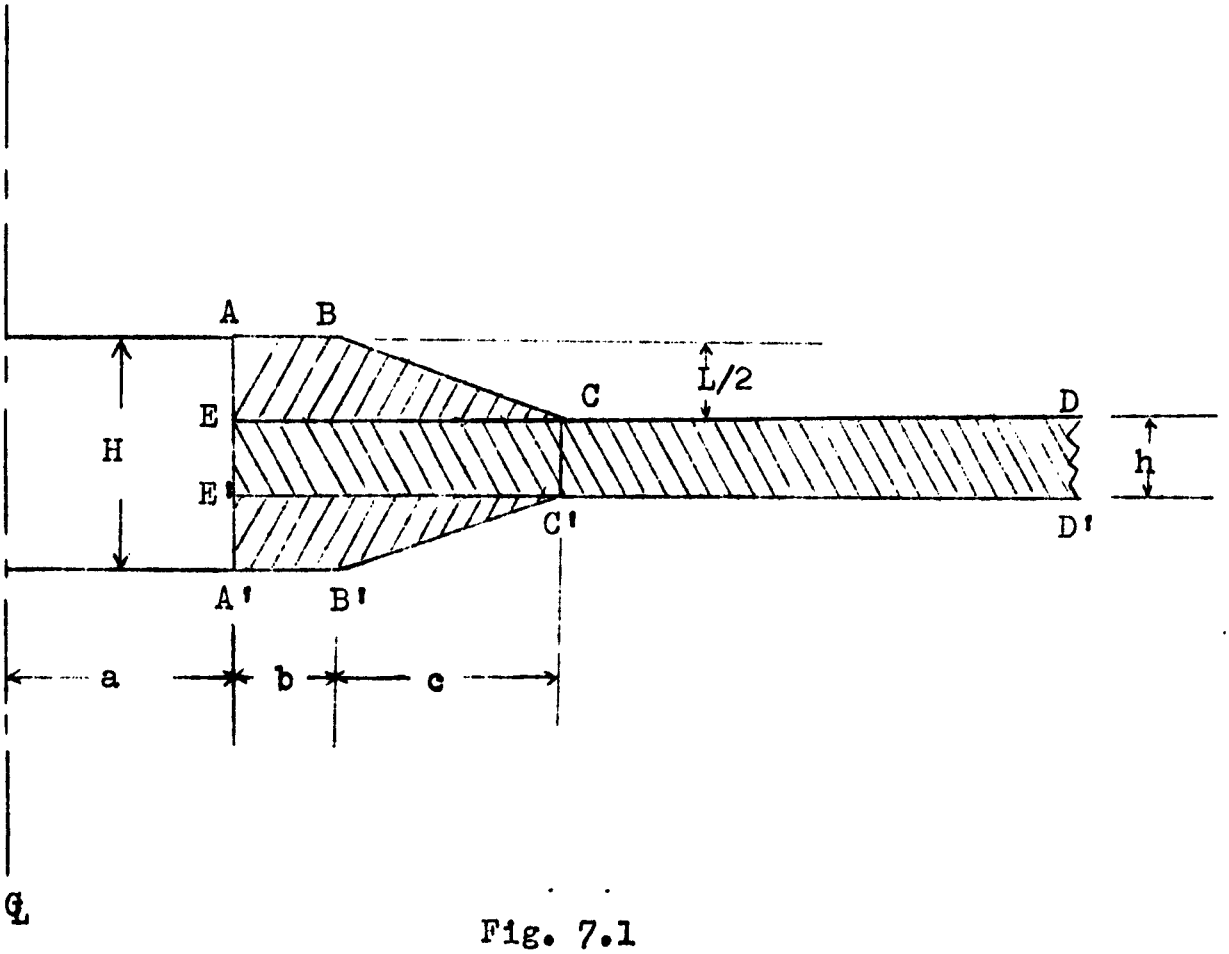

Fig. 7.1

Bevelled hub.

line of symmetry, it is convenient to take moments about the line BB' which separates the level from the sloping portion. Assuming that the outermost section yields in tension, Eqs. 5.4a take on two different forms depending upon whether the neutral axis is to the right or left of BB'. Thus, if η is positive we have

$$N = 2k[\, L\,\eta^2/c - 2H\eta - H\,b + (H + h)\,c/2\,], \tag{7.1a}$$

$$M = 2k\,[-\,2L\,\eta^2/3c + H\,\eta^2 - Hb^2/2 - Hc^2/6 - hc^2/3\,],$$

while if η is negative, the resultants are

$$N = 2k[\,-\,2H\eta\,-\,H\,b + (H + b)\,c/2\,],$$

$$M = 2k[\,H\eta^2 - Hb^2/2 - Hc^2/6 - hc^2/3\,]. \tag{7.1b}$$

It is convenient to write Eqs. 7.1 in terms of dimensionless variables defined by

$$u = NL/2kc\,H^2,$$

$$v = ML^2/2kc^2\,H^3,$$

$$A = L(Hb - Hc + Lc/2)/c\,H^2$$

$$B = L^2(Hb^2/2 + Hc^2/2 - Lc^2/3)/c\,H^3,$$

$$\xi = L\eta/cH \tag{7.2}$$

Equations 7.1 then become

$$u = \xi^2 - 2\xi - A,\quad v = -\,2/3\,\xi^3 + \xi^2 - B,\quad \xi > 0, \tag{7.3a}$$

$$u = -2\xi - A, \quad v = \xi^2 - B, \quad \xi < 0. \qquad (7.3b)$$

Similarly, the two possibilities which produce compression at the outermost surface lead to

$$u = -\xi^2 + 2\xi + A, \quad v = 2/3\ \xi^3 - \xi^2 + B, \quad \xi > 0 \qquad (7.3c)$$

$$u = 2\ \xi + A, \quad v = -\xi^2 + B, \quad \xi < 0 \qquad (7.3d)$$

The curve defined by Eqs. 7.3a has a cusp at $\xi = 1$. Therefore, it defines v as a double valued function of u for $u > A - 1$, while no real v is defined for $u < A - 1$. However, since

$$0 \leq \xi \leq L/H < 1$$

only one branch of the curve has physical meaning. In the case of 7.3a, it is readily verified that the algebraically greater branch is significant, so that, solving 7.3a for v we obtain

$$v = v_a = -(2/3 + A + B + u) + 2/3\ (1 + A + u)^{3/2}. \qquad (7.4a)$$

Similarly, only the lower branch of Eq. 7.3c is significant so that

$$v_c = (2/3 + A + B - u) - 2/3\ (1 + A - u)^{3/2}. \qquad (7.4c)$$

Finally, Eqs. 7.3b and d yield single-valued functions

$$v_b = (A + u)^2/4 - B, \qquad (7.4b)$$

$$v_d = -(A - u)^2/4 + B. \qquad (7.4d)$$

The interaction curve corresponding to Eqs. 7.4 is shown in Fig. 7.2. It is evident that the domain of safe stress resultants is defined by

$$v_a \leq v \leq v_c,$$

$$v_b \leq v \leq v_d. \qquad (7.5)$$

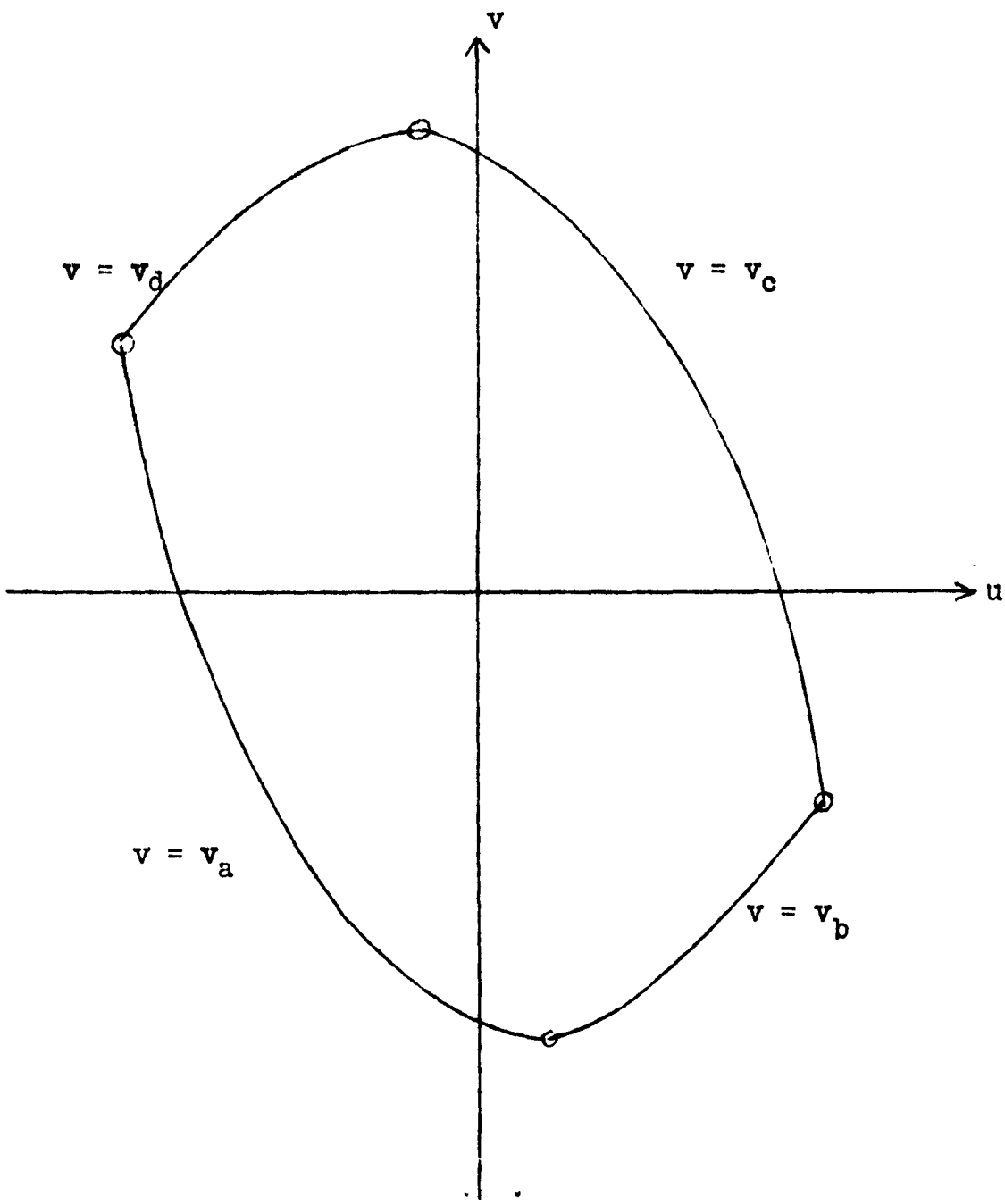

Fig. 7.2

Domain of safe stress resultants for barelled hub.

Next, we determine u and v in terms of the applied load from Eqs. 5.8. If the slab is under equal biaxial tension, $T_x = T_y = 1$ and Eqs. 5.8 furnish

$$N = 2k\lambda h(a + \delta) = 2k\lambda h(a + b + c), \quad M = M(0) \qquad (7.6)$$

obviously the best choice for the redundant moment is $M(0) = 0$, so that each section is thus stressed in pure tension. Therefore, we must have

$$N \leq 2k \text{ (Area)} = 2k\,(bH + ch + Lc/2). \qquad (7.7)$$

Comparing 7.6 and 7.7 we obtain

$$\lambda \leq \frac{bH + ch + Lc/2}{h(a + bc)}\,, \qquad (7.8)$$

for safety in biaxial loading.

In uniaxial tension $T_y = 0$, $T_x = 1$ Eqs. 5.8 furnish

$$u = D\,\lambda\,\zeta, \quad v = Y + E\,\lambda\,\zeta, \qquad (7.9)$$

where in addition to Eq. 7.2 we have introduced the notations

$$D = Lh\,(a + b + c)/c\,H^2,$$

$$E = L^2\,h\,(a + b + c)(a + b - c)/2\,c^2\,H^3,$$

$$Y = N(0)L^2 + xL^2/2kc^2\,H^3$$

$$\zeta = \sin^2\theta. \qquad (7.10)$$

The substitution of 7.9 into 7.5 yields the four inequalities

$$-(2/3 + A + B + D\lambda\zeta) + 2/3\ (1 + A + D\lambda\zeta)^{3/2} - Y - E\lambda\zeta \leq 0,$$

$$-(2/3 + A + B - D\lambda\zeta) + 2/3\ (1 + A - D\lambda\zeta)^{3/2} + Y + E\lambda\zeta \leq 0,$$

$$1/4(A + D\lambda\zeta)^2 - B - Y - E\lambda\zeta \leq 0,$$

$$1/4(A - D\lambda\zeta)^2 - B - Y + E\lambda\zeta \leq 0. \qquad (7.11)$$

Inequalities 7.11 must be satisfied for all values of ζ in $0 \leq \zeta \leq 1$. The enforcement of this condition will lead to certain inequalities not involving ζ. Each of these latter can then be solved for the redundant quantity Y. The elimination of Y then leads to various inequalities containing λ as the only unknown, and the desired value of λ is the largest one satisfying these inequalities.

Unlike the examples in the previous section, the functions of ζ on the left-hand side of 7.11 may attain their maximum value at an interior point of the interval $0 \leq \zeta \leq 1$. Therefore, it is not feasible to obtain a general solution to 7.11. For particular numerical values of the parameters, however, a solution can, of course, be obtained. For the particular case

$$H = 24,\ h = 10,\ L = 14,$$

$$a = 24,\ b = 11,\ c = 20, \qquad (7.12)$$

Levin and Hodge [6] obtained the result $\lambda = 0.98$. For the same example, 7.8 shows that $\lambda = 1$ in biaxial tension, so that the cutout is restored to at least 98% of full strength under an arbitrary uniform load.

8. Symmetric convex reinforcement for a circular cutout [9].

The techniques illustrated in the previous sections can be used, in theory, to find the yield load corresponding to any shaped cutout. However, if the hub profile is at all complex, the interaction curve will, in general, be too complicated to handle analytically. Rather than resort to straight numerical computations, it may be desirable to approximate the interaction curve.

In the first place, we observe that if the approximate domain of safe stress resultants lies entirely within the true domain of safe stress resultants, then any lower bound obtained by the approximate curve will be a true lower bound for the problem. If this is the case, the approximation will be called safe. Since, in the present chapter, we are only concerned with obtaining lower bounds, it is most desirable to know whether or not a given approximation has this property. We shall show that if the cross-section of the hub is symmetric and convex, that a simple parabolic approximation will always be safe.

To this end, let us refer the hub profile to Cartesian axes x, y which are the axes of symmetry, and let us take moments about the y axis (Fig. 8.1). Due to symmetry we need only consider the first quadrant of the hub. In this quadrant let

$$y = f(x) \tag{8.1}$$

be the equation of the hub. The boundary may contain vertical

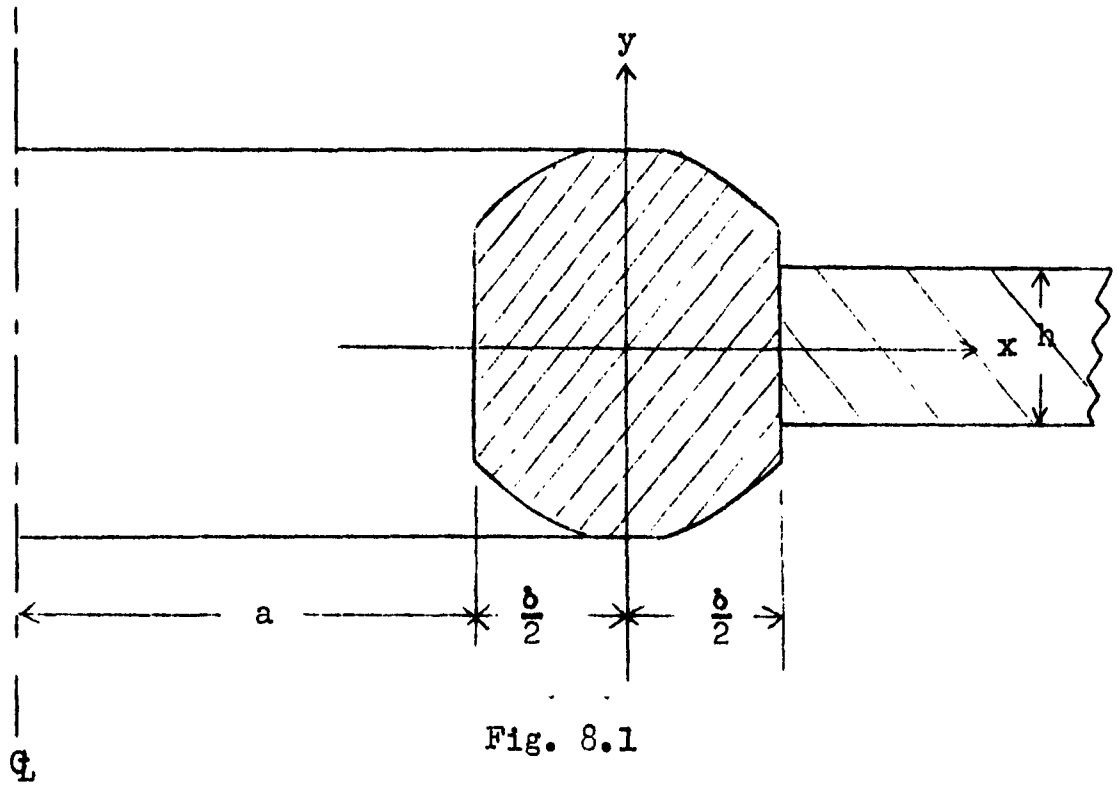

Fig. 8.1

or horizontal segments, but otherwise we assume that f is continuous and momotonically decreasing.

If $x = \zeta$ is the division between the tensile and compressive regions, Eqs. 5.4 and 5.5 may be replaced by

$$N = 4k\left|\int_{-\delta/2}^{\zeta} f(x)dx - \int_{\zeta}^{\delta/2} f(x)dx\right| = 8k\left|\int_{0}^{\zeta} f(x)dx\right|,$$

$$M = 4k\left|\int_{\delta/2}^{\zeta} xf(x)dx - \int_{\zeta}^{\delta/2} xf(x)dx\right| = 8k\left|\int_{0}^{\zeta} xf(x)dx\right|. \quad (8.2)$$

Due to symmetry, it is necessary to consider only the first quadrant of the stress-resultant plane, so that the absolute value signs in 8.2 may be dispensed with. Let

$$N_o = 8k\int_{0}^{\delta/2} f(x)dx, \quad M_o = 8k\int_{0}^{\delta/2} xf(x)dx \quad (8.3)$$

be the maximum force and moment, respectively, and define dimensionless resultants

$$\nu = \frac{N}{N_o} = \frac{\int_o^{\zeta} f(x)dx}{\int_o^{\delta/2} f(x)dx}, \quad \mu = \frac{M}{M_o} = \frac{\int_o^{\zeta} xf(x)dx}{\int_o^{\delta/2} xf(x)dx}. \qquad (8.4a,b)$$

The true interaction curve in the ν, μ plane is then obtained by eliminating ζ between Eqs. 8.4.

Let us approximate the curve 8.4 by the parabola

$$\mu = 1 - \nu^2. \qquad (8.5)$$

It follows from Eq. 6.3 that 8.4 reduces to 8.5 for a hub with rectangular section. For any other section, we wish to show that the curve 8.5 always lies below the true curve 8.4.

To this end, let us fix a value of ζ and take ν as defined in terms of ζ by Eq. 8.4a. For the true curve $\mu = \mu_T$ is given by 8.4b, while for the approximate curve, it follows from 8.5 that

$$\mu = \mu_A = 1 - \nu^2 = 1 - \left[\int_o^{\zeta} f(x)dx \Big/ \int_o^{\delta/2} f(x)dx \right]^2. \qquad (8.6)$$

Therefore, if we define

$$g(\zeta) = \mu_T - \mu_A \qquad (8.7)$$

we wish to show that $g(\zeta)$ is equal or greater than zero for $0 \leq \zeta \leq \delta/2$.

Under the assumptions on f it can be shown that [8.1]

$$g(0) = g'(0) = g(\delta/2) = 0, \; g'(\delta/2) \leq 0, \qquad (8.8)$$

and that $g'(\zeta)$ has not more than two roots in the closed interval $0 \leq \zeta \leq \delta/2$. Since $g(\zeta)$ is continuously differentiable it follows that there is a stationary point at $\zeta = 0$ and one interior stationary point. This latter must be a relative maximum of g, from the last condition 8.8. Therefore, since g is zero at the endpoints and has no relative minimum, it is everywhere non-negative.

The preceding result may be stated in words by saying that if safe stress resultants can be found for a rectangular section they can be found for any other hub section with the same δ, N_0 and M_0. Therefore, a safe approximation for any symmetric convex section can always be found in terms of a rectangular section and the analysis completed as in Sec. 6.

In particular, it is easily shown [9], that under equal biaxial tensions $2k\lambda h$ per unit length, we must have

$$\lambda \leq \lambda_1 \equiv A/[\, h(a + \delta)], \qquad (8.9)$$

where A is the total area of the section, and h the thickness of the base slab. Under uniaxial tension $2k\lambda h$ we must have

$$\lambda \leq \min\, (\lambda_1, \lambda_2), \qquad (8.10)$$

where λ_1 is given by 8.9 and

8.1 Details may be found in[9].

$$\lambda_2 \equiv \lambda_1 \left[\sqrt{2 + (aN_o/4M_o)^2} - (aN_o/4M_o) \right]. \qquad (8.11)$$

Finally, it follows from the analysis of Sec. 3 that a lower bound on the cutout factor is given by 8.10.

In [9] the above analysis is used to discuss a toroidal-type reinforcement for a circular cutout. In that example it is shown that the error introduced by approximating the interaction is negligible. In general, however, no such conclusion has been obtained.

9. Design of narrow reinforcement for full plasticity. If the reinforced cutout is to be subjected to only one type of loading, then it may be possible to design a cylindrical reinforcement for the cutout so that it will, like the "one horse shay" reach the yield stress at all points simultaneously. In other words, for a given $a(\theta)$ we wish to choose the reinforcement $\delta(\theta)$ so that the Equality 6.3 will hold at all points of the hub, rather than the Inequality 6.4.

Since the general theory becomes quite complicated [7], we shall here illustrate it by considering a circular cutout stressed in uniaxial tension.[9.1] Further we wish to design the reinforcement so as to restore the slab to full strength. Thus $T_x = 1$, $T_y = 0$, $\lambda = 1$ in Eqs. 5.8, so that the resultants are

$$N(\theta) = 2kh(a_o + \delta) \sin^2 \theta,$$

$$M(\theta) = M(0) + kha_o(a_o + \delta) \sin^2 \theta. \qquad (9.1)$$

9.1 The basic idea for this example was suggested by J.M. English [15].

We shall verify a posteriori that the quantity $\delta \sin^2 \theta$ is an increasing function of θ, so that N and M are both a maximum at $\theta = \pi/2$. Therefore, if 6.3 is to be everywhere valid, $M(\theta)$ must be everywhere less than zero except at $\theta = \pi/2$ where it will equal zero, i.e., the cutout will yield in pure tension there. With $M(\theta)$ negative, Eq. 6.3 may be written

$$- 2H\, M/k + (N/2k)^2 = H^2\, \delta^2. \tag{9.2}$$

At $\theta = 0$ Eqs. 9.1 and 9.2 show that

$$N(0) = 0,$$
$$2H\, M(0)/k = - H^2\, \delta_0^2, \tag{9.4}$$

while at $\theta = \pi/2$ they furnish

$$N(\pi/2)/2k = h\,(a + \delta_1) = H\, \delta_1,$$
$$2H\, M(\pi/2)/k = - H^2\, \delta_0^2 + 2Hha_0\,(a_0 + \delta_1) = 0, \tag{9.5}$$

where δ_1 is the value of δ at $\theta = \pi/2$. Eliminating δ_1, between Eqs. 9.5 we obtain

$$\frac{H}{h} = \frac{2\, a_0^2 + \delta_0^2}{\delta_0^2} \tag{9.6}$$

Finally, the substitution of 9.1, 9.4, and 9.6 into Eq. 9.2 shows that

$$[(1 + 2\alpha_0^2)^2 - \sin^4 \theta]\, \rho^2 + 2\alpha_0 \sin^2 \theta\, [(1 + 2\alpha_0^2) - \sin^2 \theta]\, \rho$$
$$- [(1 + 2\alpha_0^2)^2 - 2\alpha_0^2 \sin^2\theta(1 + 2\alpha_0^2) + \alpha_0^2 \sin^4 \theta\,] = 0, \tag{9.7}$$

where we have used the dimensionless variables

$$\rho(\theta) = \delta(\theta)/\delta_0, \quad \alpha_0 = a_0/\delta_0. \tag{9.8a}$$

Introducing the further abbreviation

$$f(\theta) = \sin^2\theta / (1 + 2\alpha_0^2), \tag{9.8b}$$

we may write the solution of Eq. 9.7 as

$$\rho = -\frac{\alpha_0 f}{1+f} + \sqrt{\frac{1 - 2\alpha_0^2 f/(1+f)}{1 - \cdot^2}}, \tag{9.9}$$

where the positive root is chosen since ρ must be positive.

In Figs. 9.1 and 9.2 we have sketched curves showing the shape of the reinforcement for the cases $\delta_0 = 1$ (H = 3.00 h) and $\delta_0 = 2$ (H = 1.50 h) respectively. In each figure, the dotted curve shows the circular reinforcement to full strength for the same value of H, computed from Eq. 6.13. Finally, Fig. 9.3 shows similar curves for a square cutout under various loadings. The details for this latter case may be found in [7].

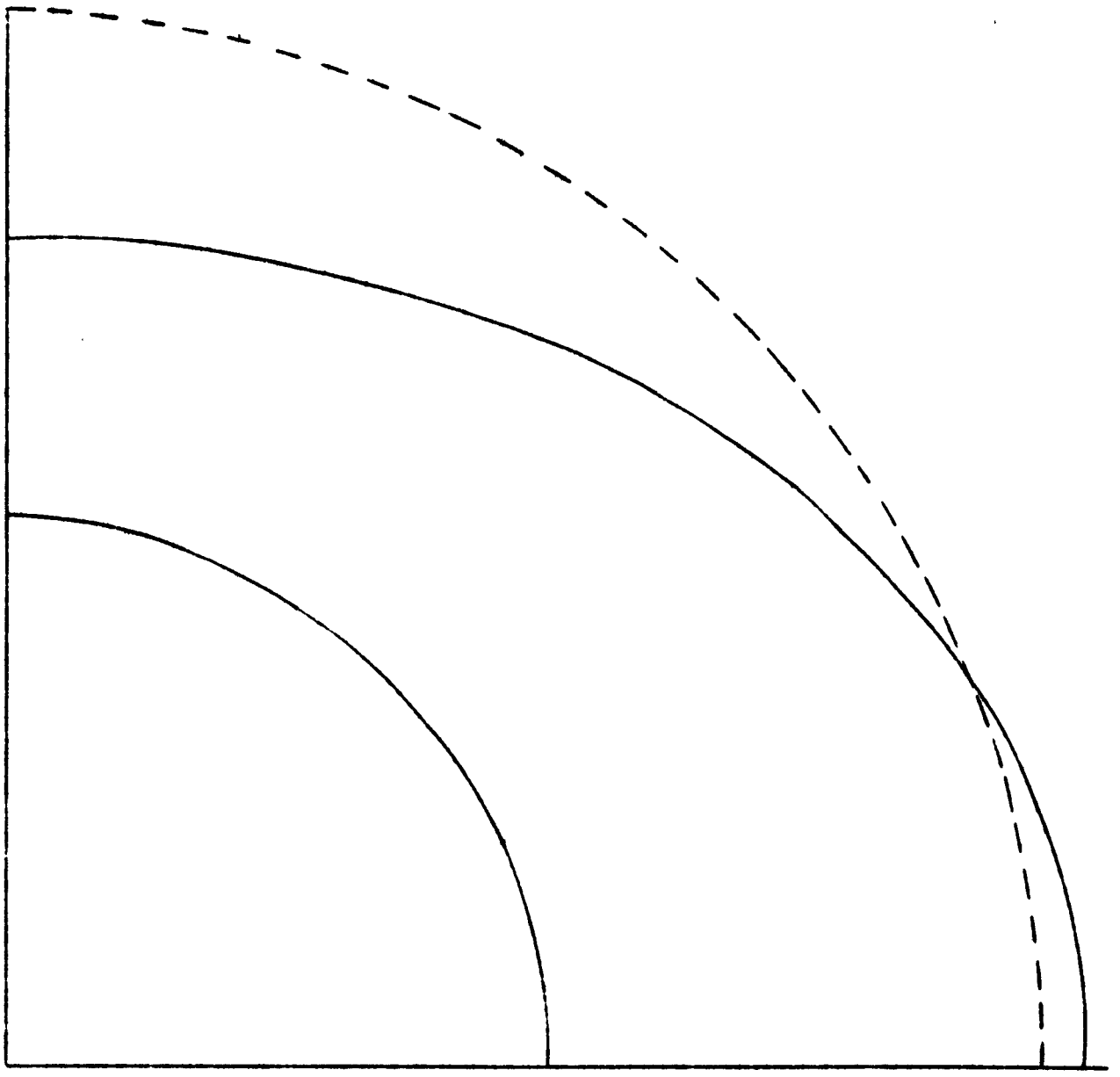

Fig. 9.1

Full reinforcement for circular cutout, $S_o = 1$.

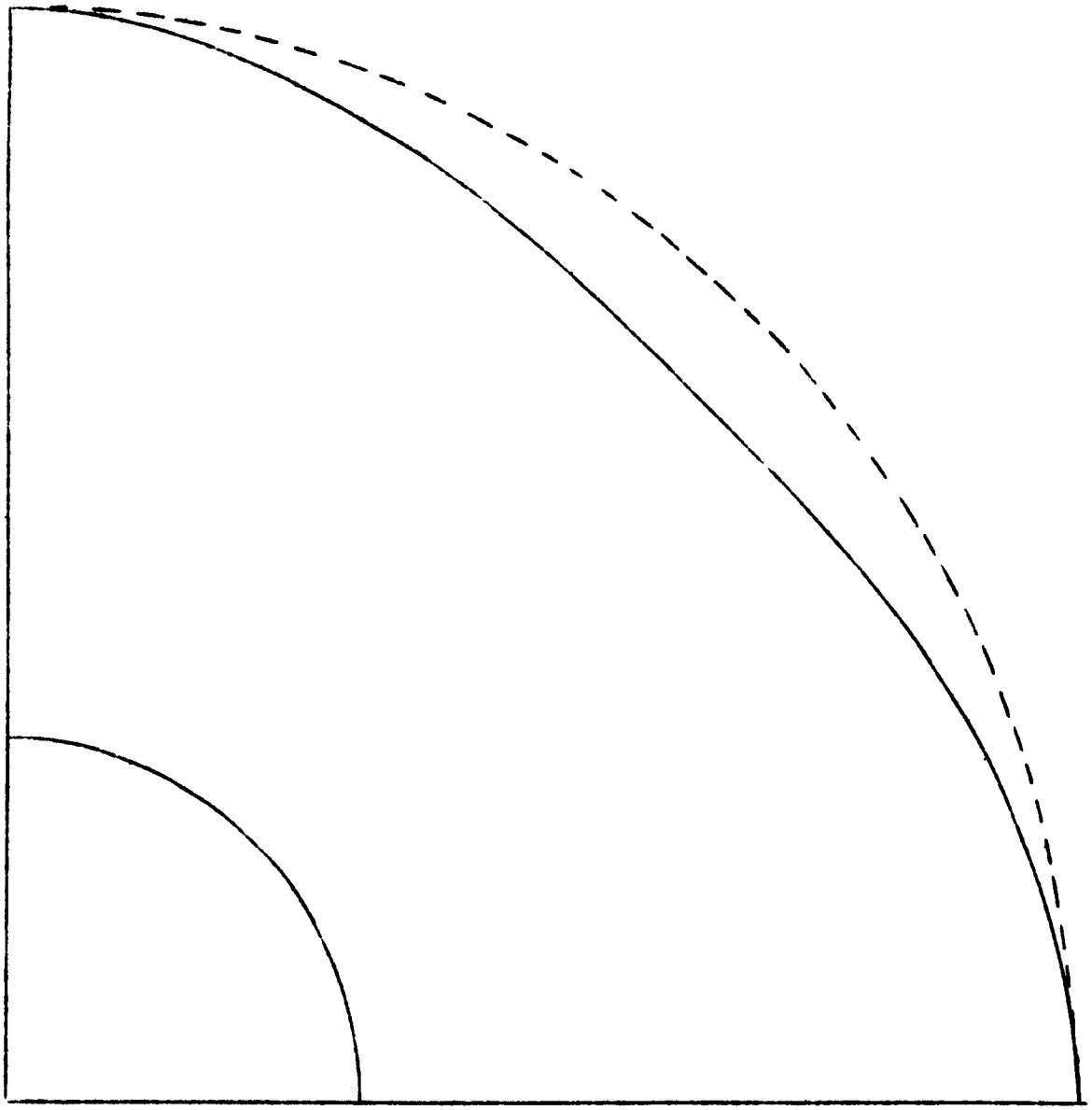

Fig. 9.2

Full reinforcement for circular cutout, $S_o = 2.$

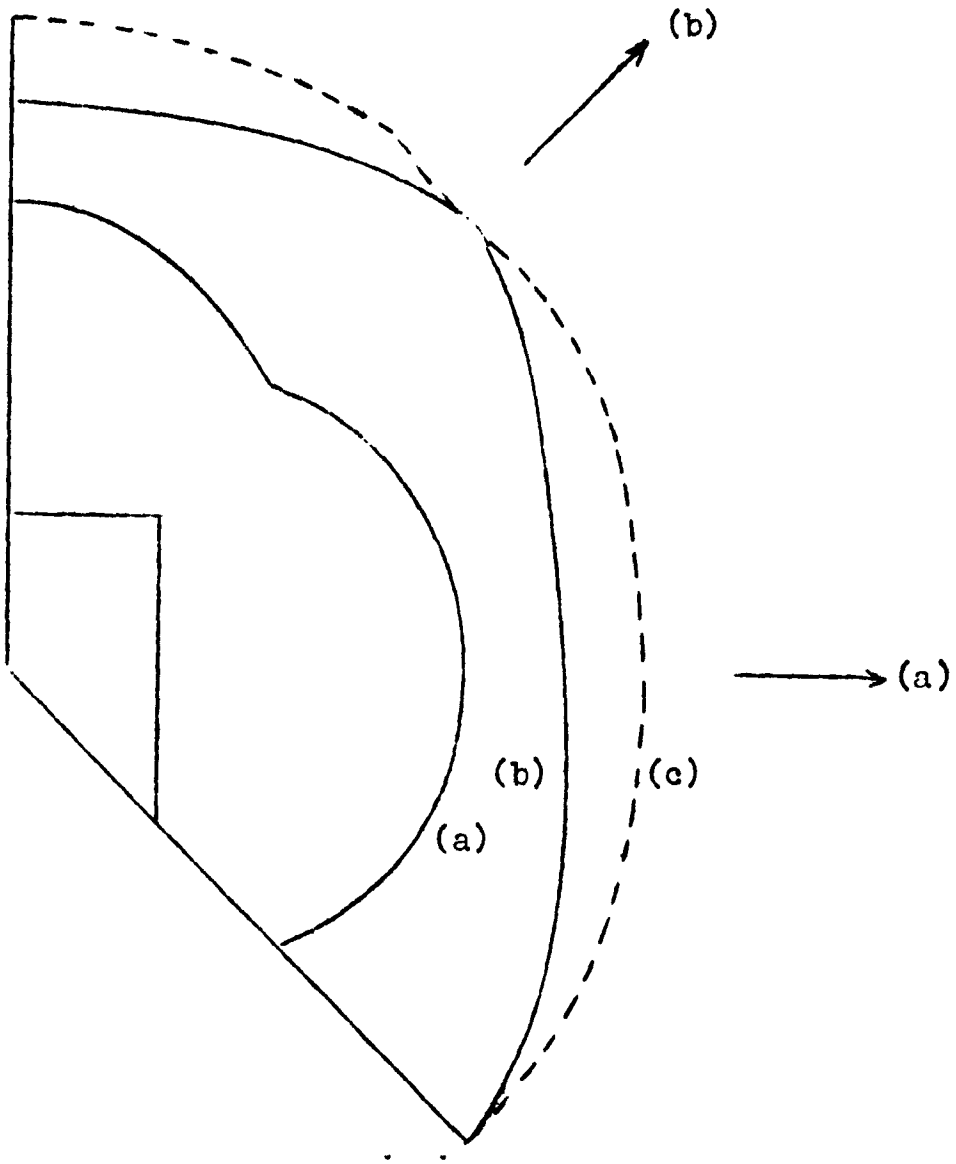

Fig. 9.3

Full reinforcements for square cutout.
(a) Uniaxial loading perpendicular to side,
(b) Uniaxial loading along diagonal,
(c) Biaxial loading.

III. UPPER BOUNDS FOR WIDE SLABS

10. Discontinuous velocity fields. The results presented in the previous chapter were concerned with a narrow reinforcement so that the hub might reasonably be approximated by a curved beam. Actually, the range of application of such techniques is rather limited, since if the ratio H/h becomes at all large there is serious question as to the carrying capacity of the hub, while if the ratio δ/a becomes large the hub is not well approximated by a beam.

A more realistic analysis in the case of wide unreinforced slabs or slabs with wide reinforcements is to approximate the actual stress state by plane stress. In this and the two succeeding chapters, we shall consider the problem of finding the yield load of unreinforced slabs, assuming a state of plane stress. We shall use both of the Drucker-Greenberg-Prager theorems in order to obtain both lower and upper bounds. The accuracy of the answer will be determined by the relative closeness of these two. In cases where the lower bound is far below the upper bound, the problem must be regarded as still unsolved.

A very simple type of velocity field which is quite useful is to assume that the slab consists of two rigid parts, and that motion occurs by the relative sliding of these two parts. In the present section we shall develop a general formula for computing the internal rate of dissipation of energy for such a motion (see also [16]).

We consider two sections of material separated by a common plane surface of area A, with one surface in motion relative to the other with a tangential velocity Δv_t (Fig. 10.1a). As mentioned in Sec. 2, such a discontinuous velocity field must be considered as the limit of a suitably chosen continuous velocity field. Let us choose coordinate axes so that the x axis is normal to the plane of sliding, and the y axis is in the direction of sliding, and consider the continuous motion defined in Fig. 10.1b. As in Fig. 10.1a, region 1 is at rest while region 3 moves upwards with velocity Δv_t. In the transition region 2, we define the velocity field

$$v_x = v_z = 0, \quad v_y = (x/\delta)\,\Delta v_t. \tag{10.1}$$

Observe that this field is incompressible, and that the combined velocity field is continuous in region 1, 2, and 3.

Since the velocity fields in regions 1 and 3 are each constant, the strains are all zero. Therefore, energy is dissipated only in region 2. In region 2, the absolutely largest principal strain rate has the constant value $\Delta v_t/2\delta$. Therefore, Eq. 2.2 yields

$$\mathcal{D}_1 = 2k \int_{V_2} (\Delta v_t/2\delta)dv = k\,(\Delta v_t/\delta)\,V_2 = kA\Delta v_t \tag{10.2}$$

independently of the value of δ. Therefore, it follows that Eq. 10.2 must also be valid for the limiting discontinuous case, $\delta = 0$.

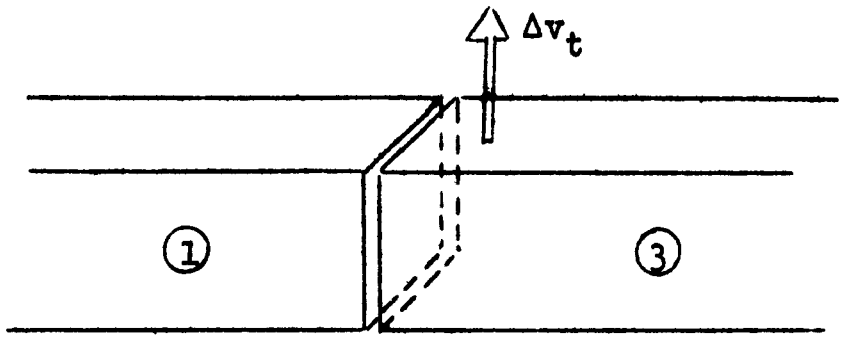

Discontinuous velocity field.

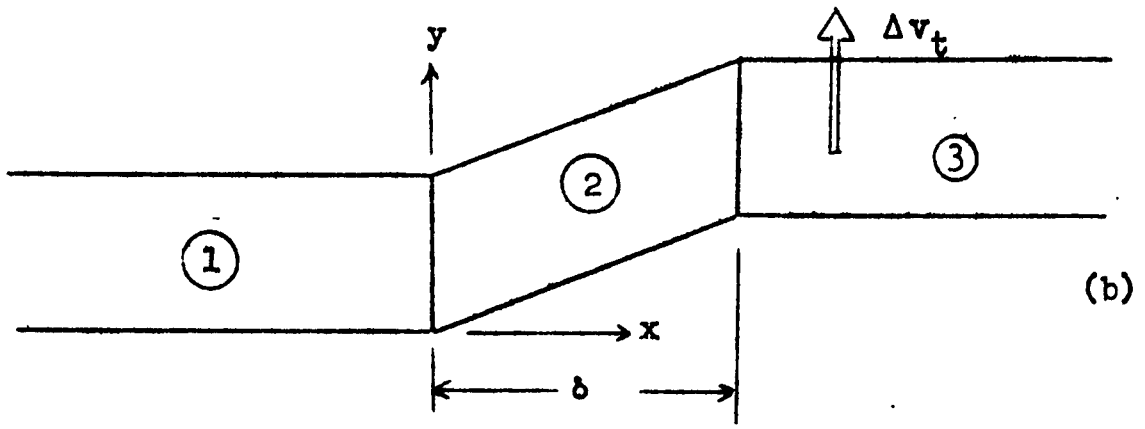

Trace of continuous velocity field.

Fig. 10.1

11. Sliding out of plane [2]. A simple upper bound for any plane slab may be found immediately by considering a shear out of the plane at 45°. Consider, for example, such a shear across the x axis of an unreinforced slab (Fig. 11.1). Since the plane of sliding is at 45° to the plane of its height will be $h\sqrt{2}$. Further, since the sliding takes place along the weakest section AB, the sliding plane consists of two rectangles, each of length $1 - a_o$. Therefore, it follows from Eq. 10.2 that the total internal rate of dissipation of energy is

$$\mathcal{D}_i = k\, 2h\sqrt{2}\,(1 - a_o)\, v \qquad (11.1)$$

The external rate of dissipation of energy is computed from Eq. 2.3. Since there is no motion in the x direction, the loads T_x do no external work. The projection of the velocity vector in the direction of the load T_y is $v/\sqrt{2}$, so that in view of 2.3,

$$\mathcal{D}_e = \int_S 2\, k\lambda T_y\, (v/\sqrt{2})ds = 2\sqrt{2}\; k\, h\, \lambda\, T_y\, V. \qquad (11.2)$$

According to Theorem 2, an upper bound for the load λ is obtained if $\mathcal{D}_e$ and $\mathcal{D}_i$ are equal. Thus

$$\lambda\, T_y \leq 1 - a_o. \qquad (11.3)$$

Since the average stress across AB is $2k\lambda T_y/(1 - a_o)$, Eq. 11.3 shows that this stress cannot exceed the yield stress. This is in marked contrast to the yielding of notched bars under conditions of plane strain [14, Sec. 33].

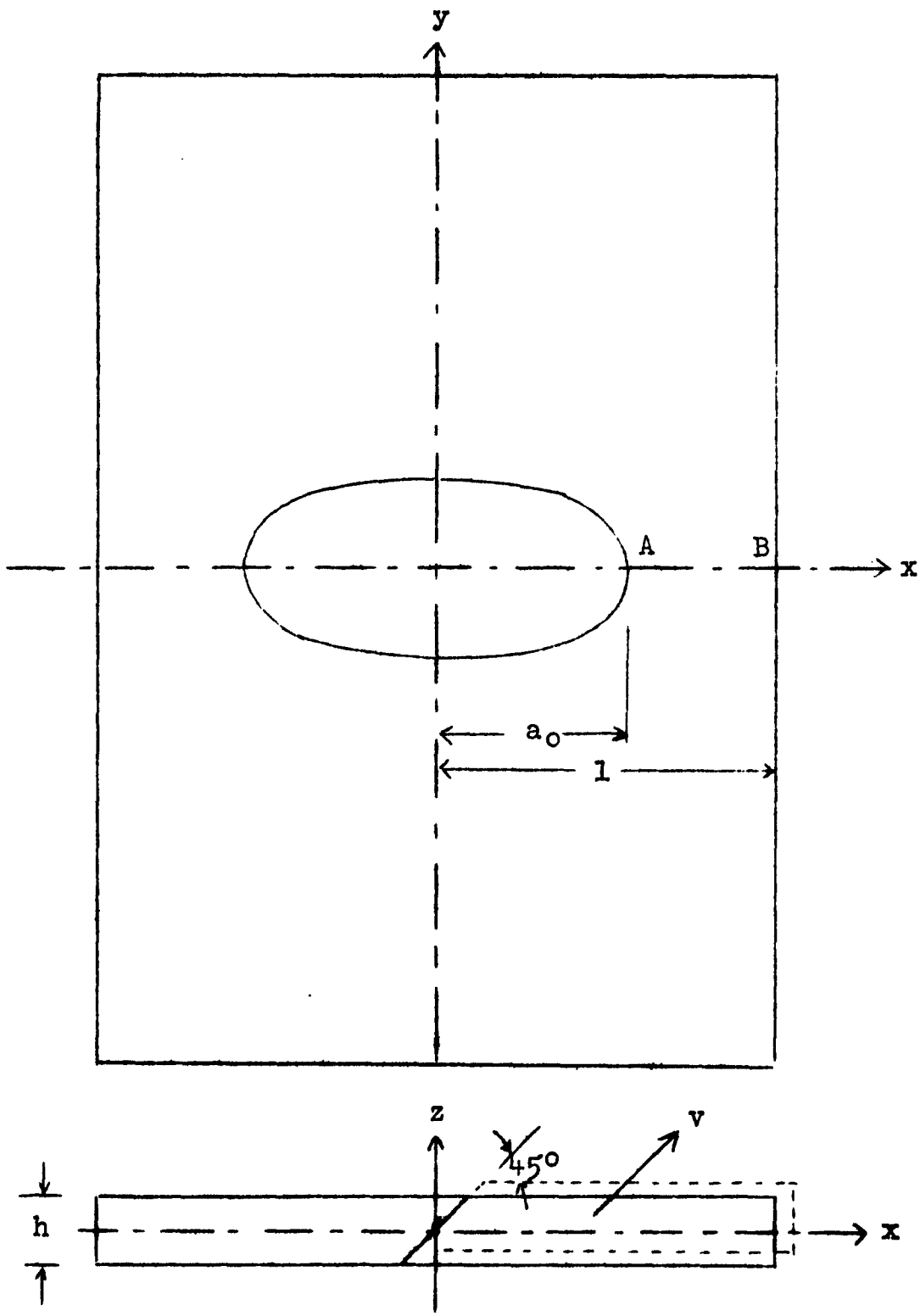

Fig. 11.1

Sliding out of plane.

12. Sliding in plane. The concept of rigid parts sliding along planes can also be used for the case where the plane of sliding is perpendicular to the slab. As an example, consider an annular slab of inner radius a and outer radius 1, sliding along four symmetrically placed lines in the plane, as indicated in Fig. 12.1. The slab is under uniaxial tension in the y direction: $T_x = 0$, $T_y = 1$.

Due to symmetry, we need consider only the first quadrant of the slab. In this quadrant the x and y components of velocity are

$$V_x = -A,\ V_y = 0 \text{ in region 1,}$$

$$V_x = 0,\ V_y = B \text{ in region 2.} \qquad (12.1)$$

However, it is more convenient to refer the motion to the directions n and t, normal and tangential to the line of discontinuity AB in Fig. 12.1. Equations 12.1 must then be replaced by

$$V_m = -A \sin \gamma,\ V_t = -A \cos \gamma \text{ in region 1,}$$

$$V_m = -B \cos \gamma,\ V_t = B \sin \gamma \text{ in region 2.} \qquad (12.2)$$

The constants A and B in Eqs. 12.2 are not independent, since the normal components of velocity must be the same in the two regions. Thus

$$B = A \tan \gamma,$$

and the discontinuity in tangential velocity is readily computed

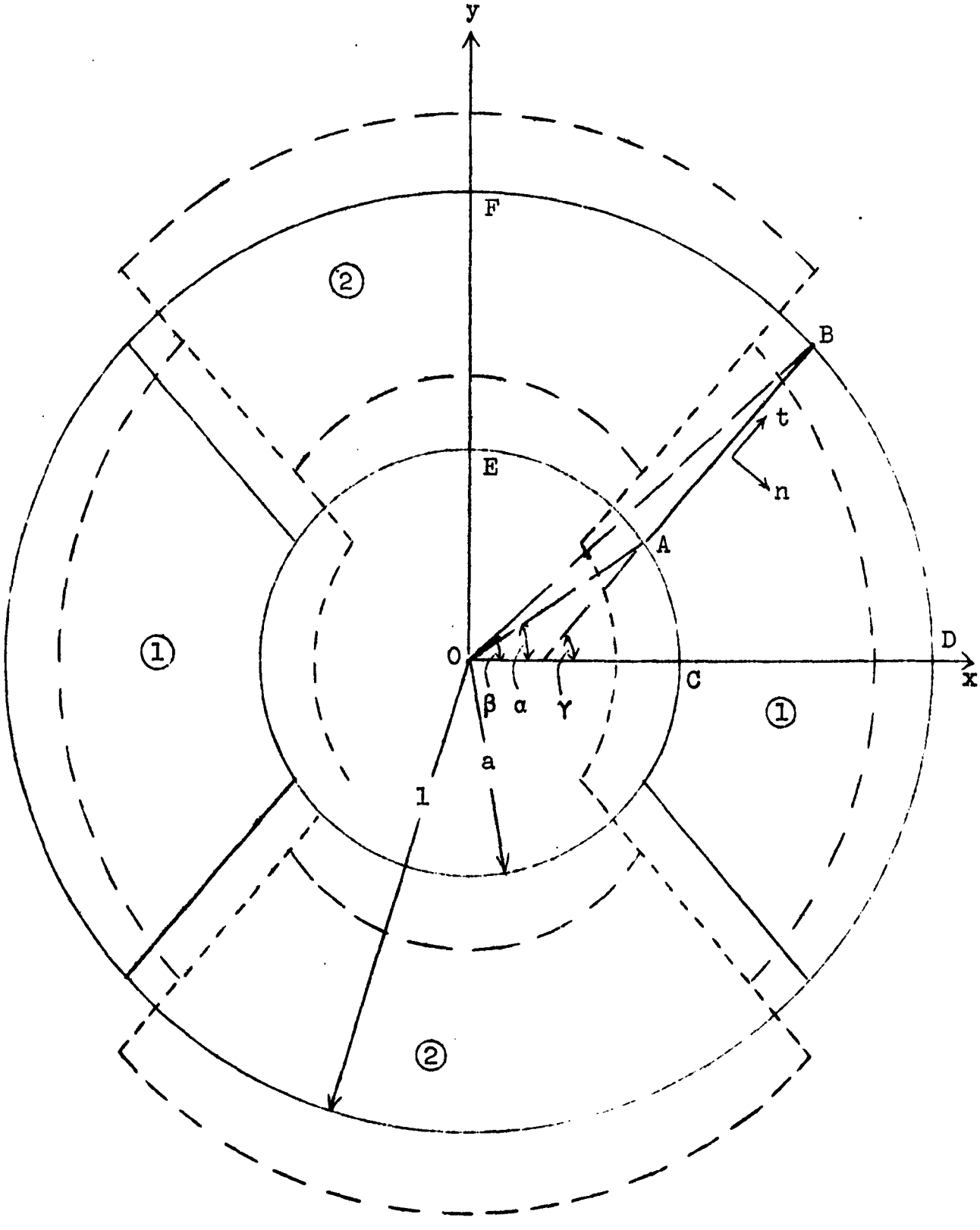

Fig. 12.1

Sliding in plane of annular slab.

to be

$$\Delta V_t = A \sec \gamma . \tag{12.3}$$

Substituting 12.3 into 10.2, we see that the internal rate of dissipation of energy is

$$\mathcal{D}_i = k\, h\, L\, A \sec \gamma , \tag{12.4}$$

where L is the length of AB.

The external rate of dissipation of energy is given by

$$\mathcal{D}_e = \int_{\beta}^{\pi/2} 2\, k\, \lambda \sin \theta\, B\, h\, d\theta = 2\, k\, \lambda\, h\, A \tan \gamma \cos \beta. \tag{12.5}$$

An upper bound on λ is then obtained by equating 12.4 and 12.6:

$$\lambda \leq \frac{L}{2 \sin \gamma \sin \beta}. \tag{12.6}$$

Note that both Eqs. 12.4 and 12.6 represent one-quarter of the total energy of the slab so that they may be equated.

The line of sliding AB has two free parameters which are conveniently taken to be the angles α and β as indicated in Fig. 12.1. In terms of these angles we have

$$\begin{aligned} L &= \sqrt{1 - 2\, a \cos (\beta - \alpha) + a^2} \ , \\ \sin \gamma &= (\sin \beta - a \sin \alpha)/L. \end{aligned} \tag{12.7}$$

Substituting 12.7 into 12.6 we obtain

$$\lambda \leq \frac{1 - 2\, a \cos (\beta - \alpha) + a^2}{2 \cos \beta (\sin \beta - a \sin \alpha)} . \tag{12.8}$$

Any values of α and β, subject to certain obvious geometric restrictions, will furnish an upper bound for λ. In particular, if AB is assumed to be a radial line, $\alpha = \beta$ and the right-hand side of 12.8 becomes $(1-a)/\sin 2\beta$. Since this can never be less than 1-a, sliding along a radial line cannot furnish a better upper bound then sliding out of the plane (Sec. 11).

Obviously the best upper bound of the type considered is obtained by choosing α and β so as to minimize the right-hand side of 12.8. To this end, let

$$u = 1 - 2a\cos(\beta - \alpha) + a^2,$$
$$v = \cos\beta\ (\sin\beta - a\sin\alpha). \tag{12.9}$$

If $f(u,v) = \frac{u}{2v}$ is to be a minimum, then

$$\frac{\partial f}{\partial \alpha} = 1/2\ \frac{v\,\partial a/\partial\alpha - u\,\partial v/\partial\alpha}{v^2} = 0,\ \frac{\partial f}{\partial\beta} = 0$$

so that

$$\frac{u}{v} = \frac{\partial u/\partial\alpha}{\partial v/\partial\alpha} = \frac{\partial u/\partial\beta}{\partial v/\partial\beta}, \tag{12.10}$$

or

$$\frac{1 - 2a\cos(\beta-\alpha) + a^2}{\sin\beta\cos\beta - a\sin\alpha\cos\beta} = \frac{2\sin(\beta-\alpha)}{\cos\beta\cos\alpha} = \frac{2a\sin(\beta-\alpha)}{\cos 2\beta + a\sin\alpha\sin\beta}. \tag{12.11}$$

Equating the last two and first two members of the continued equality 12.11, we obtain

$$a \cos \beta \cos \alpha - a \sin \beta \sin \alpha = \cos 2\beta,$$

$$(a^2 + \cos 2\beta) \cos \alpha + \sin 2\beta \sin \alpha = 2a \cos \beta. \quad (12.12)$$

Equations 12.11 may be formally identified with simultaneous linear algebraic equations in cos α and sin α and solved to yield

$$\cos \alpha = \frac{2 \cos \beta (\cos 2\beta + a^2)}{a (2 \cos 2\beta + 1 + a^2)},$$

$$\sin \alpha = \frac{\cos^2 2\beta - a^2}{-a \sin \beta (2 \cos 2\beta + 1 + a^2)}. \quad (12.13)$$

Substituting 12.13 into the identity $\sin^2 \alpha + \cos^2 \alpha = 1$ and introducing the notation

$$\zeta = \cos 2\beta \quad (12.14)$$

we obtain, after some simplification,

$$(1 - a^2)(2\zeta^2 + a^2 \zeta - a^2) = 0.$$

Since a must be actually less than one, the second factor must vanish, so that

$$\zeta = (a/4)(-a \pm \sqrt{a^2 + 8}). \quad (12.15)$$

Now, it follows from Eq. 10 that the minimum value of f is

$$f = 1/2 \frac{u}{v} = 1/2 \frac{\partial u/\partial \alpha}{\partial v/\partial \alpha} = \tan \beta - \tan \alpha. \quad (12.16)$$

Replacing α and β in Eq. 12.16 by their values in terms of ζ as given by Eqs. 12.14 and 12.13, we obtain finally

$$\lambda \leq f = \frac{\zeta (1 - a^2)}{(\zeta + a^2)\sqrt{1 - \zeta^2}} \qquad (12.17)$$

where ζ is given in terms of a by Eq. 12.15. It is readily verified that the upper sign in 12.15 will furnish a lower value of f and hence is the correct choice. In Fig. 12.2 we have sketched the upper bound on λ as a function of a. Before accepting this result, it was necessary to find β and α from Eqs. 12.14 and 12.13 and verify that they were geometrically admissible angles. This was found to be the case for all values of a. Observe that for all values of a we have obtained an improved result for this case over that obtained in Sec. 11, as shown by the dashed line in Fig. 12.2.

13. Bending in plane. A totally different type of yielding is suggested by the approximate analysis of the preceding chapter. If the slab were to be replaced by a curved beam, the beam would fail by means of yield hinges. That is, there would be certain sections of the beam where there would be a concentrated rotation and extension [17] (or, equivalently, an off center rotation [18]), with the remainder of the beam remaining rigid. There must be just enough of these yield hinges to form a mechanism.

Let us, then, consider such a yield hinge from a plane stress viewpoint. Choosing the y axis to be normal to the beam at the yield hinge, and the plane of bending to be the x,y plane, consider a rotation about the point A in Fig. 13.1.

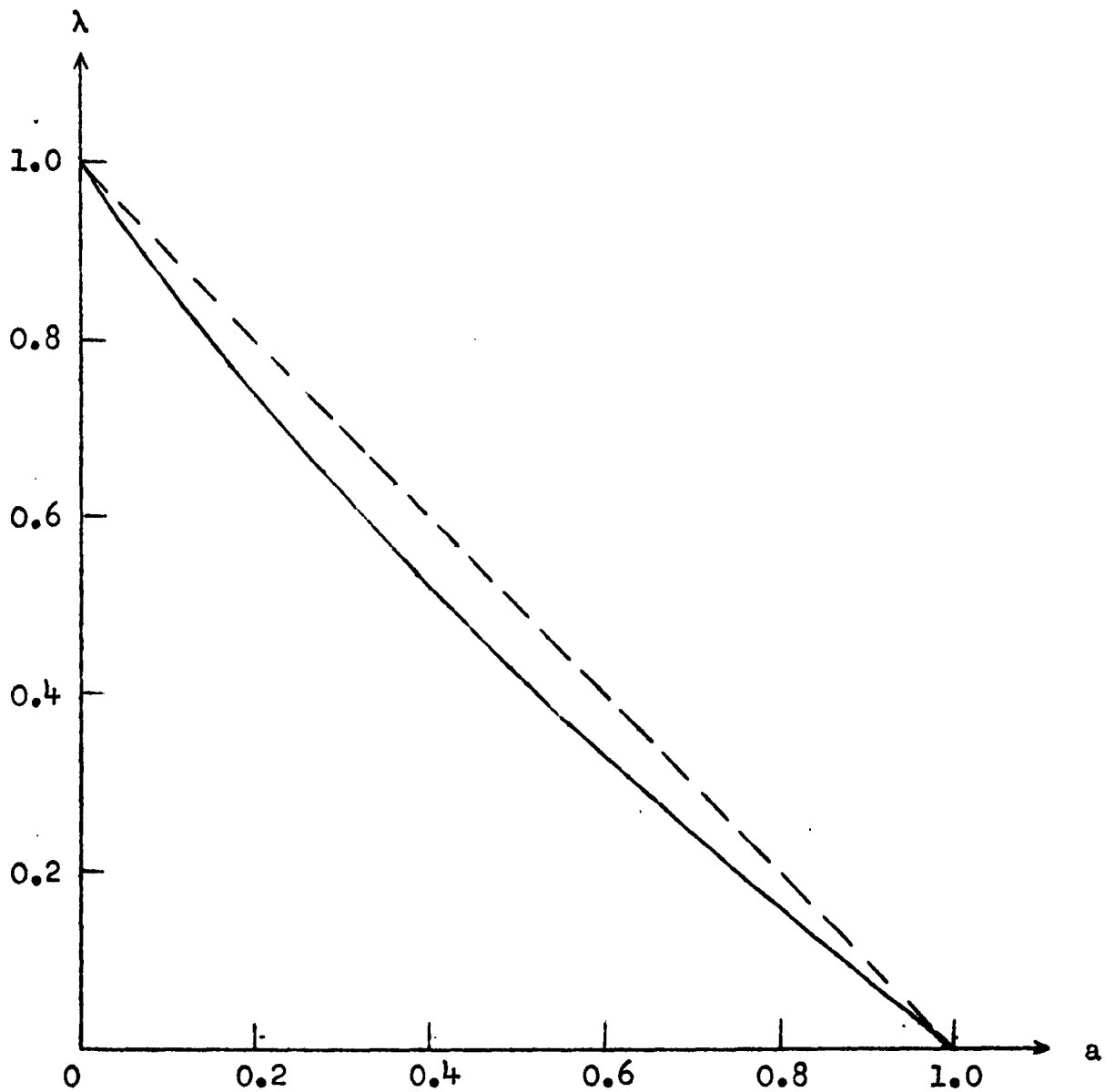

Fig. 12.2

Upper bound on yield load of annular slab.

——— sliding in plane
– – – – – – – – sliding out of plane

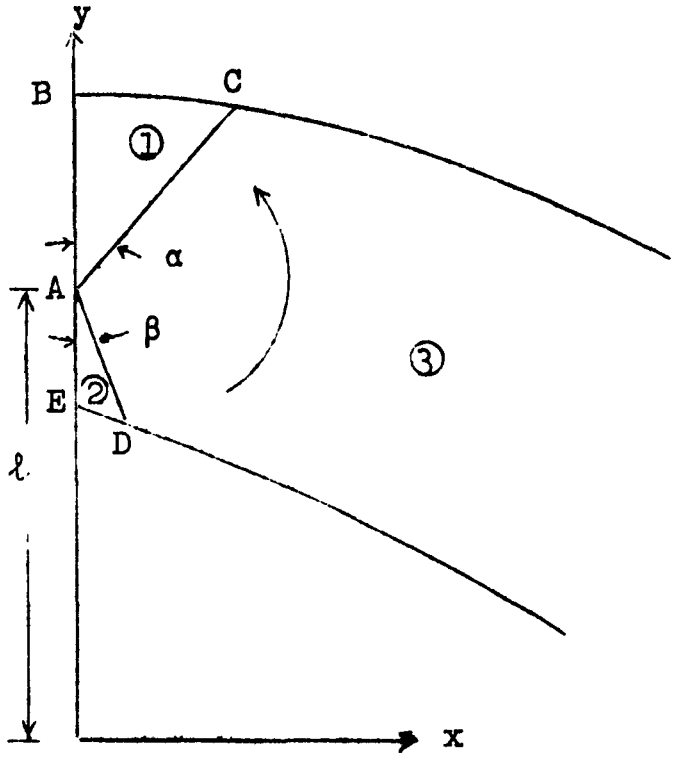

Fig. 13.1
"Yield hinge" in plane stress.

The rigid portion of the beam, region 3 will rotate about the point A with an angular velocity $\dot{\theta}$. Therefore

$$u_3 = -\dot{\theta}\,(y - \ell),\quad v_3 = \dot{\theta}\,x \qquad (13.1)$$

where u_3 and v_3 are the velocity components in the direction of the x and y axes, respectively. In region 1 u must equal zero along AB by symmetry, and must be continuous with u_3 along AC. Similarly, v must be continuous along AC, and there is to be no shearing strain in the vertical direction. Such a velocity field is given by

$$u_1 = -\dot{\theta}\,x\cot\alpha\,,\quad v_1 = \dot{\theta}\,(y - \ell)\tan\alpha. \qquad (13.3)$$

Similar considerations show that

$$u_2 = \dot{\theta}\, x \tan\beta\ ,\ v_2 = \dot{\theta}\,(\ell - y)\tan\beta\ . \qquad (13.3)$$

There are no strains in region 3, while in region 1 the principal strain rates are

$$\varepsilon_x = -\dot{\theta}\cot\alpha,\ \varepsilon_y = \dot{\theta}\tan\alpha\ ,\ \varepsilon_z = \dot{\theta}\,(\cot\alpha - \tan\alpha\,). \qquad (13.4)$$

Observe that the axial velocity w is thus not strictly continuous. However, for a sufficiently thin slab its action is reasonably neglected. Separate analyses must be made for greater or less than $\pi/4$. For definiteness we shall take $\alpha < \pi/4$ so that the absolutely largest principle strain rate has the value

$$\max|\,\varepsilon\,| = \dot{\theta}\cot\alpha\ . \qquad (13.5)$$

Substituting 13.5 into 2.2, we find that the internal rate of dissipation of energy is

$$\mathcal{D}_1^{(1)} = 2\,k\,\dot{\theta}\,h\cot\alpha\ A_1 \qquad (13.6a)$$

where A_1 is the area of region 1. Similarly, if $\beta < \pi/4$,

$$\mathcal{D}_1^{(2)} = 2\,k\,\dot{\theta}\,h\cot\beta\ A_2. \qquad (13.6b)$$

Since $\mathcal{D}_1^{(3)} = 0$ the total internal energy is the sum of the two Eqs. 13.6.

As an example, consider a square hole in a square slab under uniaxial tension (Fig. 13.2). The velocity of the rigid

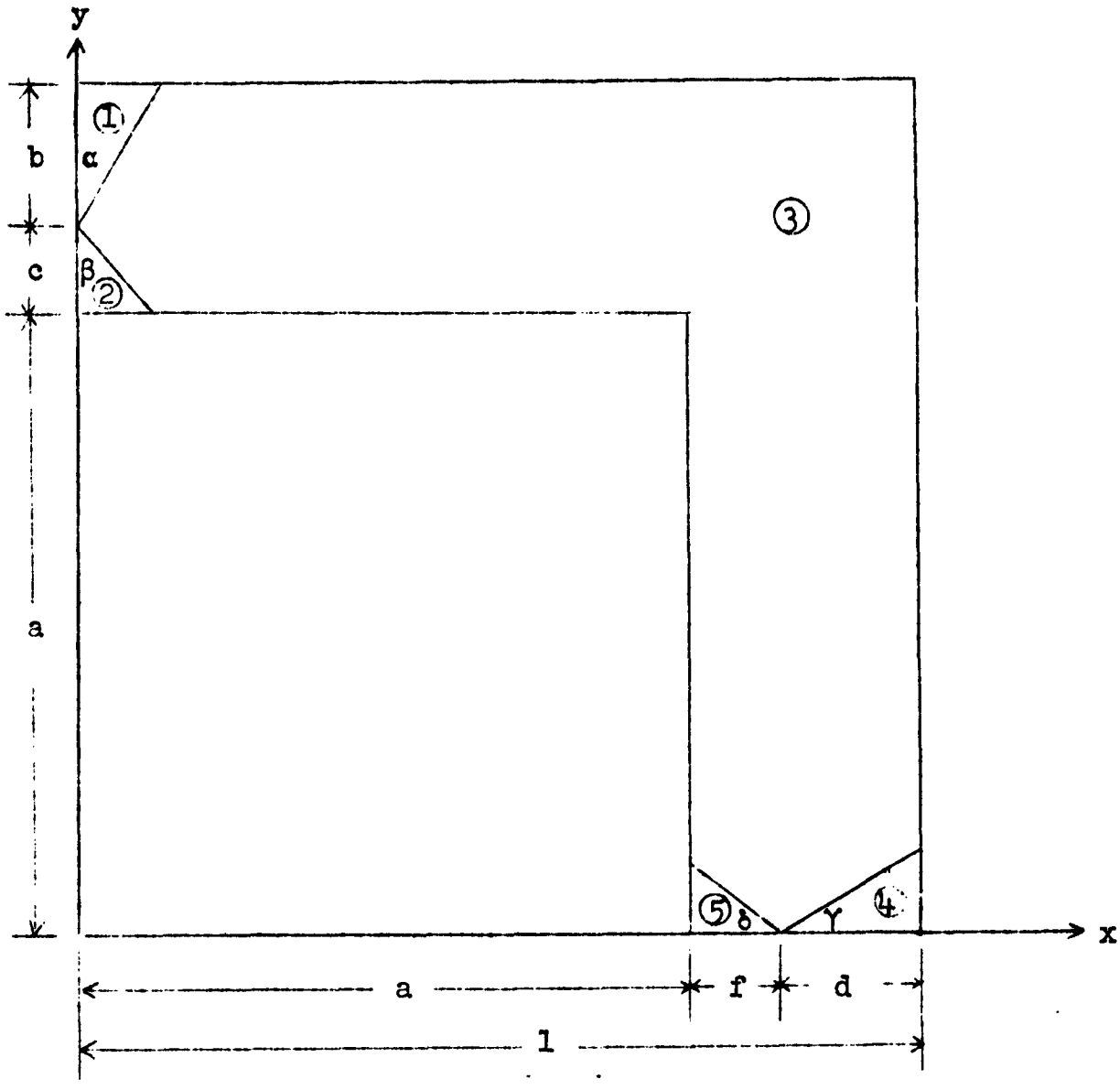

Fig. 13.2

"Bending" velocity field for square slab with square cutout.

part of the material is

$$u = \dot{\theta}\,(y - a - c),\quad v = -\,\dot{\theta}\,(x - a - f). \tag{13.7}$$

In this case, the area of region 1 is

$$A_1 = 1/2\ b^2 \tan \alpha,$$

so that

$$\mathcal{D}_1^{(1)} = k\ h\ \dot{\theta}\ b^2, \tag{13.8}$$

independently of the angle α.

Since we seek the lowest possible upper bound, we generally desire to choose the parameters of a problem so as to minimize the internal and maximize the external energy dissipation rates. Since $\mathcal{D}_1^{(1)}$ is independent of α, we may therefore choose α so as to maximize $\mathcal{D}_e$. In view of Eq. 2.3,

$$\mathcal{D}_e = \int_0^1 2\ k\ \lambda\ h\ v\ d\ x = 2\ k\ \lambda\ h \int_0^1 v\ d\ x \tag{13.9}$$

so that we wish to choose v as large as possible. Since

$$v_1 = -\ \dot{\theta}\ [\tan \alpha\ (y - a - c) - (a + f)\ ]$$

is less than v_3 along the top surface, it is advantageous to make region 1 as small as possible, i.e., to choose the limiting case $\alpha = 0$. Therefore, we may use 13.7 in the entire integral 13.9 to obtain

$$\mathcal{D}_e = 2\ k\ \lambda\ h\ \dot{\theta}\ (a + f - 1/2). \tag{13.10}$$

The total internal energy dissipation rate is given by four terms similar to 13.8:

$$\mathcal{D}_i = k\ h\ \dot{\theta}\ (b^2 + c^2 + d^2 + f^2)$$

$$= k\ h\ \dot{\theta}\ [b^2 + (1 - a - b)^2 + f^2 + (1 - a - f)^2\ ]. \tag{13.11}$$

Therefore an upper bound is given by

$$\lambda \leq \frac{b^2 + (1 - a - b)^2 + f^2 + (1 - a - f)^2}{2a + 2f - 1} \qquad (13.12)$$

for any geometrically admissible choice of b and f.

Since the denominator is independent of b, the best choice is

$$b = \frac{1 - a}{2}$$

which locates the hinge at the midpoint of the section. Therefore, 13.12 becomes

$$\lambda \leq \lambda_o = \frac{1/2(1 - a)^2 + f^2 + (1 - a - f)^2}{2a + 2f - 1} \qquad (13.13a)$$

If $a < 1/3$, the minimum value of λ_o occurs for $f = 1 - a$, i.e., the hinge is at the outer edge. However, for $1/3 < a$, λ_o has a relative minimum at

$$f = 1/2(1 + \sqrt{2 - 4a + 3a^2} - a. \qquad (13.13b)$$

With this value of f, the resulting λ_o represents the best upper bound of the type considered. Figure 13.3 shows that we have obtained an improvement over the result of Sec. 11 for all $a > 1/3$.

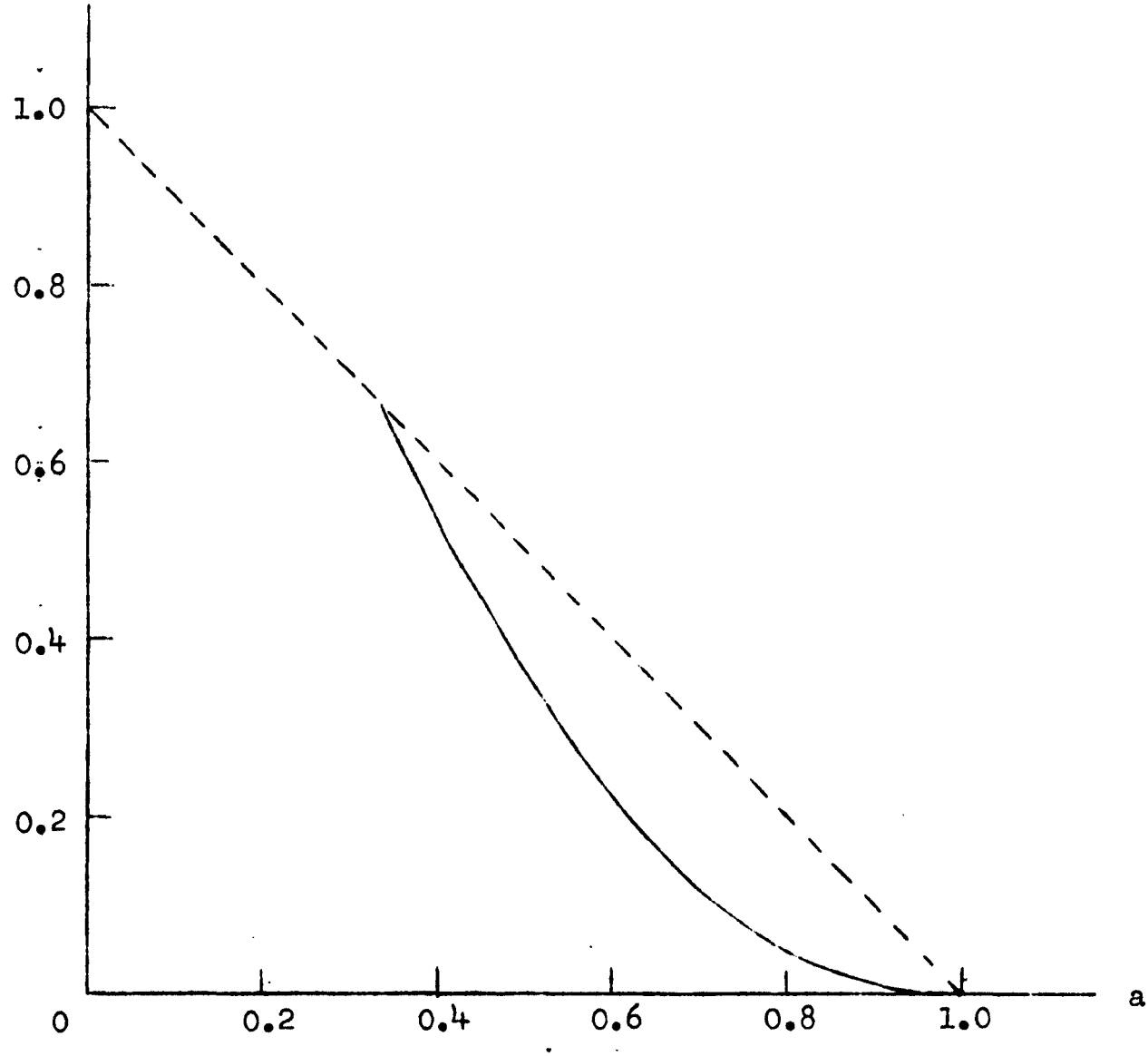

Fig. 13.3

Upeer bounds for square slab with square cutout.

———— bending
---------- sliding out of plane

IV. LOWER BOUNDS FOR WIDE SLABS

14. Discontinuous stress fields [3]. As we have seen in the previous chapter, it is not difficult to construct upper bounds for the yielding of slabs with cutouts. However, the determination of statically admissible stress fields is, in general, more difficult.

In the case where we are concerned primarily with uniform loads on rectangular boundaries, it is often possible to construct a discontinuous stress field consisting of several regions of constant stress separated by straight lines of discontinuity. This approach has also been used for problems in plane strain [14, Sec. 33].

We shall find it convenient to define the stress field in terms of the principal stresses and a representative angle. To this end, let θ be the smallest non-negative angle between the x axis and a principal direction, let s be the principal stress across the element inclined at θ to the x axis, and let r be the other principle stress in the plane of the slab. Let ω be the reduced mean normal stress and χ the reduced principal stress difference:

$$\omega = (r + s)/2k, \qquad \chi = (r - s)/2k. \tag{14.1}$$

Let N and T be the normal and tangential stresses across an element inclined to the x axis at an angle α. In terms of the new variables

$$\frac{N}{k} = \omega - \chi \cos 2(\theta - \alpha), \quad \frac{T}{k} = -\chi \sin 2(\theta - \alpha). \tag{14.2}$$

Across any line of discontinuity, these exterior components of

stress must be continuous, but the remaining interior component of stress may be discontinuous. Thus, if α_{kj} is the angle between the x axis and the straight line of discontinuity separating regions k and j, we must have

$$\begin{aligned} \omega_j - \chi_j \cos 2(\theta_j - \alpha_{kj}) &= \omega_k - \chi_k \cos 2(\theta_k - \alpha_{kj}), \\ \chi_j \sin 2(\theta_j - \alpha_{kj}) &= \chi_k \sin 2(\theta_k - \alpha_{kj}). \end{aligned} \tag{14.3}$$

Any stress field which satisfies 14.3 and the stress boundary conditions will be in equilibrium. If it is to be statically admissible, it must also satisfy the yield condition. In terms of the present variables this may be written

$$\max\left[\left|\frac{r}{2k}\right|, \quad \left|\frac{s}{2k}\right|, \quad |\chi|\right] \leq 1. \tag{14.4}$$

As an example, let us consider a square slab with a square cutout under uniform uniaxial tension. The assumed discontinuous stress field is shown in Fig. 14.1. Symmetry demands that the principal directions in regions 1, 3, and 4 be parallel to the coordinate axes, so that

$$\theta_1 = \theta_3 = \theta_4 = 0. \tag{14.5a}$$

Due to this symmetry we need consider only the first quadrant of the slab. In regions 1, 3, and 4 the stress normal to the boundary must be in equilibrium with the load, so that

$$s_1 = 2k\lambda, \quad s_4 = 0, \quad r_3 = 0. \tag{14.5b}$$

There will be three pairs of Eqs. 14.3 corresponding to the three lines of discontinuity in the first quadrant. Since

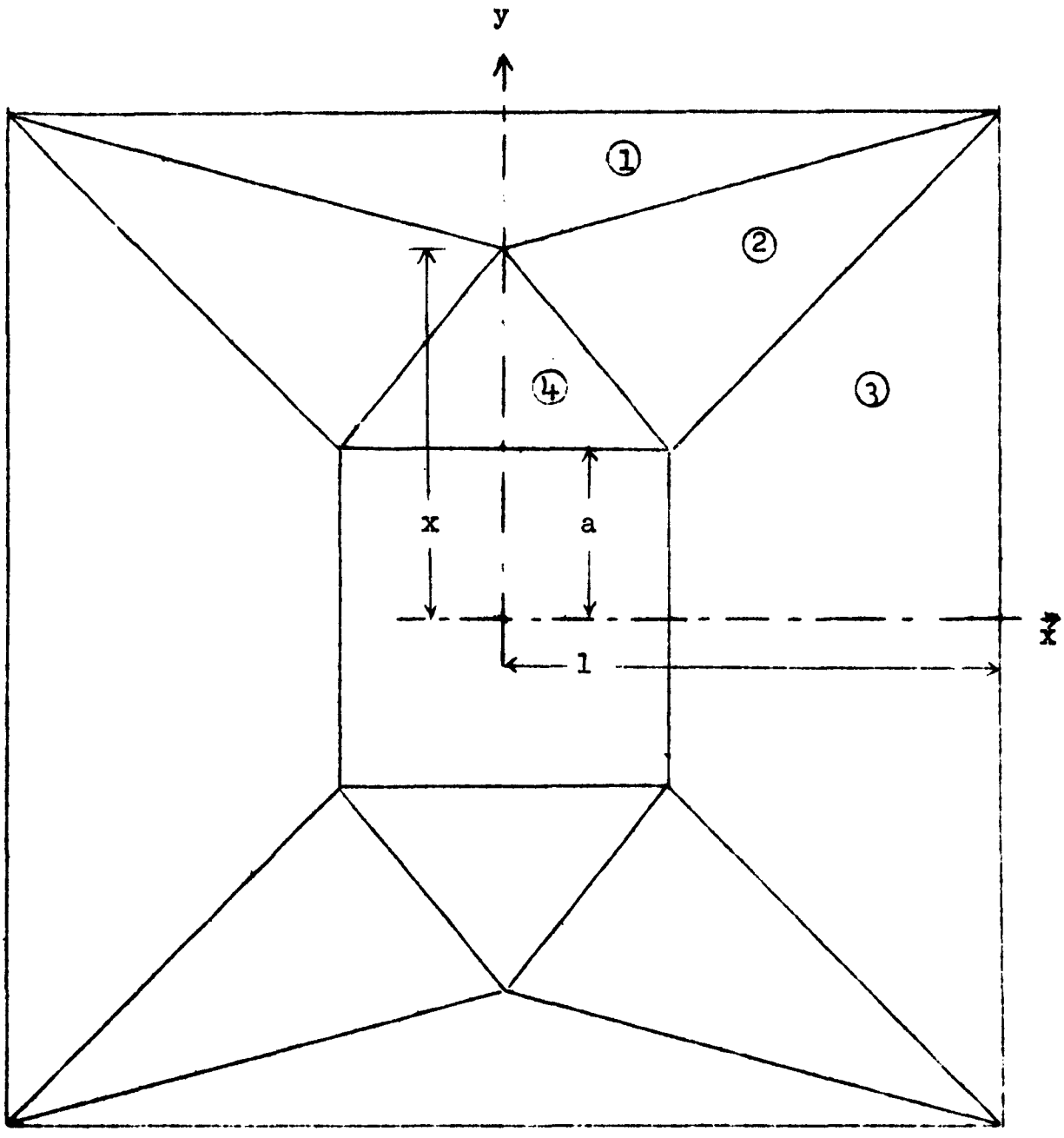

Fig. 14.1

Discontinuous stress fields.

$\alpha_{23} = \pi/4$ these may be written

$$\omega_2 - \chi_2 \cos 2(\theta_3 - \alpha_{12}) = (\frac{r_1}{2k})(1 - \cos 2\alpha_{12}) + \lambda(1 + \cos 2\alpha_{12}),$$

$$\omega_2 - \chi_2 \cos 2(\theta_3 - \alpha_{24}) = (\frac{r_4}{2k})(1 - \cos 2\alpha_{24}),$$

$$\omega_2 - \chi_2 \sin 2\theta_2 = \frac{s_3}{2k}, \qquad (14.6)$$

$$\chi_2 \sin 2(\theta_2 - \alpha_{12}) = (\lambda - \frac{r_1}{2k})\sin 2\alpha_{12},$$

$$\chi_2 \sin 2(\theta_2 - \alpha_{24}) = -(\frac{r_4}{2k})\sin 2\alpha_{24},$$

$$-\chi_2 \cos 2\theta_2 = \frac{s_3}{2k}.$$

The geometry of the stress field is entirely determined by the choice of the parameter x (Fig. 14.1). Indeed, we have

$$\tan \alpha_{12} = 1 - x, \quad \tan \alpha_{24} = 1 - \frac{x}{a}. \qquad (14.7)$$

Therefore, Eqs. 14.6 may be solved for the six unknown quantities in terms of x:

$$\tan 2\theta_2 = \frac{2a}{x},$$

$$\chi_2 = -\frac{\lambda}{1 - a}\frac{\sqrt{x^2 + 4a^2}}{x},$$

$$\omega_2 = \frac{\lambda}{1 - a}[1 - \frac{2a}{x}],$$

$$\frac{r_1}{2k} = \frac{\lambda a}{(1 - a)(1 - x)}, \qquad (14.8)$$

$$\frac{r_4}{2k} = \frac{\lambda a}{(1 - a)(1 - x)},$$

$$\frac{s_3}{2k} = \frac{\lambda}{1 - a}.$$

As a check on the computations it may be verified that the resulting stresses satisfy overall equilibrium requirements across the x and y axes.

The problem, then, is to determine the largest value of λ for which 14.4 will be satisfied in each of the four regions. In each region, that inequality which would be violated for the smallest value of λ will be called the governing inequality. In the present example it may be determined by inspection in each region. The four governing inequalities obtained by substituting 14.8 into 14.4 may then be written

$$\lambda a \leq (1 - a)(1 - x), \tag{14.9a}$$

$$\lambda \sqrt{x^2 + 4a^2} \leq x(1 - a), \tag{14.9b}$$

$$\lambda \leq 1 - a, \tag{14.9c}$$

$$\lambda a \leq (1 - a)(x - a). \tag{14.9d}$$

Since $x/\sqrt{x^2 + 4a^2}$ is always less than 1, Inequality 14.9c is obviously satisfied whenever 14.9b is, so that 14.9 are equivalent to

$$\lambda \leq (1 - a)(1 - x)/a, \tag{14.10a}$$

$$\lambda \leq x(1 - a)/\sqrt{x^2 + 4a^2}, \tag{14.10b}$$

$$\lambda \leq (1 - a)(x - a)/a. \tag{14.10c}$$

Subject to the geometric restriction $a \leq x \leq 1$, we may choose x in 14.10 so as to obtain the maximum possible value of λ. While x may be formally eliminated from the inequalities as in Sec. 6, the resulting functions of λ cannot be handled in closed form.

Therefore, the following procedure seems more appropriate.

The general character of the right-hand sides of 14.10, considered as functions of x in the interval $a \leq x \leq 1$ is independent of a. Thus 14.10a is a straight line falling from $(1 - a)^2/a$ at $x = a$ to 0 at $x = 1$, while 14.10c is a straight line rising from 0 to $(1 - a)^2/a$ in the same interval. Finally, 14.10b is monotonically increasing and positive in $a \leq x \leq 1$. These curves are sketched in Fig. 14.2. We must distinguish two cases depending upon whether curve (b) passes above or below the intersection of (a) and (c). In the former case, we must take x as the intersection of (a) and (c) in order to maximize λ, while in the latter case x is chosen as the intersection of (b) and (c). After some computation [3] we find

$$x = \tfrac{1}{2}(1 + a), \quad \lambda = (1 - a)^2/2a, \qquad \text{if } a > 0.443, \tag{14.11}$$

$$a = \frac{x(1 - x)}{\sqrt{(3x - 2)(2 - x)}}, \quad \lambda = \frac{(1 - a)(1 - x)}{a}, \quad \text{if } a < 0.443.$$

The resulting lower bound on the collapse load is shown in Fig. 14.3. Also shown is the result for biaxial tension which will be obtained in Sec. 18.

15. Stress functions. While the method of discontinuous constant stress fields is easy to apply in a few examples, it does not adapt itself to non-rectangular domains. A second technique, which holds great theoretical promise although an efficient means of exploitation is yet to be found, is to construct a stress function. As is well known, if the stress components are derived from a stress function ψ by means of

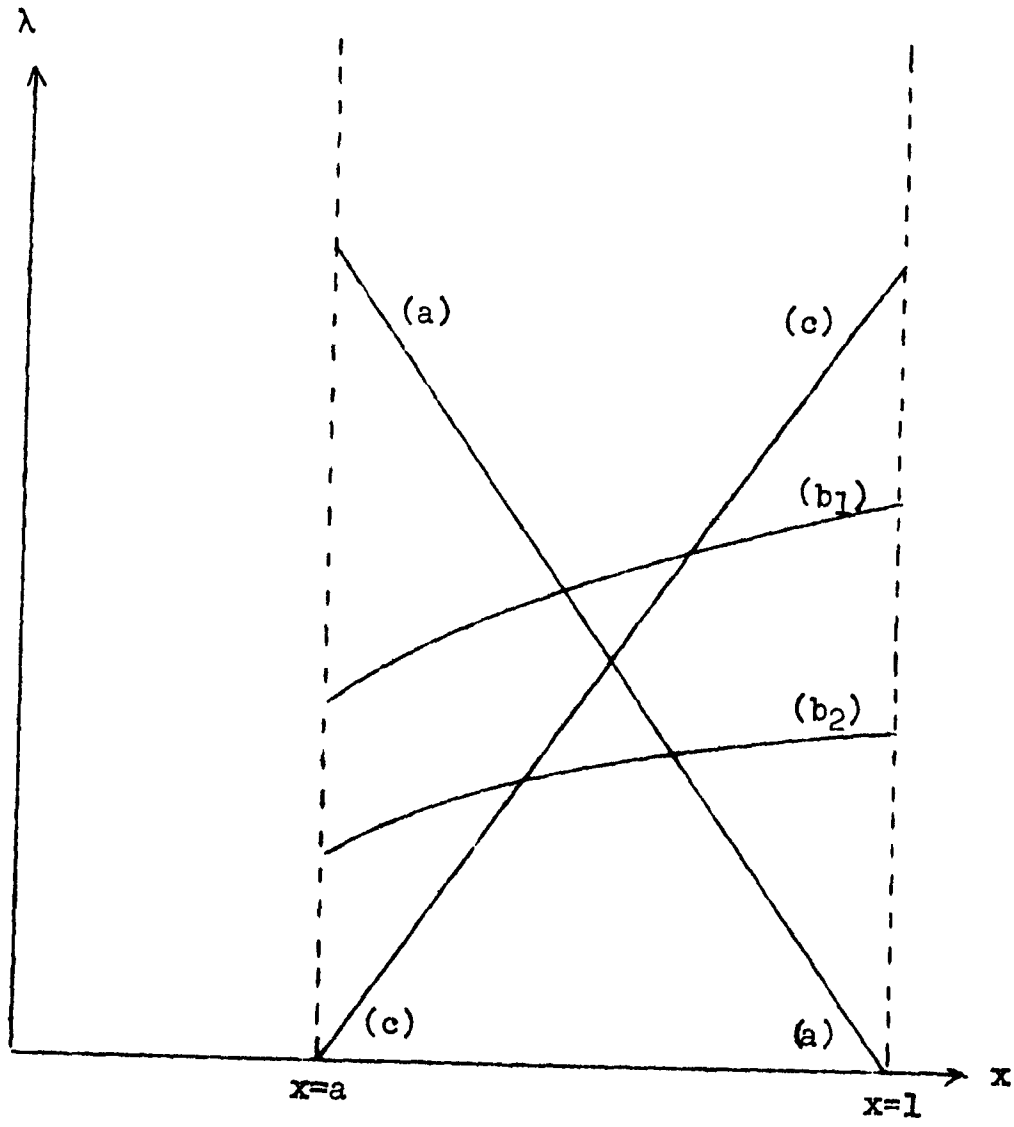

Fig. 14.2

Inequalities 14.10.

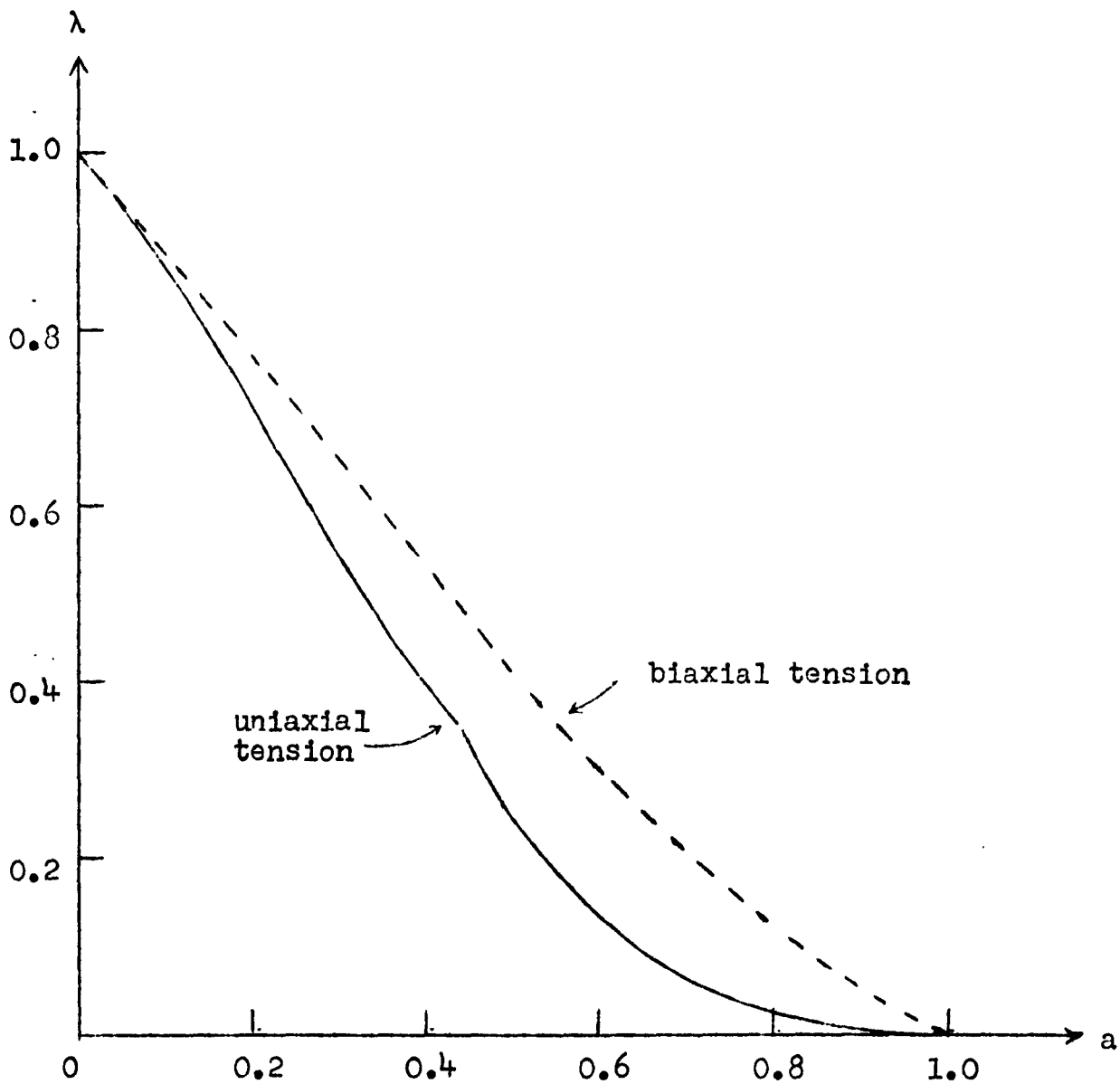

Fig. 14.3

Lower bounds for square slab with square cutout.
——— uniaxial tension
------- biaxial tension

$$\sigma_x = \frac{\partial^2\psi}{\partial y^2}, \quad \sigma_y = \frac{\partial^2\psi}{\partial x^2}, \quad \tau_{xy} = -\frac{\partial^2\psi}{\partial x \partial y}, \tag{15.1}$$

then the equilibrium equations 0.2 are satisfied identically. For the elastic problem, ψ must satisfy the biharmonic equation

$$\nabla^4\psi = \frac{\partial^4\psi}{\partial x^4} + 2\frac{\partial^4\psi}{\partial x^2 \partial y^2} + \frac{\partial^4\psi}{\partial y^4} = 0, \tag{15.2}$$

and the boundary conditions. However, Eq. 15.2 is derived from Hooke's law and does not apply when we seek only a statically admissible stress field. For such a purpose we may choose <u>any</u> function ψ which satisfies the boundary conditions.

Once ψ is chosen, the stress components are determined from 15.1. The principal stresses are then given by [19, Sec. 9]

$$\left.\begin{matrix}\sigma_1 \\ \sigma_2\end{matrix}\right\} = \frac{\sigma_x + \sigma_y}{2} \pm \sqrt{\left(\frac{\sigma_x - \sigma_y}{2}\right)^2 + \tau_{xy}^2}. \tag{15.3}$$

By definitely identifying σ_1 and σ_2 as indicated by the signs in 15.3, the yield condition 1.1 then states that

$$\max[\sigma_1, -\sigma_2, \sigma_1 - \sigma_2] \leq 2k. \tag{15.4}$$

If 15.4 is everywhere satisfied, then the constructed stress field is statically admissible and will furnish a lower bound on the load. More generally, if the load is expressed in terms of the parameter λ, any value of λ which satisfies 15.4 is a lower bound.

The stress function may be used advantageously with other coordinate systems. Thus, in polar coordinates r, θ the stress components defined by

$$\sigma_r = \frac{1}{r}\frac{\partial\psi}{\partial r} + \frac{1}{r^2}\frac{\partial^2\psi}{\partial\theta^2},$$
$$\sigma_\theta = \frac{\partial^2\psi}{\partial r^2}, \qquad (15.5)$$
$$\tau_{r\theta} = -\frac{\partial}{\partial r}\left(\frac{1}{r}\frac{\partial\psi}{\partial\theta}\right),$$

will satisfy the equilibrium equations identically. The principal stress are then given by equations analgous to 15.4:

$$\left.\begin{matrix}\sigma_1\\ \sigma_2\end{matrix}\right\} = \frac{\sigma_r + \sigma_\theta}{2} \pm \sqrt{\left(\frac{\sigma_r - \sigma_\theta}{2}\right)^2 + \tau_{r\theta}^2}. \qquad (15.6)$$

As an example, let us consider the annular slab (Fig. 12.1) for which an upper bound was found in Sec. 12. For uniaxial tension the boundary conditions on the stresses are

$$\begin{aligned} &\text{at } r = a: \quad \sigma_r = 0, \quad \tau_{r\theta} = 0; \\ &\text{at } r = 1: \quad \sigma_r = k\lambda(1 - \cos 2\theta), \quad \tau_{r\theta} = k\lambda \sin 2\theta. \end{aligned} \qquad (15.7)$$

In view of the dependence of the boundary conditions upon θ, we are led to try a stress function of the type

$$\psi = f(r) + g(r)\cos 2\theta \qquad (15.8)$$

where f and g are to be determined. It then follows from 15.5 that the stress components are

$$\sigma_r = \frac{f'}{r} + \frac{rg' - 4g}{r^2}\cos 2\theta,$$
$$\sigma_\theta = f'' + g'' \cos 2\theta, \qquad (15.9)$$
$$\tau_{r\theta} = 2\frac{rg' - g}{r^2}\sin 2\theta,$$

where primes indicate differentiation with respect to r.

Substituting 15.9 into 15.7 we obtain the boundary conditions for f and g:

$$f'(a) = g(a) = g'(a) = 0, \qquad f'(1) = k\lambda, \quad g(1) = \tfrac{1}{2} k\lambda, \quad g'(1) = k\lambda. \tag{15.10a}$$

Next, let us consider possible discontinuous stress fields derived from stress functions. As previously discussed, the normal and tangential stress must be continuous across any curve, but the other normal stress need not be. For the annular slab, 15.8 implies that the stress function is analytic as a function of θ, hence the only possible curve of discontinuity is a circle $r = r_k$. Across such a circle, σ_r and $\tau_{r\theta}$ must be continuous, but σ_θ may exhibit a jump. It follows from 15.9 that f and g must be continuously differentiable but may have discontinuous second derivatives. Thus,

$$f'(r_k^+) = f'(r_k^-), \quad g(r_k^+) = g(r_k^-), \quad g'(r_k^+) = g'(r_k^-). \tag{15.11}$$

Subject to Eqs. 15.10 and 15.11, we can choose any functions f and g. Once these are chosen, the principal stresses are determined by 15.9 and 15.6 and λ is then taken to be the largest number such that the yield inequality 15.4 is valid at all points of the slab.

The difficulty with using the method described above is that even when the functions f and g are chosen as simply as possible so as to satisfy the boundary conditions 15.10, the resulting values of σ_1 and σ_2 become quite complicated, so that an analysis in closed form becomes impossible. In the remaining sections of this chapter we shall indicate two possible methods of alleviating this situation which are currently being investigated.

16. Numerical techniques.[16.1] As indicated in the previous section, even a simple choice of the functions f and g in Eq. 15.8 will lead to a complicated function of r and θ when substituted into the yield condition 15.4. To obtain a lower bound for the load, it is necessary to find that point in the slab where the left hand side of 15.4 achieves its maximum. However, for complex functions this cannot be done in closed form and it becomes necessary to use numerical techniques.

A primary disadvantage of numerical methods is that a separate problem must be solved for each value of the cutout radius a. However, if an efficient means of utilizing modern high-speed computing machines can be devised, this drawback becomes less serious.

In the present section we shall discuss some preliminary steps which have been made in this connection, and indicate possible extensions. The problem has only recently been looked into, and the results and suggestions are purely tentative. Indeed, it is impossible to say whether such techniques will ever prove useful.

As a first step, let us replace f and g in Eq. 15.8 by two new functions each, defined by

$$\begin{aligned} f'(r) &= k\lambda A(r)[1 + (1 - r)B(r)], \\ g(r) &= k\lambda C(r)[1 + (1 - r)^2 D(r)]. \end{aligned} \tag{16.1}$$

Substituting 16.1 into the boundary conditions 15.10, we see that

---

16.1 The results of this section were obtained by E. Levin.

B and D are entirely arbitrary (provided, of course, that they remain finite throughout the slab), and that A and C must be such that

$$A(a) = C(a) = C'(a) = 0,$$
$$A(1) = 1, \quad C(1) = \tfrac{1}{2}, \quad C'(1) = 1. \tag{16.2}$$

For any A and C satisfying 16.2, we express successively the stress function ψ (Eq. 15.8), the stress components σ_r, σ_θ, $\tau_{r\theta}$ (Eqs. 15.5), the principal stresses σ_1, σ_2 (Eq. 15.6), and the yield condition (15.4) in terms of the four functions A, B, C, D and the angle θ. The result will be three inequalities which may be written

$$\lambda F_1[A, B, C, D; \theta] \leq 2,$$
$$\lambda F_2[A, B, C, D; \theta] \leq 2, \tag{16.3}$$
$$\lambda F_3[A, B, C, D; \theta] \leq 2.$$

The constant λ must be such that all three Inequalities 16.3 are satisfied at each point of the slab. Any choice of the functions A, B, C, D, together with sufficient computations, will furnish such a λ. The problem then is to choose A, B, C, D so as to obtain the largest possible value of λ.

Without going into the details of computation, it is evident that since σ_θ depends upon the second derivative of f and g, the values of F_1, F_2, and F_3 will depend upon B and D, even on the boundaries r = a, r = 1. However, a minor change in the definitions 16.1 will eliminate this. Let us, then, replace 16.1 by the definitions

$$f'(r) = k\lambda A(r)[1 + (1 - r)^2(r - a)B(r)],$$
$$g(r) = k\lambda C(r)[1 + (1 - r)^3(r - a)D(r)]. \qquad (16.4)$$

The advantage of this is if A and C can once be chosen so that the maximum value of $2kF_i$ on the boundaries appears to give a reasonable value for λ, an attempt can be made to adjust low values of F_i in the interior by manipulating B and D. Therefore, in deciding upon the "best" functions A and C, it is necessary to consider only values at the boundaries r = a, r = 1.

At the inner boundary r = a, it follows from the boundary conditions that σ_r and τ are both zero, so that the yield inequality becomes

$$|\sigma_\theta| \leq 2k.$$

Replacing σ_θ at r = a by its value in terms of A and C, we obtain

$$-2 \leq \lambda(A' + C'' \cos 2\theta) \leq 2. \qquad (16.5)$$

Inequality 16.5 represents a necessary restriction on A and C. Since the middle member is linear in cos 2θ, the extreme values are at θ = 0 and θ = π/2. If the assumed stress field is to be at all close to the actual one, σ_θ will be algebraically greater at θ = 0 than at θ = π/2, so that C should be positive at r = a.

As an example, let us consider the particular case $a = \frac{1}{3}$, and take simple polynomials satisfying the boundary conditions:

$$A = \tfrac{1}{2}(3r - 1), \quad B = 0, \quad D = 0,$$
$$C = (3r - 1)^2(2 - r)/8. \qquad (16.6)$$

Since only a preliminary analysis is intended, the resulting

functions F_k are evaluated numerically for a coarse mesh in r and θ. The results on the boundaries are given in Table 16.1

	θ	0	30°	45°	60°	90°
r = a	Max F_i	5.25	3.38	1.50	0.38	2.25
r = 1	F_1	0.75	1.84	2.06	1.77	0.25
	F_2	0.75	1.73	2.28	2.57	2.25
	F_3	0	0.11	-0.22	-0.80	-2.00

Table 16.1

Values of max F_i on the boundary for Eq. 16.6.

Since the maximum value of F occurs at the inner boundary at $\theta = 0$, it follows from 16.3 that a <u>necessary</u> restriction on λ is

$$\lambda \leq \frac{2}{5.25} = 0.38. \qquad (16.7)$$

That this stress field cannot furnish a "good" lower bound can be seen as follows. Actual plastic yielding cannot take place until a plastic region extends continuously from at least one point on the inner boundary to at least one point on the outer boundary, since otherwise there will be a determinate elastic structure remaining which can sustain a greater load. A <u>necessary</u> condition that this be the case is that max F_i has the same value on both the inner and outer boundaries, which is far from the case in Table 16.1.

Therefore, as an improvement, let us keep the same value of C, but take A identically zero on the inner boundary.

Thus, let

$$A = (3r - 1)^2/4, \quad B = 0, \quad D = 0, \qquad C = (3r - 1)^2(2r - 1)/8. \tag{16.8}$$

The values on the boundaries are then given in Table 16.2.

	θ	0°	30°	45°	60°	90°
r = a	max F_i	3.75	1.88	0	1.88	3.75
	F_1	2.25	2.74	2.83	2.55	1.75
	F_2	2.25	2.93	3.41	3.71	3.75
	F_3	0	-0.19	-0.59	-1.16	-2.00

Table 16.2

Values of max F_i on the boundary for Eq. 16.8.

In this case, the maximum boundary value of 3.75 occurs on the inner boundary at $\theta = 0^\circ$ and $\theta = 90^\circ$, and occurs on the outer boundary at $\theta = 90^\circ$. The corresponding necessary restriction on λ is

$$\lambda \leq \frac{2}{3.75} = 0.53. \tag{16.9}$$

In Sec. 12 an upper bound for this problem was obtained. Setting $a = \frac{1}{3}$ in Eq. 12.17 (or reading from Fig. 12.2) we find that $\lambda = 0.59$ is an upper bound. Since 16.9 is reasonably close to that upper bound it would appear that we have obtained a reasonably close solution <u>on the boundary</u>.

However, 16.9 is only an upper bound on the lower bound. To obtain a true lower bound for the assumed function, we must compute max F_i throughout the slab. The results are shown in Table 16.3.

r \ θ	0°	30°	45°	60°	90°
1/3	3.75	1.88	0	1.88	3.75
1/2	3.38	3.52	3.56	3.08	1.88
2/3	3.30	3.80	3.92	3.26	0.56
5/6	2.63	4.70	5.11	4.34	1.88
1	2.25	2.93	3.41	3.71	3.75

Table 16.3

Values of max F_i in slab for Eqs. 16.8.

The maximum value for the mesh considered is 5.11, occurring at $r = \frac{5}{6}$, $\theta = 45°$. Therefore, it follows from 16.3 that

$$\lambda \leq 0.39. \qquad (16.10)$$

The next logical step is to keep the values for A and C given by Eqs. 16.8, and to try non-zero values for B and D in an attempt to reduce some of the high values in the interior. Due to limitations of time, we are unable to include any further results of this technique in the present report.

It should be pointed out that 16.10 represents only a crude approximation, due to the large mesh size used. However, it appears reasonable to use a large mesh to obtain information as to "good" functions A, B, C, and D. Once this is done, the results should be computed for a much smaller mesh to obtain a more precise location and valuation of the maximum value of F_i.

17. Approximate yield conditions. An alternative to a completely numerical approach to a statically admissible stress field is to consider an approximation to the yield condition sufficiently simple so that analytic techniques may be employed. It follows from Eqs. 15.6 and 15.4 that the actual yield condition consists of the three inequalities

$$u + \sqrt{v^2 + \tau^2} \leq 2k, \tag{17.1a}$$

$$-u + \sqrt{v^2 + \tau^2} \leq 2k, \tag{17.1b}$$

$$\sqrt{v^2 + \tau^2} \leq k, \tag{17.1c}$$

where we have introduced the notations

$$u = (\sigma_r + \sigma_\theta)/2, \qquad v = (\sigma_r - \sigma_\theta)/2. \tag{17.2}$$

If we sketch the surfaces represented by the equality signs in 17.1 in a Cartesian space with coordinates u, v, and τ, we obtain a surface which may be described as follows. The u axis is an axis of rotation; for $|u| \leq k$ the surface is a cylinder of radius k; for $k \leq |u| \leq 2k$ the surface is a pair of right circular cones capping either end of the cylinder with vertices at $u = \pm 2k$. The first octant of such a surface is sketched in Fig. 17.1.

Since we are concerned with finding a lower bound on the yield load, we shall consider only approximations to Fig. 17.1 which lie wholly within the actual yield surface. If this is done, then any lower bound obtained using an approximate yield condition will be a true lower bound for the problem.

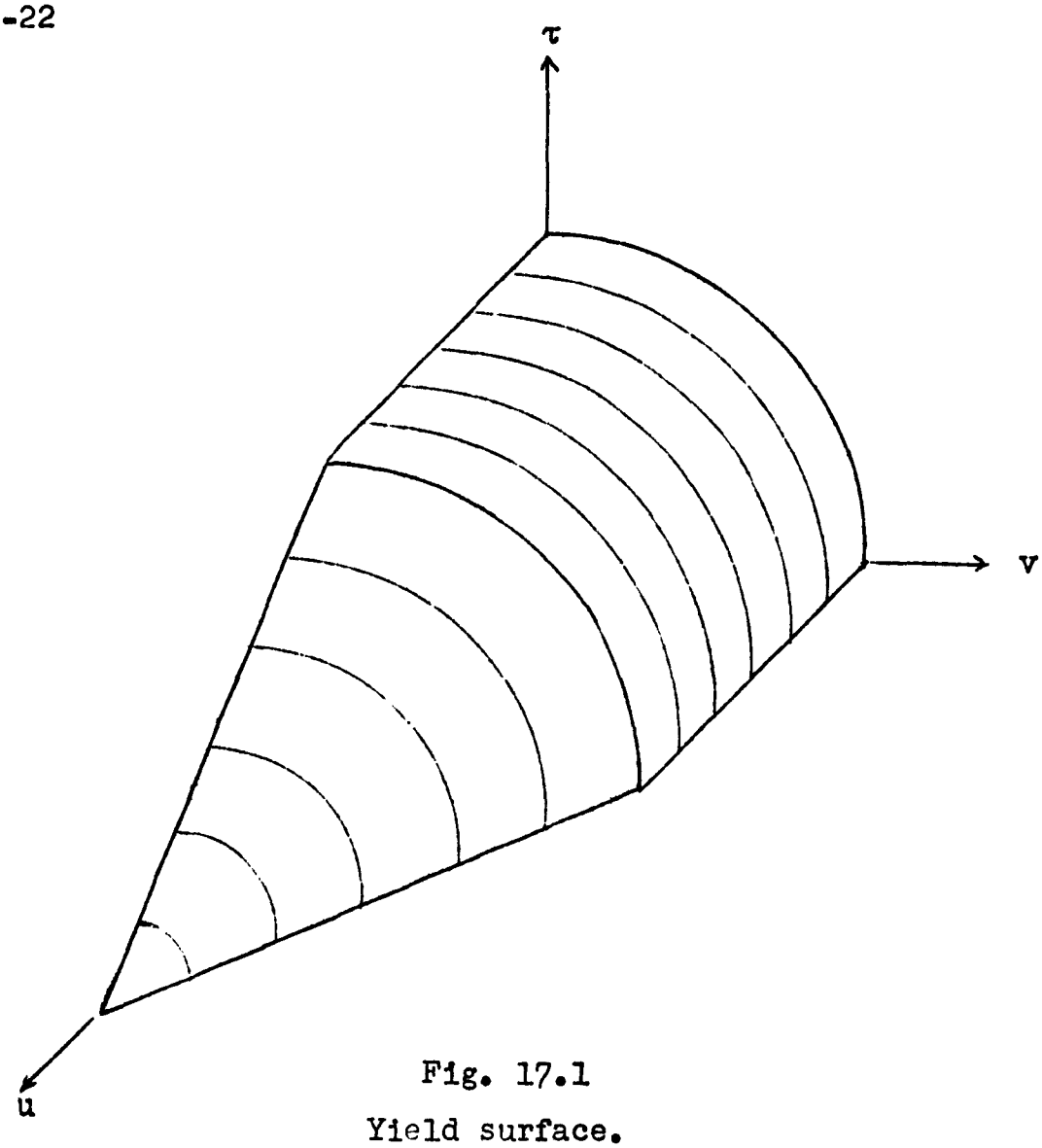

Fig. 17.1
Yield surface.

The difficulty with using the actual yield condition is primarily due to the fact that the stresses contain both sin 2θ and cos 2θ (see Eqs. 15.9) and hence by the time θ is eliminated, the resulting functions of r have become quite complex. Therefore, we seek an approximation which will simplify the dependence on θ. Since τ is the only stress component which contains sin 2θ, while u and v contain only cos 2θ, we would like to separate 17.1 into inequalities containing only τ and those not containing τ. Geometrically, this means that we wish to inscribe a right cylinder or prism with generators parallel to the τ axis in

Fig. 17.1.

As the simplest such inscribed prism, consider a hexagonal prism oriented the same as the trace of the true yield surface in the u,v plane and bounded by the planes $\tau = \pm k/\sqrt{2}$. Analytically this is described by the inequalities

$$|\tau| \leq k/\sqrt{2}\ , \quad |v| \leq k/\sqrt{2}, \qquad (17.3)$$

$$\sigma_r \leq (2 - \tfrac{1}{\sqrt{2}})k, \quad \sigma_\theta \leq (2 - \tfrac{1}{\sqrt{2}}\ k).$$

The choice of $k/\sqrt{2}$ as the height of the above prism was entirely arbitrary and there is no assurance that it will produce a reasonable approximation. To obtain a better approximation, let us consider separately the cylindrical and conical portions of the yield surface. In the cylindrical portion (Eq. 17.1c), it is sufficient to let τ and v satisfy

$$|v| = k \cos\beta, \quad |\tau| \leq k \sin\beta. \qquad (17.4)$$

In the most general case, β can be a function of r and θ, but such generality would destroy the simplicity desired. A reasonable basis for choice would be to divide the slab into a finite number of regions. In each such region let the numerically largest values of v and τ be denoted by $k\lambda v_n$ and $k\lambda\tau_n$ respectively. In each region, β is then chosen so that the two inequalities 17.4 are equally restrictive. Thus, for the correct choice of β

$$k\lambda v_n = k \cos\beta, \quad k\lambda\tau_n = k \sin\beta,$$

hence β is given by

$$\beta = \tan^{-1} \frac{v_n}{\tau_n}\ , \qquad (17.5a)$$

and the cut-out factor must satisfy

$$\lambda \leq \sin \beta/\tau_n. \tag{17.5b}$$

In the conical section, we construct an approximating prism by first inscribing a pyramid in the cone, and then a prism in the pyramid. Since, in the only examples considered thus far the most restrictive part of the yield condition corresponds to the cylinder, the weaker approximation under the cone appears reasonable. Analytically, then, we note that 17.1a, b will both be satisfied if

$$|u| + |v| + |\tau| \leq 2k.$$

Therefore, we demand that

$$|u| + |v| \leq 2k\alpha, \quad |\tau| \leq 2k(1 - \alpha). \tag{17.6}$$

The parameter α is determined in the same way as the parameter β in Eq. 17.4. In particular, if α is constant throughout some region, then

$$\alpha = \frac{u_n + v_n}{u_n + v_n + \tau_n}, \tag{17.7a}$$

and

$$\lambda \leq \frac{2\alpha}{u_n + v_n}. \tag{17.7b}$$

If Eqs. 15.9 are substituted into 17.3, each of the resulting inequalities are linear in either sin 2θ or cos 2θ. Since all inequalities must be satisfied for all values of θ, it is thus necessary and sufficient to satisfy them at the extreme values. Therefore, the quantities u_n, v_n, τ_n appearing in Eqs. 17.5 and 17.7 are independent of θ.

Let us assume for simplicity that each of the regions is a complete annulus. In terms of the functions f and g

appearing in Eqs. 15.9, we then have

$$|v_n| = \frac{1}{2}\left|\frac{f'}{r} - f''\right| + \frac{1}{2}\left|g'' - \frac{g'}{r} + 4\frac{g}{r^2}\right|,$$

$$|\tau_n| = \left|\frac{2g'}{r} - \frac{2g}{r^2}\right|, \qquad (17.8)$$

$$u_n + v_n = \max\left[\left|\frac{f'}{r}\right| + \left|\frac{4g}{r^2} - \frac{g'}{r}\right|, \quad |f''| + |g''|\right].$$

The possibility of investigating the annular slab by these approximate yield conditions is only now being investigated. Unfortunately time has not permitted the inclusion of any examples of the technique illustrated by Eqs. 17.4 through 17.8. In the only example worked out so far by means of Eqs. 17.3 (see Sec. 21), the resulting lower bound is disappointingly low. However, at least part of the reason appears to be due to the choice of stress function, rather than to the use of an approximate yield condition. Further investigations of this approach are being undertaken and will be reported on elsewhere.

V. EXAMPLES

18. Square slab with square cutout. We have already considered this problem in uniaxial tension in Secs. 13 and 14. Therefore, it follows from Sec. 3 that we need only find a lower bound in equal biaxial tension in order to find a bound under any loading. As in the case of uniaxial tension, it is useful to consider a piecewise constant stress field, as shown in Fig. 18.1. Due to symmetry, it is here necessary only to consider one-eighth of the slab. Thus we seek to determine the stresses in regions 1, 2, and 3 of Fig. 18.1. Symmetry at once determines the value of θ in each region:

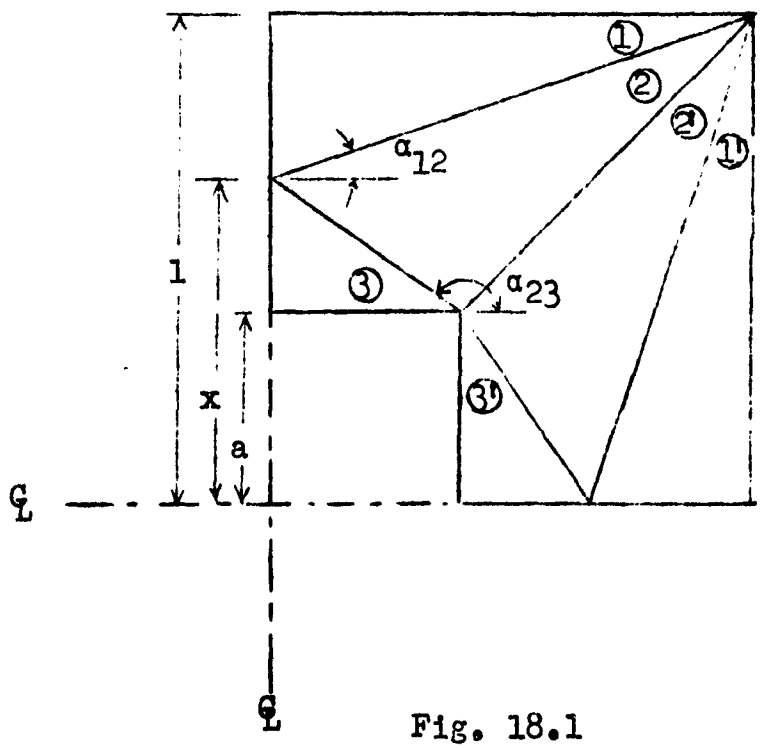

Fig. 18.1

Square slab in biaxial tension.

$$\theta_1 = \theta_3 = 0, \quad \theta_2 = \frac{\pi}{4}, \tag{18.1}$$

while the boundary conditions show immediately that

$$s_1 = 2k\lambda, \quad s_3 = 0. \tag{18.2}$$

Applying Eqs. 14.3 to each of the two lines of discontinuity and using 18.1 and 18.2 we obtain

$$\begin{aligned}
(\tfrac{r_1}{2k})(1 - \cos 2\alpha_{12}) + \lambda(1 + \cos \alpha_{12}) &= \omega_2 - \chi_2 \sin 2\alpha_{12}, \\
(\tfrac{r_2}{2k})(1 - \cos 2\alpha_{23}) &= \omega_2 - \chi_2 \sin 2\alpha_{23}, \\
(\lambda - \tfrac{r_1}{2k})\sin 2\alpha_{12} &= \chi_2 \cos 2\alpha_{12}, \\
-(\tfrac{r_3}{2k})\sin 2\alpha_{23} &= \chi_2 \cos 2\alpha_{23}.
\end{aligned} \tag{18.3}$$

These equations are easily solved for the four unknown quantities, the results being

$$\chi_2 = -\frac{2\lambda}{\tan \alpha_{13} - \tan \alpha_{23}}, \quad \omega_2 = -\frac{2\lambda \tan \alpha_{23}}{\tan \alpha_{12} - \tan \alpha_{23}}, \tag{18.4}$$

$$\frac{r_1}{2k} = \lambda \frac{1 - \tan \alpha_{12} \tan \alpha_{23}}{\tan \alpha_{12}(\tan \alpha_{12} - \tan \alpha_{23})}, \quad \frac{r_3}{2k} = \lambda \frac{1 - \tan^2 \alpha_{23}}{\tan \alpha_{23}(\tan \alpha_{12} - \tan \alpha_{23})}.$$

The two angles appearing in 18.4 are not independent, but may both be expressed in terms of the cutout half-side and the parameter x. Thus, from Fig. 18.1,

$$\tan \alpha_{12} = 1 - x, \quad \tan \alpha_{23} = -(x - a)/a. \tag{18.5}$$

Substituting 18.5 into 18.4 we obtain

$$\chi_2 = \frac{-2\lambda a}{(1-a)x}, \qquad \omega_2 = 2\lambda \frac{x-a}{(1-a)x},$$

$$\frac{r_1}{2k} = \lambda \frac{1-x+a}{(1-x)(1-a)}, \qquad \frac{r_3}{2k} = -\lambda \frac{2a-x}{(x-a)(1-a)}. \tag{18.6}$$

The value of λ must now be determined so that all of 14.4 are valid. The governing inequality in regions 2 and 3 may depend upon the values of x and a, so that on first analysis we must solve the following five inequalities:

$$\frac{r_1}{2k} = \lambda \frac{1-x+a}{(1-x)(1-a)} \leq 1, \tag{18.7a}$$

$$\frac{r_3}{2k} = \lambda \frac{x-2a}{(x-a)(1-a)} \leq 1, \tag{18.7b}$$

$$-\frac{r_3}{2k} = \lambda \frac{2a-x}{(x-a)(1-a)} \leq 1, \tag{18.7c}$$

$$\frac{s_2}{2k} = \frac{\lambda}{1-a} \leq 1, \tag{18.7d}$$

$$-\frac{\chi_2}{2k} = \frac{2\lambda a}{x(1-a)} \leq 1. \tag{18.7e}$$

It is convenient to distinguish two cases, depending upon the sign of x - 2a. If x - 2a is positive, it is evident that all of 18.7 will be valid if 18.7a is. However, the largest λ allowable by 18.7a occurs for the smallest allowable x, which in this case is x = 2a. Since this case can also be considered under the hypothesis that x - 2a is non-positive, it suffices to examine 18.7 for

$$x - 2a \leq 0.$$

Inequalities 18.7b and 18.7d are then obviously valid if the others are, so that we seek the largest λ such that

$$\lambda \leq \begin{cases} \dfrac{(1-a)(1-x)}{1-x+a}, & (18.8a) \\ \dfrac{x}{2a}, & \\ \dfrac{(1-a)(x-a)}{2a-x}. & (18.8c) \end{cases}$$

Considering the right hand sides of 18.8 as functions of x, it is evident that all three are monotone and positive in the interval $a \leq x \leq \min(2a, 1)$ under consideration. Since the right hand sides of 18.8a and 18.8c are decreasing functions of x, while 18.8b is increasing, the situation may be discussed qualitatively as in the case of uniaxial tension, Fig. 14.2. The optimum choice for x will be the intersection of 18.8b with either 18.8a or 18.8c, whichever yields the lower value of λ. After some computation it can be verified that

$$x = \tfrac{1}{2}\left[1 + 2a - \sqrt{(1-a)^2 + a^2}\,\right],$$

$$\lambda = \frac{1}{1-a}\left[\sqrt{(1-a)^2 + a^2} - a\right],$$

$$\text{for } \tfrac{1}{7}(\sqrt{8} - 1) \leq a \leq 1; \qquad (18.9)$$

$$x = \tfrac{1}{2}\left[1 + 3a - \sqrt{(1-a)^2 + 8a^2}\right],$$

$$\lambda = \frac{1}{4a}\left[1 + 3a - \sqrt{(1-a)^2 + 8a^2}\right],$$

$$\text{for } 0 \leq a \leq \tfrac{1}{7}(\sqrt{8} - 1).$$

The resulting function of λ is shown as the dashed curve in Fig. 14.3. Since the solid curve, representing the lower bound in uniaxial tension is everywhere below this curve, it follows that the lower bound obtained in Sec. 14 (Eqs. 14.11)

is safe for any loading.

In Fig. 18.2 we have redrawn this lower bound, together with the upper bound determined in Sec. 13 (Eqs. 13.13). For $a < \frac{1}{3}$, a better upper bound is given by the method of Sec. 11. Setting $T_y = 1$, $a_0 = a$ in Eq. 11.3 the latter becomes

$$\lambda \leq 1 - a. \tag{18.10}$$

Therefore, for a given value of a, the cutout factor λ must lie in the narrow region between the two groups of curves in Fig. 18.2. For practical purposes, we would appear to have solved this example to a reasonable degree of accuracy.

19. Square slab with a slit [5]. In the previous example we were able to obtain a lower bound very close to the upper bound by using a piecewise constant stress field. In the case of a square slab with a slit we can do even better than that and obtain the actual yield load.

The discontinuous stress field for uniaxial tension is shown in Fig. 19.1. The method of solution is similar to that used in Sec. 14 and the results are as follows (for details of the computations see [5]):

$$\begin{aligned}
&\theta_1 = 0, \quad s_1 = 2k\lambda, \quad r_1 = 2k\lambda a/(1 - x), \\
&\tan 2\theta_2 = 2a/[x + a(1 - a)], \\
&\omega_2 = \lambda[x - a(1 - a)]/[a + x(1 - a)], \\
&\chi_2 = -\lambda \left\{ [x + a(1 - a)]^2 + 4a^2 \right\}^{1/2}/[a+x(1-a)], \\
&\theta_3 = 0, \quad r_3 = 0, \quad s_3 = 2k\lambda/(1 - a), \\
&\theta_4 = 0, \quad s_4 = 0, \quad r_4 = -2k\lambda a/x.
\end{aligned} \tag{19.1}$$

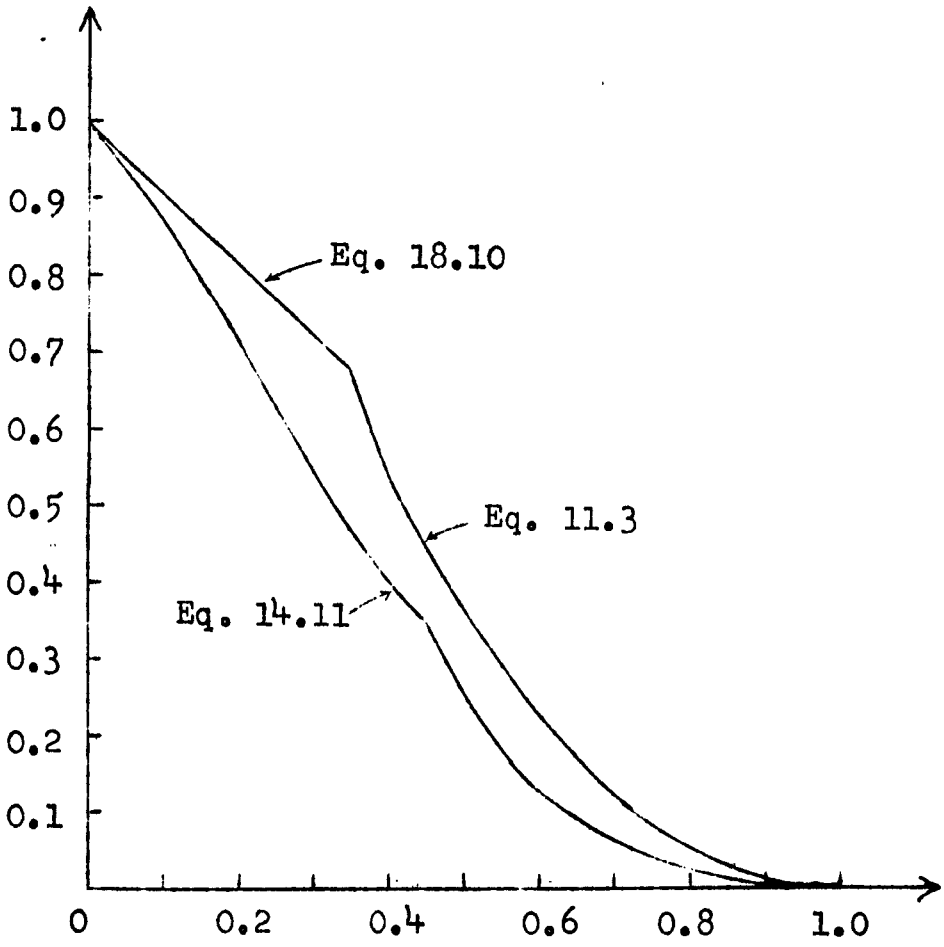

Fig. 18.2

Upper and lower bounds
on yield load of square slab
with square cutout.

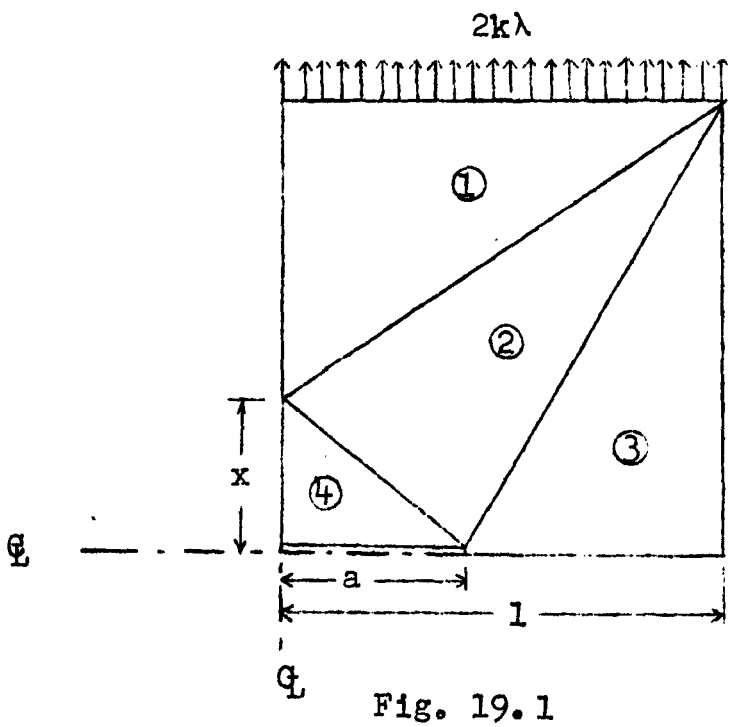

Fig. 19.1

Square slab with a slit-uniaxial tension.

Substituting 19.1 into 14.4 and determining the governing inequality in each region we obtain finally

$$\begin{aligned} &\lambda a \le 1 - x, \\ &\lambda\sqrt{[x + a(1 - a)]^2 + 4a^2} \le a + x(1 - a), \\ &\lambda \le 1 - a, \\ &\lambda a \le x. \end{aligned} \tag{19.2}$$

It is readily verified that if we choose

$$x = 1 - a + a^2, \tag{19.3}$$

then $$\lambda = 1 - a \tag{19.4}$$

will satisfy all of 19.2 so that 1 - a is a lower bound on the yield load.

That 1 - a is also an upper bound for uniaxial tension follows from the analysis of Sec. 11, provided we assume the idealized "slit" to be equal in width to the thickness of the slab.

Since the slab is not symmetric with respect to its diagonals, we must consider both biaxial tension and uniaxial tension in the x direction in order to show that 1 - a is the cutout factor. The latter is trivially true since in this case the slit has no effect and the slab would support a load $\lambda = 1$. The case of biaxial tension can be handled with a piecewise constant stress field as in the previous example (see [5]). However, it is interesting to construct an entirely different statically admissible stress field as follows.

We divide the slab into three regions as indicated in Fig. 19.2. The region interior to a circle of radius a (region 1) we take to be stress free, while the regions exterior to a unit circle (regions 3) are assigned the equal biaxial stress field.

$$\sigma_x = \sigma_y = \sigma_r = \sigma_\theta = 2k\lambda, \quad \tau = 0 \tag{19.5}$$

Region 2 adapts itself naturally to polar coordinates, and we consider the stress field

$$\begin{aligned} \sigma_r &= 2k\lambda(1 - a/r)/(1 - a), \\ \sigma_\theta &= 2k\lambda/(1 - a), \quad \tau_{r\theta} = 0. \end{aligned} \tag{19.6}$$

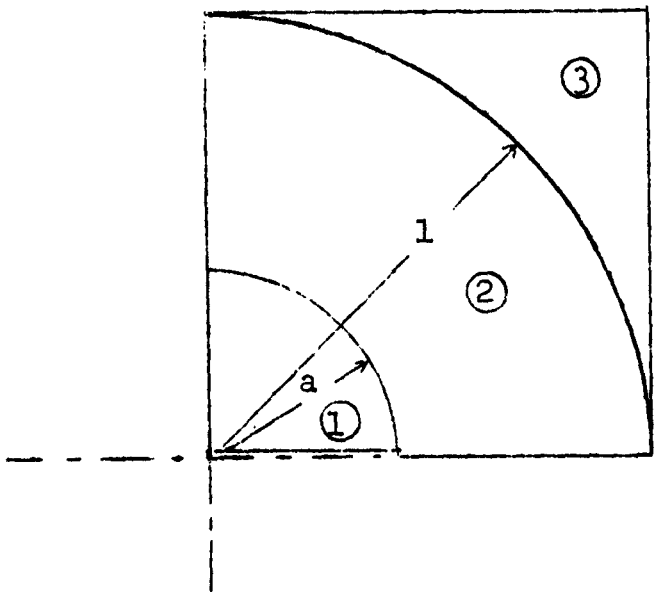

Fig. 19.2

Square slab with a slit-biaxial tension.

Observe that 19.6 furnishes continuous tractions with the stress fields in regions 1 and 3, and satisfies the equilibrium equation

$$\frac{d}{dr}(r\sigma_r) - \sigma_\theta = 0 \qquad (19.7)$$

in region 2. It remains only to satisfy the yield condition 1.1. Since the principle stresses are in the coordinate directions and satisfy

$$\sigma_\theta \geq \sigma_r \geq 0, \qquad (19.8)$$

this means that we require

$$\sigma_\theta = 2k\lambda/(1 - a) \leq 2k, \qquad (19.9)$$

or

$$\lambda \leq 1 - a \qquad (19.10)$$

in agreement with 19.4.

The preceding types of stress and velocity fields can also be applied to slits in rectangular slabs. If the direction perpendicular to the slit is the longer dimension, we again obtain $\lambda = 1 - a$ as the cutout factor. Indeed, the same upper bound applies as before, while a statically admissible stress field may be constructed as indicated in Fig. 19.3. Region 1 is constant stress

$$\sigma_x = 0, \quad \sigma_y = 2k\lambda, \quad \tau_{xy} = 0$$

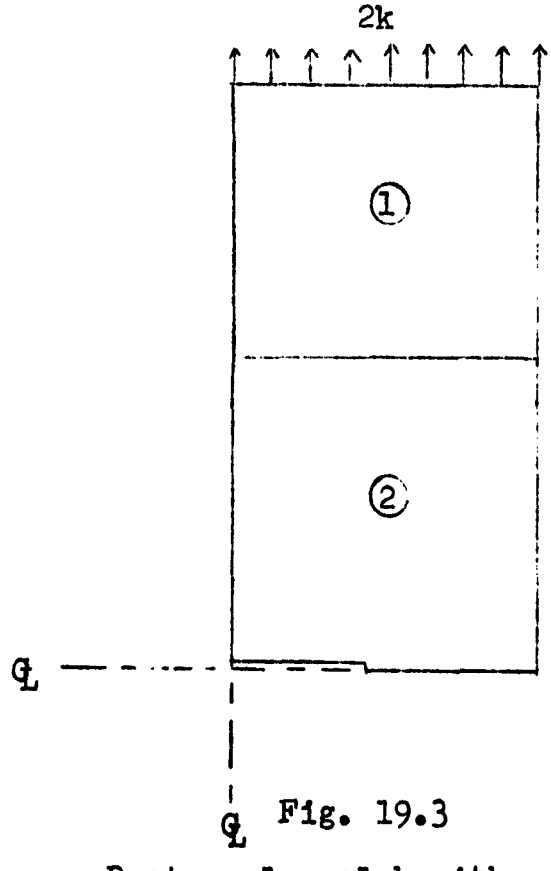

Fig. 19.3
Rectangular slab with a slit.

while region 2 is the same piecewise constant stress field considered for the square slab.

If the shorter side is perpendicular to the slit, the upper and lower bounds obtained no longer coincide. A few results are known [20], but they do not provide good approximations and will not be reviewed here.

20. Square slab with a circular cutout [3]. An important corollary to the first Prager-Greenberg-Drucker theorem is that the yield load of an elastic-perfectly plastic body cannot be lowered by the addition of material adjacent to a stress free boundary. Indeed, it is merely necessary to assign a zero state of stress to the new material and complete the stress field as if it were not there. It was this idea which we used in finding a biaxial lower bound in the previous section.

The example under consideration can be regarded as a square cutout, with additional material added to change it to a circle, as indicated in Fig. 20.1. Therefore, it follows

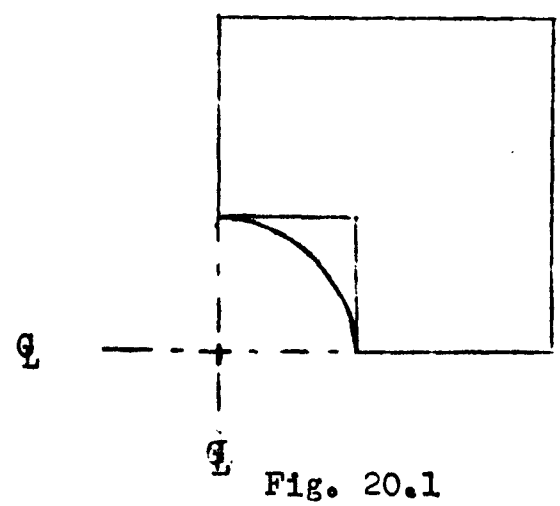

Fig. 20.1

Square slab with circular cutout.

immediately that the lower bounds obtained for the square cutout in Secs. 14 and 18 are also lower bounds in this case.

The solution of Sec. 13 also provides an upper bound for the present example. To be sure, if we take the regions of bending to have any finite width, then Eq. 13.8 is no longer valid. However, in Sec. 13 we purposefully chose one of the angles to passing to its limiting value of zero, and left the other three angles (β, γ, and δ in Fig. 13.2) undetermined. In the present application let all four angles be arbitrarily close to zero. In the limit we again obtain Eq. 13.11 for the internal rate of dissipation of energy. Since the external energy dissipation rate is unchanged it follows that Eqs. 13.13 are valid in this case also. Therefore, upper and lower bounds on the yield load are again given by Fig. 18.2.

21. Annular slab. In the examples previously considered we have been able to obtain upper and lower bounds which were reasonably close together. However, for an annular slab this is yet to be done, and the best upper and lower bounds obtained so far differ considerably from each other. This is unfortunate from a practical viewpoint, because probably the most common type of reinforced cutout is a circular hole with an annular reinforcement. Therefore, if we could solve the annular slab problem, we could use the method of Sec. 4 to solve the slab-independent reinforcement problem. Further, as we shall see in the next chapter, the only direct methods evolved so far for the reinforced slab depend heavily on the results of the unreinforced cutout problem.

In view of the importance of the annular slab, it seems

worthwhile to discuss such meager results as have been obtained so far, inconclusive as these may be. The methods used have been discussed in some detail in previous sections, and we shall here merely collect the results.

We first of all observe that the case of equal biaxial tension can be easily disposed of, by considering the stress field [1]

$$\sigma_r = 2k\lambda(1 - \frac{a}{r})/(1 - a), \qquad (21.1)$$

$$\sigma_\theta = 2k\lambda/(1 - a), \quad \tau_{r\theta} = 0.$$

Observe that this is the same stress field used in region 2 of Fig. 19.2 for the slab with a slit. Therefore, just as in Sec. 19 we obtain a lower bound of $\lambda = 1 - a$ for equal biaxial tension. Also, using sliding out of the plane (Sec. 11) we obtain $\lambda = 1 - a$ as an upper bound so that the cutout factor in equal biaxial tension is

$$\lambda = 1 - a. \qquad (21.2)$$

It remains, therefore, to consider uniaxial tension. Upper bounds for uniaxial tension can be found by the methods of Secs. 12 and 13. Equations 12.15 and 12.17 provide an upper bound which is less than $1 - a$ for all values of a, thus showing that the limit in uniaxial tension is definitely less than in equal biaxial tension. However, for large values of a, the concept of bending, as illustrated in Sec. 13 provides a still lower upper bound. Since the results obtained for the hollow square slab (Fig. 13.2) were independent of the angles α, β, γ, δ we may, as in the previous section, set each of these angles equal to zero and hence Eqs. 13.13 are valid for the annular slab as

well. As a matter of fact, since for the annular slab an increase of α or γ from zero would decrease the total internal rate of dissipation of energy in regions 1 and 4, (Fig. 13.2) respectively, a still lower upper bound could be obtained by variation of these angles. This has not been done, however. In Fig. 21.1, the upper curve shows the resultant upper bound obtained by taking the lower value of λ as given by Eqs. 12.17 or 13.13.

For any stress function, a lower bound may be obtained using Eqs. 17.3. R. K. Froyd has used these equations with stress functions defined by

$$\left.\begin{aligned} f' &= 0 \quad g = \frac{k\lambda}{2}\frac{(1+a)}{(1-a)^2}(r-a)^2, && a \le r \le \frac{1+a}{2}, \\ f' &= \frac{2k\lambda}{1-a}\left[r + \frac{1+a}{2}\right], \\ g &= \frac{k\lambda}{2}\frac{(1+a)}{(1+a)^2}\left[\frac{1-3a}{1+a}r^2 + 2ar - a\right] && \frac{1+a}{2} \le r \le 1 \end{aligned}\right\} \qquad (21.3)$$

Considering only the case $a \ge \frac{1}{3}$ he obtained a lower bound

$$\lambda \le \frac{1-a^2}{\sqrt{2}\,(1+3a)}, \quad \frac{1}{3} \le a \le \frac{1}{2},$$

$$\lambda \le \frac{(1+a)(1-a)^2}{\sqrt{2}\,a(3-a)}, \quad \frac{1}{2} \le a \le \frac{6\sqrt{2}-5+\sqrt{97-68\sqrt{2}}}{4\sqrt{2}} \simeq 0.78, \qquad (21.4)$$

$$\lambda \le \frac{4-\sqrt{2}}{2}\frac{(1-a)^2}{1+a}\frac{6\sqrt{2}-5+\sqrt{97-68\sqrt{2}}}{4\sqrt{2}} \le a \le 1.$$

The resulting lower bound is sketched in Fig. 21.1.

For the particular case $a = \frac{1}{3}$ E. Levin has considered numerically the stress function defined by

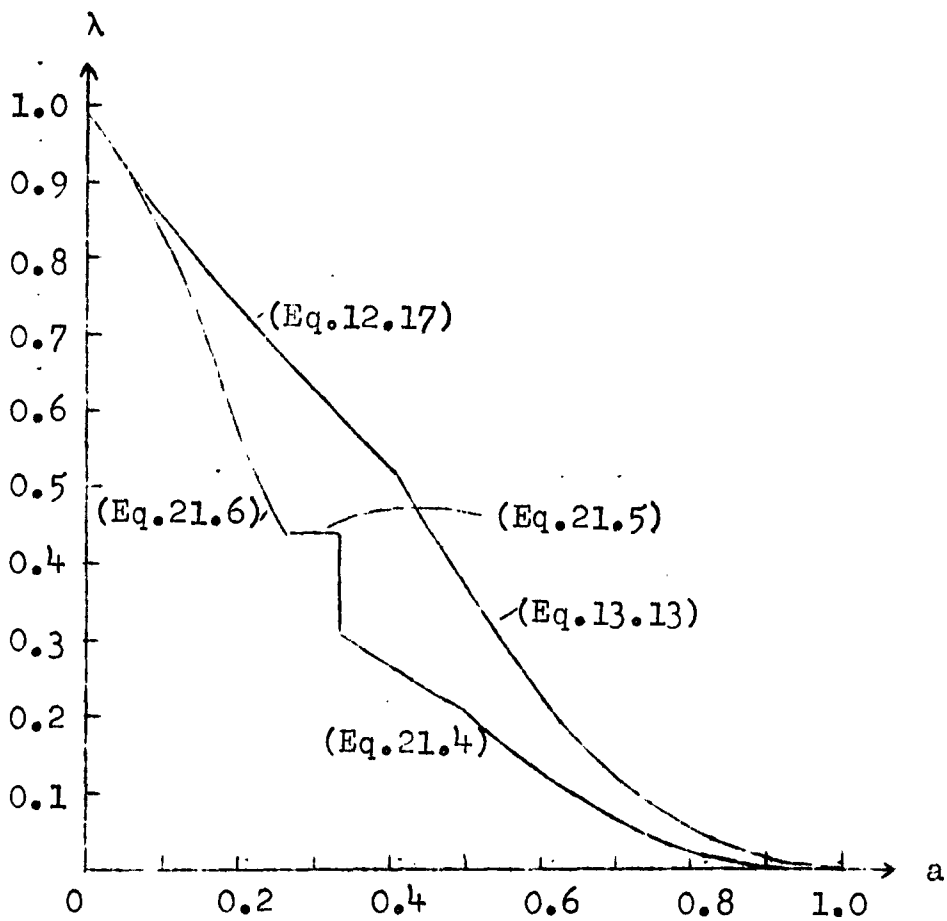

Fig. 21.1

Upper and lower bounds for annular slab.

$$
\left.\begin{aligned} f' &= k\lambda\,(r - \tfrac{1}{3}), \\ g &= (k\tfrac{\lambda}{6})(3r - 1)^2, \end{aligned}\right\} \tfrac{1}{3} \le r \le \tfrac{2}{3},
$$

$$
\left.\begin{aligned} f' &= k\lambda\,(r - \tfrac{1}{3}), \\ g &= k\lambda\,(r - \tfrac{1}{2}), \end{aligned}\right\} \tfrac{2}{3} \le r \le \tfrac{5}{6}, \qquad (21.5)
$$

$$
\left.\begin{aligned} f' &= k\lambda\,(3r - 2), \\ g &= k\lambda\,(r - \tfrac{1}{2}). \end{aligned}\right\} \tfrac{5}{6} \le r \le 1.
$$

The worst point was found to occur at $\theta = \pi/4$, $r = 2/3$. The result is subject to some question, of course, as a rather course mesh was used. However, since the functions involved are simple ones, it appears reasonable that the worst point would be at the end point of an interval in r, so that Levin's result may be tentatively accepted. It would, however, be desirable to check it analytically, at least using the approximate yield condition.

Levin's result is considerably higher than any bound so far obtained for an arbitrary value of a. Therefore, for a a little less than 1/3, the best bound available at present is to combine 21.5 with a stress-free region for $r < 1/3$. This accounts for the horizontal portion of the lower curve in Fig. 21.1.

Finally, for a less than about 0.265, the best lower bound has been obtained by inscribing a hollow square in the annulus. That part of the annulus exterior to the square is taken to have a constant stress state, while that part interior to the cutout in the square is taken to be stress-free. Within the

hollow square, the discontinuous stress field of Sec. 14 is used. Since the exterior side of the square is $\sqrt{2}$ in length, while a length 2 was assumed in obtaining Eqs. 14.11, the result for the present case is

$$\lambda_A(a) = \lambda_s(a\sqrt{2}) \tag{21.6}$$

where λ_s is the cutout factor for the square as given by Eqs. 14.11 (Eq. 14.11b is the applicable one in the range of interest for a), and λ_A is the desired cutout factor for the annulus.

Figure 21.1 shows the best upper and lower bound corresponding to each value of a. As previously admitted, the solution is by no means satisfactory and the investigation is being continued in the hope of obtaining better bounds.

VI. REINFORCED CUTOUTS

22. Reinforcement to full strength. In Sec. 4, a method was indicated by which a reinforcement for full strength could be designed on the basis of the analysis of the hub alone. Intuitively, one might expect that such an analysis would always be conservative, and that a consideration of the stresses in the base slab would lead to substantially reduced hub dimensions. However, as we shall see, this is not always the case.

As an example, let us consider a square slab of half-side d with a circular cutout of radius a, reinforced by concentric circular cylindrical rings of outer radius b. The thickness of the hub is H, and the slab is subjected to equal biaxial tensions $2k\lambda$ (Fig. 22.1).

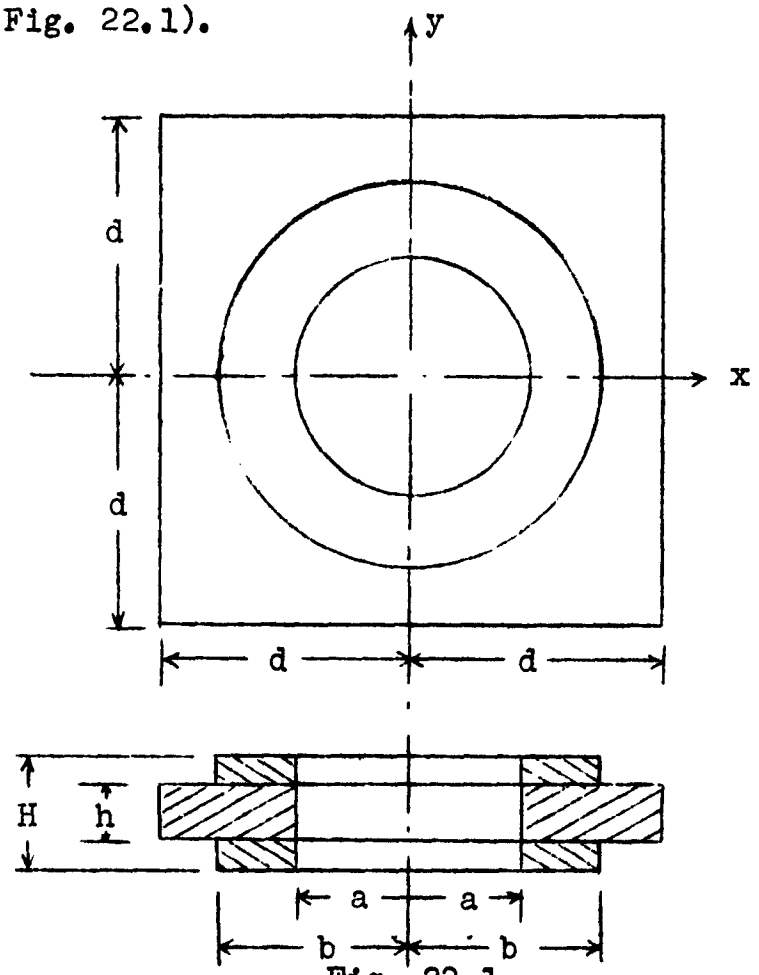

Fig. 22.1
Slab reinforced by rings

Consider first the radially symmetric stress field [1]

$$\sigma_r = 2k(1 - \frac{a}{r}), \quad \sigma_\theta = 2k, \quad a \leq r \leq b$$

$$\sigma_r = 2k\left\{1 - \frac{b}{r}[1 - \frac{H}{h}(1 - \frac{a}{b})]\right\}, \quad \sigma_\theta = 2k, \quad b \leq r \leq 1, \tag{22.1}$$

$$\sigma_r = 2k\lambda, \quad \sigma_\theta = 2k\lambda, \quad r > b.$$

Observe that this stress field satisfies the equilibrium equation (Eq. 19.7) in each of the three regions, and the boundary condition $\sigma_r = 0$ at $r = 0$. Further, at the hub boundary $r = b$ the traction per unit length is

$$2kH(1 - \frac{a}{b})$$

computed from either side. Finally, the tractions applied at $r = 1$ will be in equilibrium provided that

$$\lambda = 1 - \frac{b}{d} + (\frac{H}{h})(b - a)/d. \tag{22.2}$$

Therefore, Eqs. 22.1 furnish an equilibrium stress field. If we impose the additional condition that

$$\frac{H}{h} \leq \frac{b}{b - a} \tag{22.3}$$

then at all points of the reinforced slab

$$\sigma_r \geq \sigma_\theta \geq 0 \tag{22.4}$$

so that the stress field 22.1 is statically admissible. It follows from Theorem 1 that

$$\lambda \geq 1 - \frac{b}{d} + (\frac{H}{h})(b - a)/d. \tag{22.5}$$

Next, we may construct a kinematically admissible velocity field based on sliding out of the plane, as in Sec. 11.

An elementary computation then shows that $1 - b + (H/h)(b - a)$ is also an upper bound for the yield load λ. Therefore, the load and hub thickness are related by Eq. 22.2.

If the reinforcement is to be designed for full strength, then we may set $\lambda = 1$ in Eq. 22.2 and obtain

$$\frac{H}{h} = \frac{b}{b - a}. \tag{22.6}$$

This result is independent of the dimension d which characterizes the slab. Indeed, the same result could have been more easily obtained by the method of Sec. 4. For a plane annular slab of inner and outer radii a and b respectively, the yield load under biaxial tension is easily shown to be [1],

$$\lambda = 1 - \frac{a}{b}. \tag{22.7}$$

Substituting this into 4.1 yields 22.6 immediately.

Although reinforcement to full strength is independent of d, the same is not true if we wish to reinforce to some value less than full strength. Solving 22.5 for H/h, we obtain

$$\frac{H}{h} = \frac{b}{b - a} - \frac{1 - \lambda}{b - a} d. \tag{22.8}$$

In Fig. 22.2 we have sketched H/h as a function of d for the particular case $a = 1$, $b = 2$ for different values of λ. Observe that for any value of $\lambda < 1$ a sufficiently large value of d brings the slab to the required strength without any reinforcement ($H/h = 1$).

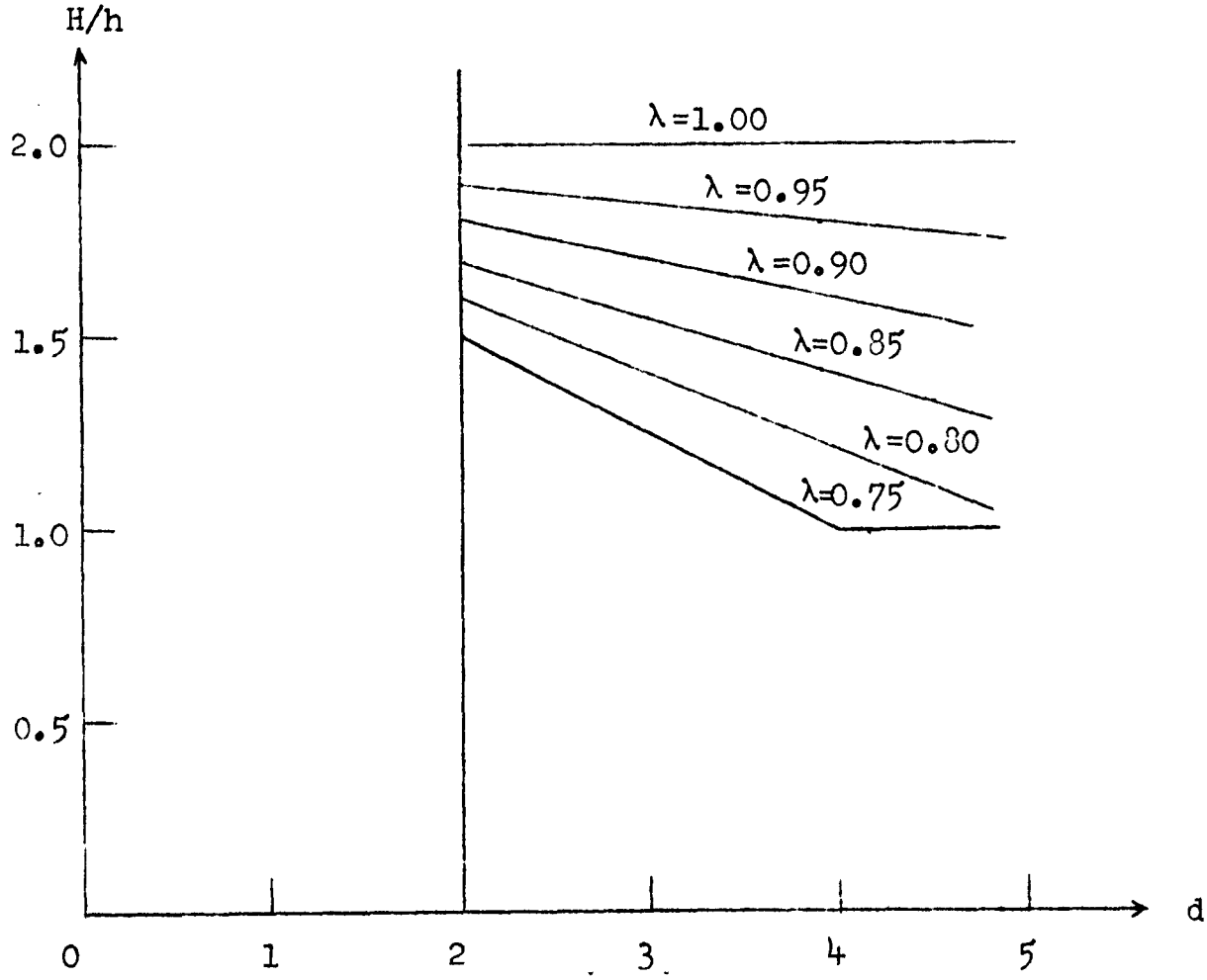

Fig. 22.2

Reinforcement to less than full strength.

23. Wide square reinforcement. As a second example of direct computation of reinforced cutouts, consider a square reinforcement of a square coutout in a square slab (Fig. 23.1). The state of stress in the hub, as well as in the base slab, is to be approximated by plane stress.

Let us consider a piecewise constant stress field, dividing the base slab into four regions as in the previous section, and dividing the hub into four similar regions (Fig. 23.1). In each of regions 1, 3, 4, 5, 7 and 8, symmetry demands that the principal directions be the coordinate directions so that

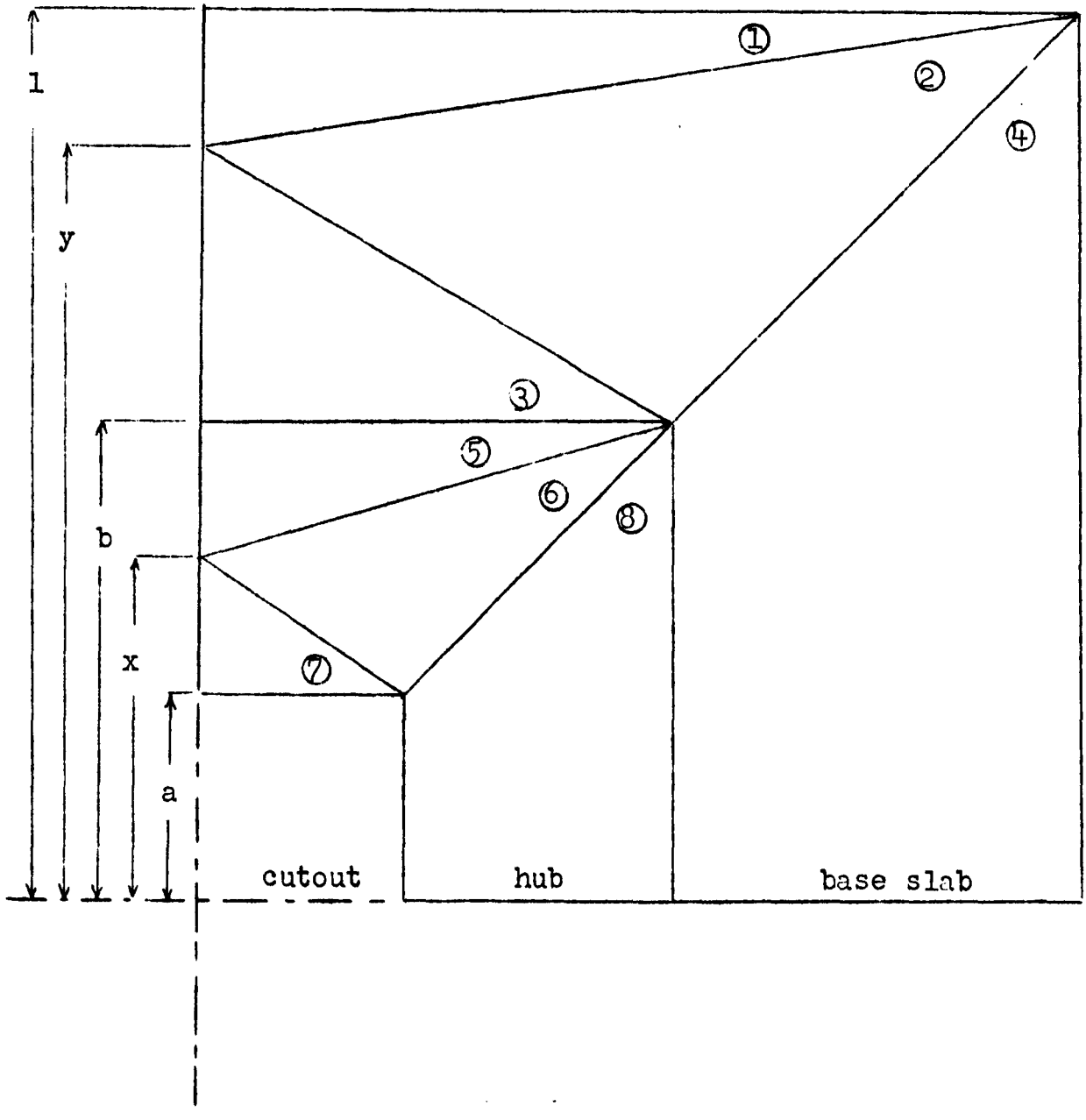

Fig. 23.1

Wide square reinforcement of square slab with square cutout.

$$\theta_1 = \theta_3 = \theta_4 = \theta_5 = \theta_7 = \theta_8 = 0. \tag{23.1a}$$

Equilibrium with the applied boundary tractions determines

$$\begin{aligned} s_1 &= 2k\lambda, \quad s_7 = 0, \\ r_4 &= 0, \quad r_8 = 0. \end{aligned} \tag{23.1b}$$

Next, if we denote σ_y in region 3 by $2k\mu$, and define

$$\eta = \frac{h}{H}$$

as the ratio of base slab height to hub height, equilibrium between regions 3 and 5 furnishes

$$s_3 = 2k\mu, \quad s_5 = 2k\mu\eta. \tag{23.1c}$$

In an example such as the present one which contains several regions, it is desirable to linearize the equilibrium equations between adjoining regions (Eqs. 14.3) by defining

$$u = \chi \cos 2\theta, \quad v = \chi \sin 2\theta. \tag{23.2a}$$

Using the further notation

$$\rho = \frac{r}{2k}, \quad \sigma = \frac{s}{2k}$$

the situation in each region is given in Table 23.1.

Since we have already satisfied the boundary conditions at the inner and outer boundaries and between the hub and base slab, there are a total of twelve Eqs. 14.3 as follows:

Region	Θ	ρ	σ	ω	χ	u	v
1	0	ρ_1	λ	$\rho_1 + \lambda$	$\rho_1 - \lambda$	$\rho_1 - \lambda$	0
2	Θ_2	ρ_2	σ_2	ω_2	χ_2	u_2	v_2
3	0	ρ_3	μ	$\rho_3 + \mu$	$\rho_3 - \mu$	$\rho_3 - \mu$	0
4	0	0	σ_4	σ_4	$-\sigma_4$	$-\sigma_4$	0
5	0	ρ_5	$\mu\eta$	$\rho_5 + \mu\eta$	$\rho_5 - \mu\eta$	$\rho_5 - \mu\eta$	0
6	Θ_6	ρ_6	σ_6	ω_6	χ_6	u_6	v_6
7	0	ρ_7	0	ρ_7	ρ_7	ρ_7	0
8	0	0	σ_8	σ_8	$-\sigma_8$	$-\sigma_8$	0

Table 23.1

Stress quantities in Fig. 23.1.

regions 1,2: $(\rho_1 + \lambda) - (\rho_1 - \lambda)C_1 = \omega_2 - u_2C_1 - v_2S_1,$

$(\rho_1 - \lambda)S_1 = u_2S_1 - v_2C_1,$

regions 3,2: $(\rho_3 + \mu) - (\rho_3 - \mu)C_3 = \omega_3 - u_2C_2 - v_2S_3,$

$(\rho_3 - \mu)S_3 = u_3S_3 - v_2C_3,$

regions 4,2: $\sigma_4 = \omega_2 - v_2,$

$-\sigma_4 = u_2,$

regions 5,6: $(\rho_5 + \mu\eta) - (\rho_5 - \mu\eta)C_5 = \omega_6 - u_6C_5 - v_6S_5,$

$(\rho_5 - \mu\eta)S_5 = u_6S_5 - v_6C_5,$

regions 7,6: $\rho_7(1 - C_7) = \omega_6 - u_6C_7 - v_6S_7,$

$\rho_7S_7 = u_6S_7 - v_6C_7,$

regions 8,6: $$\sigma_8 = \omega_6 - v_6,$$

$$-\sigma_8 = u_6,$$

where we have used the symbols

$$\begin{aligned} C_1 &= \cos 2\alpha_{12}, & S_1 &= \sin 2\alpha_{12}, \\ C_3 &= \cos 2\alpha_{32}, & S_3 &= \sin 2\alpha_{32}, \\ C_5 &= \cos 2\alpha_{56}, & S_5 &= \sin 2\alpha_{56}, \\ C_7 &= \cos 2\alpha_{76}, & S_7 &= \sin 2\alpha_{76}. \end{aligned} \tag{23.4}$$

Equations 23.3 separate into two groups of six equations each, the first six equations containing ρ_1, ρ_3, σ_4, ω_2, u_2, and v_2 as unknowns; the second group containing ρ_5, ρ_7, σ_8, ω_6, u_6 and v_6. The equations are easily solved with the use of the trignometric identities

$$\begin{aligned} \cos 2\alpha &= (1 - \tan^2\alpha)/(1 + \tan^2\alpha), \\ \sin 2\alpha &= 2\tan\alpha/(1 + \tan^2\alpha). \end{aligned} \tag{23.5}$$

Further, it follows from Fig. 23.1 that

$$\begin{aligned} \tan\alpha_{12} &= 1 - y, & \tan\alpha_{32} &= 1 - \frac{y}{b}, \\ \tan\alpha_{56} &= 1 - \frac{x}{b}, & \tan\alpha_{76} &= 1 - \frac{x}{a}. \end{aligned} \tag{23.6}$$

After some computation, then, we finally obtain

$$\rho_1 = \frac{\lambda - \mu}{1 - y} \cdot \frac{b}{1 - b},$$

$$\rho_3 = \frac{\lambda - \mu}{b - y} \cdot \frac{b}{1 - b},$$

$$\sigma_4 = \frac{\lambda - \mu b}{1 - b},$$

$$\omega_2 = \frac{\lambda - \mu b}{1 - b} - 2\frac{\lambda - \mu}{y}\frac{b}{1 - b},$$

$$
\begin{aligned}
u_2 &= -\frac{\lambda - \mu b}{1 - b}, \\
v_2 &= -2\frac{\lambda - \mu}{y} \cdot \frac{b}{1 - b}, \\
\rho_5 &= \frac{ab}{b - a} \cdot \frac{\mu \eta}{b - x}, \\
\rho_7 &= \frac{ab}{b - a} \cdot \frac{\mu \eta}{a - x}, \\
\sigma_8 &= \frac{b}{b - a} \mu \eta, \\
\omega_6 &= \frac{x - 2a}{x} \frac{b}{b - a} \mu \eta, \\
u_6 &= -\frac{b}{b - a} \mu \eta, \\
v_6 &= -\frac{2a}{x} \frac{b}{b - a} \mu \eta.
\end{aligned}
\tag{23.7}
$$

Next, we compute the governing inequality in each region. However, we first record the elementary inequalities

$$
\begin{aligned}
&0 < a < x < b < y < 1, \\
&0 < \eta \leq 1, \\
&0 \leq \mu \leq \lambda \leq 1.
\end{aligned}
\tag{23.8a}
$$

Taking 23.8a for granted wherever they are needed, we see that in region 1, ρ and σ are both positive and $\sigma < 1$ is included in 23.8a so that the governing inequality is

$$
\rho_1 = \frac{\lambda - \mu}{1 - y} \frac{b}{1 - b} \leq 1. \tag{23.8b}
$$

In region 2, $|\chi|$ is easily computed from the identity

$$
|\chi| = \sqrt{u^2 + v^2},
$$

and it can be shown that for any values of the parameters

$|\chi| > |\omega|$. Therefore, the governing inequality is

$$|\chi_2| = \frac{1}{1-b}\sqrt{(\lambda - \mu b)^2 + \left(\frac{2b}{y}\right)^2(\lambda - \mu)^2} \leq 1. \qquad (23.8c)$$

In region 3, on the other hand, we have $\sigma > 0 > \rho$ for any values of the parameters, so that the governing inequality is

$$|\chi_3| = \sigma_3 - \rho_3 = \mu + \frac{\lambda - \mu}{y - b}\frac{b}{1 - b} \leq 1. \qquad (23.8d)$$

Since $\rho = 0$ in region 4, the governing inequality is

$$\sigma_4 = \frac{\lambda - \mu b}{1 - b} \leq 1. \qquad (23.8e)$$

Finally, similar arguments for each of the four regions of the hub lead to the governing inequalities

$$\sigma_5 = \frac{ab\mu\eta}{(b - a)(b - x)} \leq 1, \qquad (23.8f)$$

$$|\chi_6| = \frac{\mu b\eta}{b - a}\sqrt{1 + \frac{4a^2}{x^2}} \leq 1, \qquad (23.8g)$$

$$-r_7 = \frac{ab}{b - a}\frac{\mu\eta}{x - a} \leq 1, \qquad (23.8h)$$

$$\sigma_8 = \frac{\mu\eta b}{b - a} \leq 1. \qquad (23.8i)$$

Inequalities 23.8 may be considered in either of two ways. On the one hand, for given values of a and b we may wish to determine the maximum value of $\eta(= h/H)$ which will restore the slab to full strength. As far as the present type of stress field is concerned, the situation is similar to that encountered in the previous section in that we obtain no improvement over the result obtained by applying the theory of Sec. 4 to the example considered in Sec. 18. To see this, we need only consider Inequality 23.8. With $\lambda = 1$, this becomes

$$1 - \mu b \leq 1 - b.$$

Since b must be positive and $\mu \leq 1$ it follows that $\mu = 1$. Therefore, the applied boundary tractions are transmitted directly to the hub, as stated.

A second problem is to find the yield load of a given reinforced slab. That is, given a, b, and η, find the maximum λ satisfying Inequalities 23.8. Since there are three parameters in the problem, it is impracticable to obtain any general results. However, a solution is easily obtained for any particular value of the parameters.

As an example, consider a reinforced slab with $a = \frac{1}{4}$, $b = \frac{1}{2}$, $\eta = \frac{1}{2}$ (observe that for a circular hole this would provide full strength). Since Inequalities 23.8e and 23.8i are consequences of 23.8c and 23.8g, respectively, we must consider the six inequalities

$$\lambda - \mu \leq 1 - y, \tag{23.9b}$$

$$4[(\lambda - \tfrac{\mu}{2})^2 + (\lambda - \mu)^2/y^2] \leq 1, \tag{23.9c}$$

$$\mu + (\lambda - \mu)/(y - \tfrac{1}{2}) \leq 1, \tag{23.9d}$$

$$\mu \leq 2 - 4x, \tag{23.9f}$$

$$\mu \sqrt{1 + \frac{1}{4x^2}} \leq 1, \tag{23.9g}$$

$$\mu \leq 4x - 1. \tag{23.9h}$$

Since $\mu \leq \lambda$, it is obvious that a larger value of μ will always allow a larger value of λ in Inequalities 23.9b, c. An elementary calculation shows that the same result is valid for

23.9d. Since these are the only three inequalities which contain λ and y, while the remaining three are the only ones which contain x, it follows that we wish to determine x in 23.9f, g, h so as to maximize μ in those inequalities. An analysis similar to that used in Sec. 14 shows that we must choose

$$x = \frac{3}{8}, \quad \mu = \frac{1}{2}. \tag{23.10}$$

With this value of μ, the first three Inequalities 23.9 become

$$\lambda \leq \frac{3}{2} - y, \tag{23.11b}$$

$$2\sqrt{(\lambda - \tfrac{1}{4})^2 + (\lambda - \tfrac{1}{2})^2/y^2} \leq 1, \tag{23.11c}$$

$$\lambda \leq \frac{1}{2}y + \frac{1}{4}. \tag{23.11d}$$

These inequalities are again similar to those considered in Sec. 14. Let us try the value of y for which 23.11b, d are both equalities. Then

$$y = \frac{5}{6}, \quad \lambda = \frac{2}{3}. \tag{23.12}$$

It is readily verified that these values also satisfy 23.11c so that we have obtained the best value of λ for the considered stress field.

By way of comparison, the method of Sec. 14 together with the results of Sec. 14 would furnish a lower bound of $\lambda = \frac{1}{2}$.

The upper bound obtained by considering sliding out of the plane is easily seen to be $\lambda = 1$, corresponding to full strength. However, by using a bending type velocity field as in Sec. 13, we can show that full strength is not attained. For simplicity, we shall assign convenient values to the hinge centers-

by varying these values we could presumably reduce the upper bound still further. Thus, with reference to Fig. 13.2, take $b = \frac{1}{2}$, $c = \frac{1}{4}$, $d = 0$, $f = \frac{3}{4}$. Observe that this locates the top hinge at the junction of hub and base slab, and the lower hinge at the outer edge of the slab. The internal energy dissipation rates are given by Eqs. 13.6, where h must be replaced by $H = 2h$ in areas corresponding to the hub. The resulting total is

$$\mathcal{D}_i = [(\tfrac{1}{4}) + (\tfrac{1}{8}) + 0 + (\tfrac{9}{16})]kh\dot{\theta} = 15\ kh\dot{\theta}/16. \qquad (23.13)$$

Since the external rate of dissipation of energy is still given by 13.10, we have

$$\mathcal{D}_e = 2k\lambda h\dot{\theta}(\tfrac{1}{4} + \tfrac{3}{4} - \tfrac{1}{2}) = kh\dot{\theta}\lambda. \qquad (23.14)$$

Comparing 23.13 and 23.14 we obtain the upper bound

$$\lambda \leq \frac{15}{16}. \qquad (23.15)$$

24. Wide slabs with narrow reinforcements. If the hub is sufficiently narrow to be approximated by a curved beam, as in Chap. II, then the methods of Chaps. II and IV can be combined to furnish a lower bound.

As an example, let us consider a circular cutout with an annular cylindrical reinforcement subject to uniaxial tension. We divide the base slab into several regions as indicated in Fig. 24.1. Regions 1 through 5 constitute the base slab and region 6 is the hub. The stress distribution in the hub is expressed in terms of stress resultants, as in Chap. II. The stress distribution in regions 1 through 4 is similar to that discussed in the base slab in the previous section. The component of stress

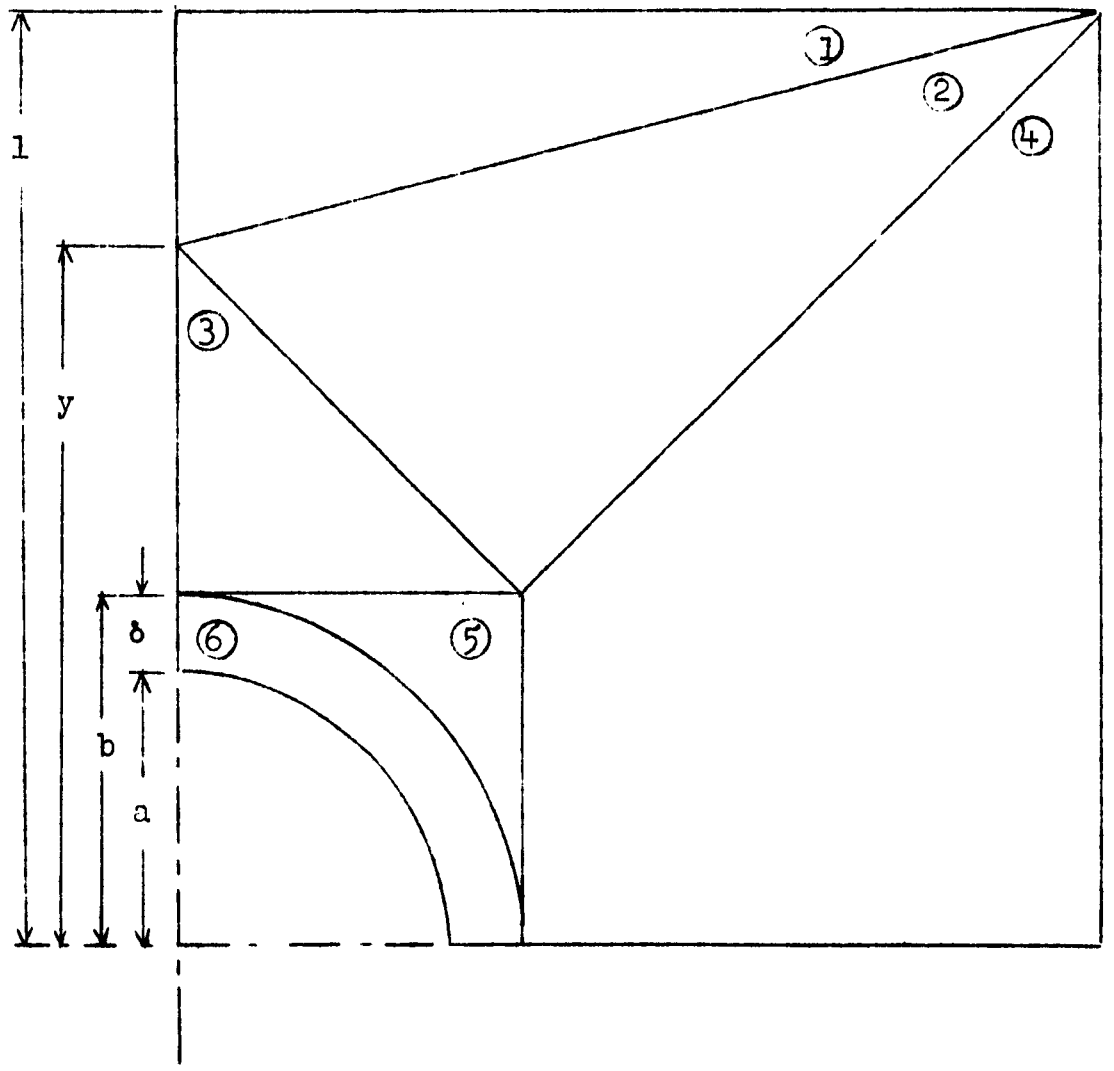

Fig. 24.1

Square slab with narrow annular reinforcement.

σ_y is $2\lambda k$ in region 1 to be in equilibrium with the applied load, while in region 3 it is $2k\mu$ where μ is a constant to be determined. In region 5, the stress is determined by regions 3 and 4 to be

$$\sigma_x = 0, \quad \sigma_y = 2k\mu, \quad \tau_{xy} = 0.$$

Therefore, it follows that the hub is acted upon by a uniformly distributed vertical force of magnitude $2k\mu h$ per unit length.

The forces acting upon regions 1 through 4 are exactly the same as those acting on the corresponding regions in Fig. 23.1, considered in the previous section. Therefore, the same stress distribution will subsist and hence the same governing inequalities. From Eqs. 23.8b through e we have then

$$\frac{\lambda - \mu}{1 - y} \frac{b}{1 - b} \leq 1, \tag{24.1a}$$

$$(\lambda - \mu b)^2 + \left(\frac{2b}{y}\right)^2 (\lambda - \mu)^2 \leq (1 - b)^2, \tag{24.1b}$$

$$\mu + \frac{\lambda - \mu}{y - b} \frac{b}{1 - b} \leq 1, \tag{24.1c}$$

$$\lambda - \mu b \leq 1 - b.$$

The last of these inequalities is a consequence of 24.1b and hence will not be considered further. Region 5, of course, does not add any new inequalities. The inequalities in region 6 are obtained from Eqs. 6.12, replacing λ by μ. Thus

$$\mu \leq \frac{H}{h} \frac{\delta}{a + \delta}, \tag{24.2a}$$

$$\mu \leq \frac{H}{h} \frac{\sqrt{a^2 + 2\delta^2} - 1}{a + \delta}. \tag{24.2b}$$

Next, we observe that the left hand sides of 24.1a and c are decreasing functions of μ for all values of y and b, while

the same will be true for 24.1b if

$$y < b(2 - b)/(1 - b). \qquad (24.3)$$

It is found that this is generally the case, so that we shall assume that the left hand sides of all three Inequalities 24.1 are decreasing functions of μ. It follows that since μ is bounded only from above by inequalities 24.2, we should choose μ to be the largest value permitted by these equations. Then μ becomes a known quantity and inequalities 24.1 are to be solved, determining y so as to maximize λ. It should be pointed out that if b and y should turn out to be such that 24.3 is reversed, this will not lead to an invalid result, since for <u>any</u> choice of μ and y a legitimate lower bound on λ is obtained. It merely means that the best possible lower bound for the given data would not be obtained.

With μ fixed, then, the general character of inequalities 24.1 is the same as that illustrated in Fig. 14.2 for inequalities 14.10. Thus, depending upon the values of the parameters, the best value for y will be the intersection of 24.1c with either 24.1a or 24.1b. After some computation it is found that

$$\lambda \geq \min(\lambda_1, \lambda_2), \qquad (24.4)$$

where

$$\lambda_1 = \mu + \left(\frac{1 - \mu}{2 - \mu}\right) \frac{(1 - b)^2}{b}, \qquad (24.5a)$$

and λ_2 is defined implicitly by

$$\left[1 - \frac{(\lambda_2 - \mu)b}{1 - b}\right]^2 = \frac{4b^2(\lambda_2 - \mu)^2}{(1 - b)^2 - (\lambda_2 - b\mu)^2}. \qquad (24.5b)$$

A convenient upper bound for the above example is obtained by considering sliding out of the plane:

$$\lambda \leq 1 - b + (b - a)(\frac{H}{h}). \qquad (24.6)$$

Other upper bounds can also be obtained by considering bending as in the previous section. Some specific examples will be given in Sec. 26.

The same approach can be used for any shaped hub. In each case μ is obtained by the methods of Chap. II, and λ is then given by 24.4. Thus, for a square cutout with a square reinforcement, it follows from 6.18 that

$$\mu = \min \frac{H}{h}\left[\frac{\delta}{\sqrt{2}\,(a + \delta)}, \frac{H}{h}\,\frac{-a + \sqrt{a^2 + 4\delta^2}}{2(a + \delta)}\right]. \qquad (24.7)$$

As an example, let us consider the reinforced slab for which a plane stress bound was found in Sec. 23. With $a = \delta = 1/4$, $H/h = 2$ Eq. 24.7 furnished $\mu = \frac{1}{2}(\sqrt{5} - 1) = 0.62$. Substituting this into 24.5a we obtain $\lambda_1 = 0.76$. It is easily shown that λ_2 is greater than λ_1, in this case, so that

$$\lambda = 0.76 \qquad (24.8)$$

is a lower bound. Comparing this with Eqs. 23.12 and 23.15 we see that this type of approach gives a value between the upper and lower bounds furnished by the plane stress approach.

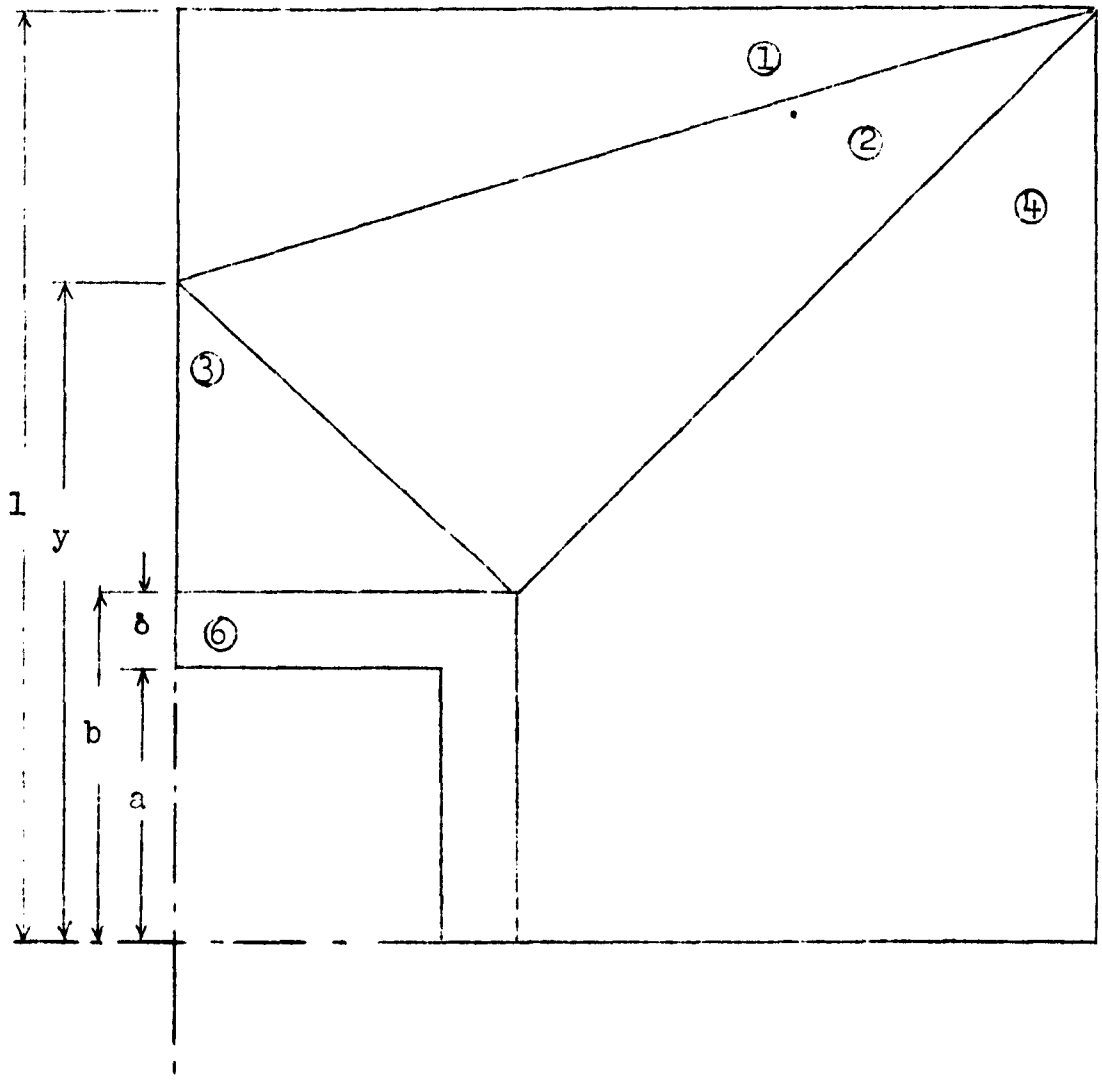

Fig. 24.2

Square slab with narrow hollow square reinforcement.

25. Other loading conditions. Up to now we have been considering only the situation where a uniform load has been applied to the boundary. However, in applications, it may be that only the resultant load is known, and not the load distribution. In the present section we shall discuss this situation more generally.

In the first place, we observe that an assumption must be made that the load intensity per unit length is nowhere greater than 2kh, since otherwise the material of the slab would fail locally. Secondly, it is evident that the slab is generally stronger if the load is applied near the edge of the slab, away from the cutout. Therefore, we may consider two extreme cases as indicated in Fig. 25.1. In each case, a vertical load of intensity 2kh per unit length is applied over a length c in each quadrant. In Fig. 25.1a the load is at the outer edge, and in Fig. 25.1b at the center. In either case we may define a design problem: to determine a reinforcement which will support a given load span c; or an analysis problem: to determine the maximum c for a given slab.

Let us consider first an unreinforced slab with an outer load applied. For the case $c = 1 - a_o$ a statically admissible stress field may be trivially constructed as indicated in Fig. 25.2. Region 1 is stress free, while in region 2

$$\sigma_y = \tau_{xy} = 0, \quad \sigma_x = 2k.$$

Therefore, it follows that $1 - a_o$ is a lower bound for c. On the other hand, a kinematically admissible velocity field consisting of sliding out of the plane shows that $1 - a_o$ is also an upper bound, so that in this case

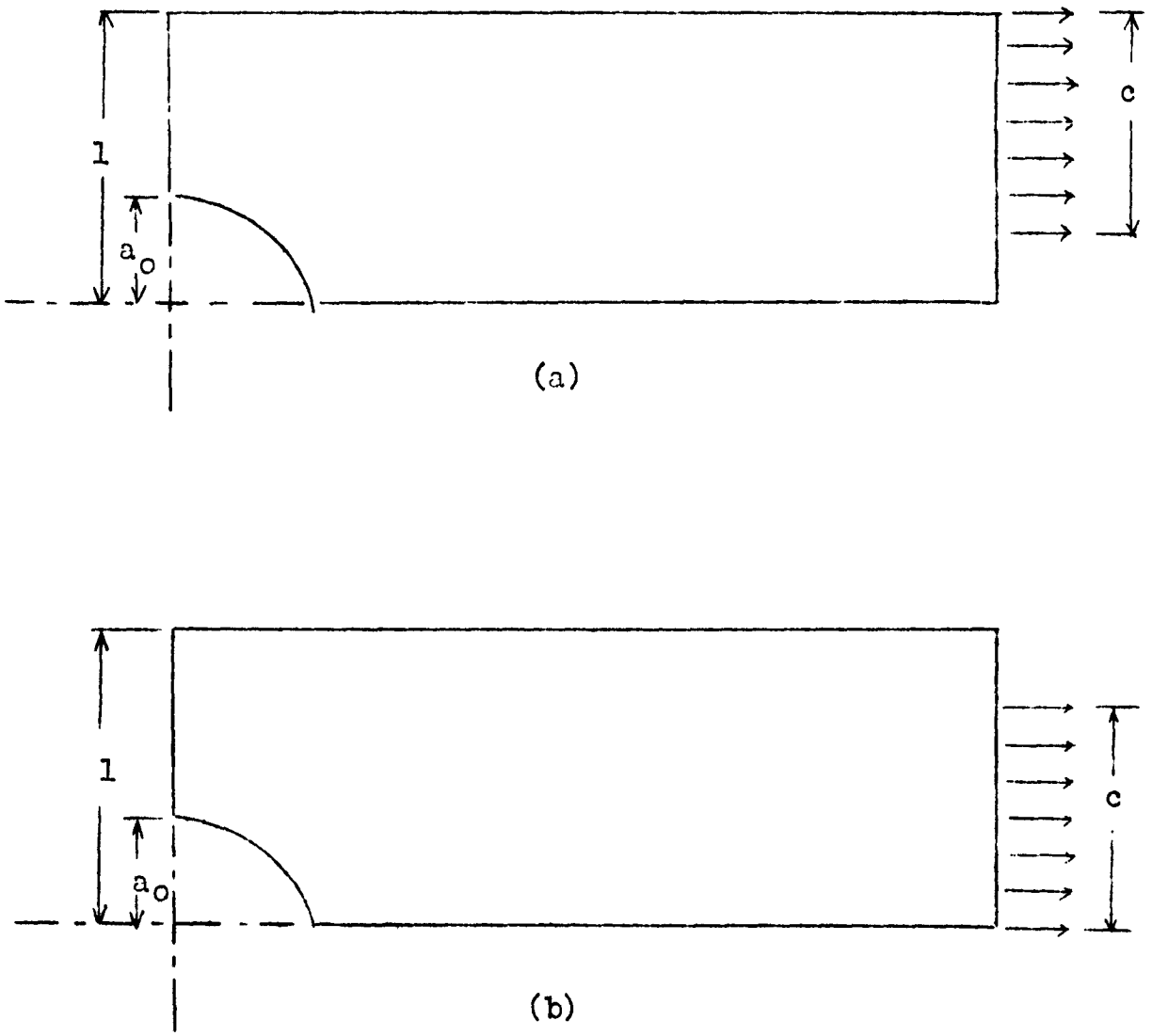

Fig. 25.1

Extreme load distributions.

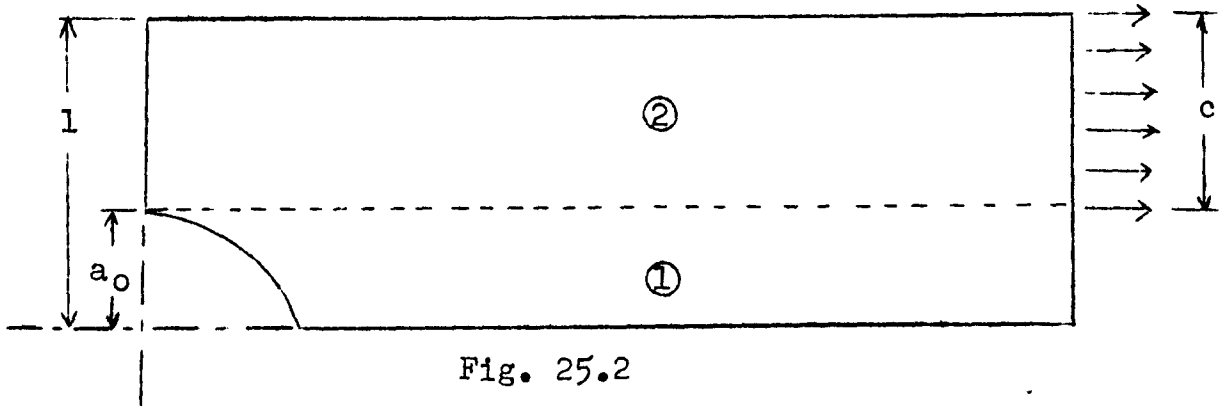

Fig. 25.2

Statically admissible stress field for extreme load.

$$c = 1 - a_o. \qquad (25.1)$$

As an application of this type of analysis, consider a test slab which is clamped perfectly rigidly at either end (Fig. 25.3). If the clamp is perfectly rigid and indefinitely strong then <u>any</u> equilibrium stress field in the clamp is statically admissible. Such a stress field can always be found for any prescribed boundary stresses, for example, the elastic solution.

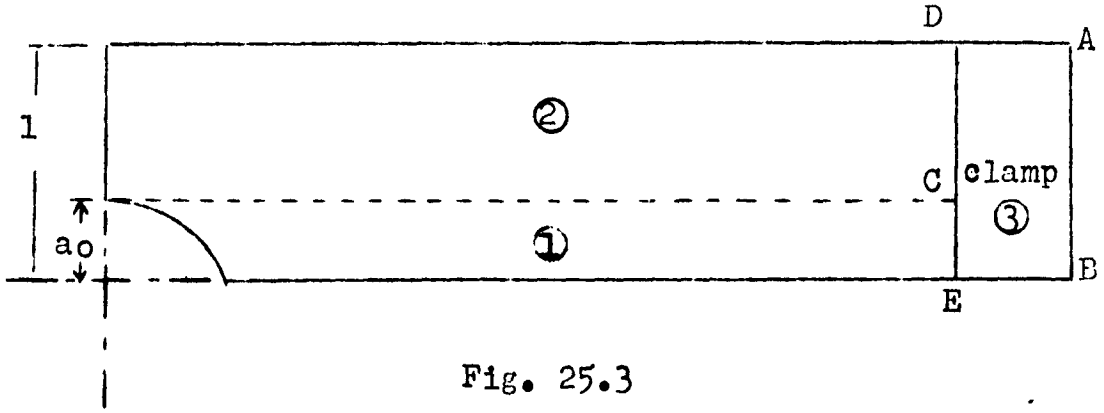

Fig. 25.3

Statically admissible stress field for clamped slab.

Therefore, in Fig. 25.3, let the stress field in the clamp be such that it is in equilibrium a total load of $2k\lambda$ on AB (in whatever manner it is actually applied), no load on EC, and a uniform load $2k\lambda/(1 - a_o)$ on CD. The other sides are stress free and there are no shearing tractions. Region 1 is taken as stress free, while in region 2

$$\sigma_y = \tau_{xy} = 0, \quad \sigma_x = 2k\lambda/(1 - a_o).$$

The above stress field will be statically admissible for the entire assembly of clamp and slab provided that σ_y in region 2 is less than the yeild stress. Thus a lower bound for λ is $1 - a_o$. Since it follows from Eq. 11.3 that this is also an upper bound, we have

$$\lambda = 1 - a_o. \tag{25.2}$$

Therefore, for a perfectly rigid and strong clamp the collapse load is determined.

In actual practice, the clamp may not be perfect, so that 25.2 is not exact. While conceivably the actual load as it reaches the slab could be as indicated in Fig. 25.1b, in practice this seems most unlikely, so that the true collapse load is probably somewhere in between 25.2 and the uniform load analysis considered in the preceding section.

For a reinforced cutout the analysis is not quite so trivial. As a matter of fact, for reinforcement to full strength the present viewpoint offers no improvement. However, for analysis under a given load less than full strength, modifications of the above procedure can certainly be used to advantage.

As an example, consider the reinforced slab discussed

in the previous section, pulled in uniaxial tension by a perfect clamp (Fig. 25.4). The stress distribution in the slab is the same as in Fig. 25.3, where the length c is chosen so that the tractions transmitted across AB onto the slab are 2kh per unit length. The base slab stresses are then statically admissible, and it remains only to consider the hub.

The hub is subjected to a horizontal force of magnitude 2kh per unit length for $\Theta_1 \leq \Theta \leq \pi/2$ and to no force for $0 \leq \Theta \leq \Theta_1$. The resultants may be computed by equations analogous to 5.8, and it is found that

$$\left.\begin{aligned} N(\Theta) &= 0, \quad M(\Theta) = M(0), \quad 0 \leq \Theta \leq \Theta_1, \\ N(\Theta) &= 2khb(\sin\Theta - \sin\Theta_1)\sin\Theta, \\ M(\Theta) &= M(0) + khb(\sin\Theta - \sin\Theta_1)(a\sin\Theta - b\sin\Theta_1), \end{aligned}\right\} \quad 0 \leq \Theta \leq \pi/2. \tag{25.3}$$

Using the notations

$$\begin{aligned} \zeta &= \sin\Theta, \quad \zeta_1 = \sin\Theta_1, \\ \eta &= h/H, \quad \alpha = a/b, \\ Y &= 2HM(0)/kh^2b^2, \end{aligned} \tag{25.4}$$

and substituting 25.3 into 6.3 we obtain the yield inequalities

$$\left|Y + \left(\frac{2}{\eta}\right)(\zeta - \zeta_1)(\alpha\zeta - \zeta_1)\right| + (\zeta - \zeta_1)^2\zeta^2 \leq (1 - \alpha^2)/\eta^2. \tag{25.5}$$

Inequality 25.5 must be satisfied for all $\zeta_1 \leq \zeta \leq \pi/2$, and Y is to be chosen so that ζ_1 is a minimum. It follows from Fig. 25.4 that the resultant load on the quarter is given in terms of ζ_1 by

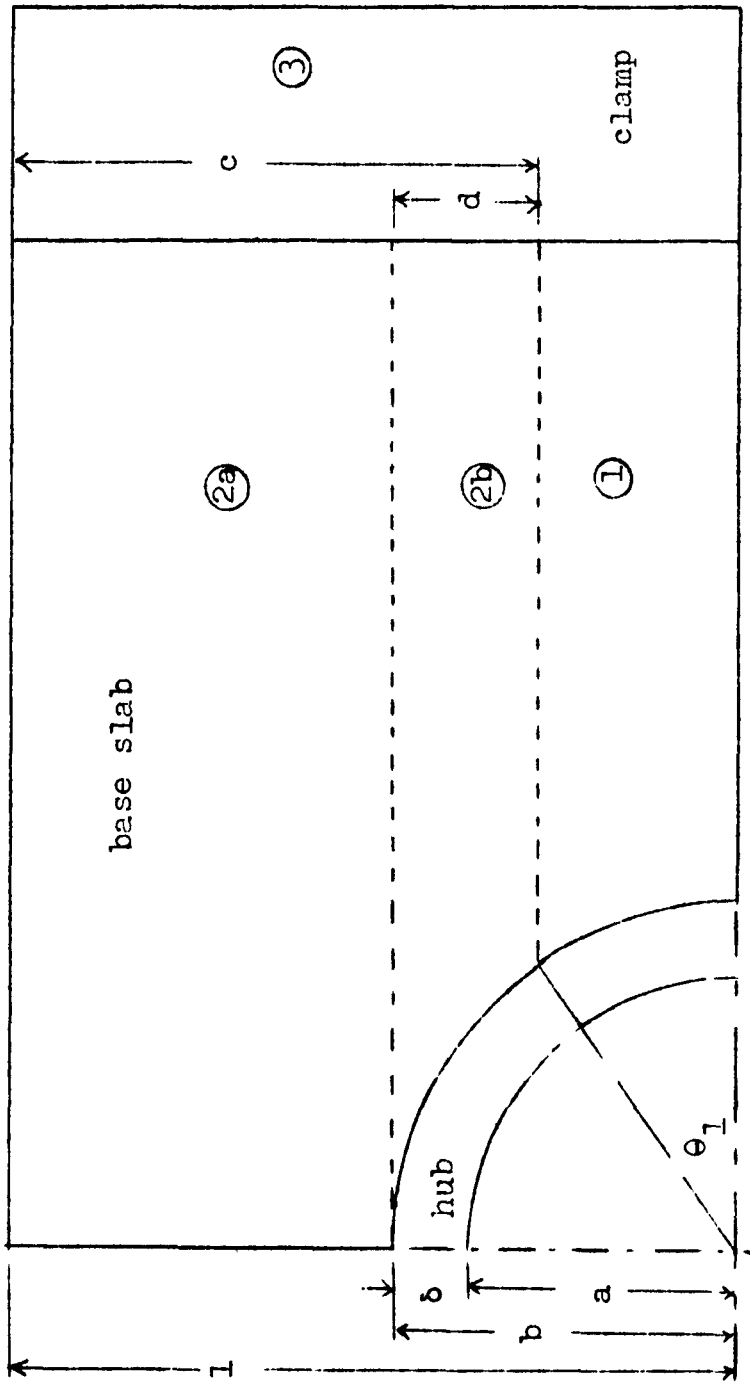

Fig. 25.4

Statically admissible stress field for clamped reinforced slab.

$$2k\lambda h = 2k\lambda c = 2kh(1 - b\zeta_1),$$

so that the reinforced cutout factor is

$$\lambda = 1 - b\zeta_1. \tag{25.6}$$

The solution of inequalities 25.5 is not simple, even numerically for specified values of η and α and no examples have been computed as yet. Possibly some of the techniques for the limit analysis of arches [17] can be used to advantage.

A somewhat simpler (although in general not as good) lower bound can be obtained by assuming full yield stress in region 2a (Fig. 25.4) as before, but a constant traction $2kh\mu$ in regions 1 and 2b. The hub analysis is then identical with that in Sec. 6, except that λ is to be replaced by μ. Thus, from Eqs. 6.12,

$$\mu = \frac{H\delta}{h(a + \delta)} \qquad \text{if } \frac{\delta}{a} \geq 2,$$

$$\mu = H\,\frac{\sqrt{a + 2\delta^2} - a}{h(a + \delta)} \quad \text{if } \frac{\delta}{a} \leq 2. \tag{25.7}$$

Since the total load is

$$2kh\lambda = 2kh(1 - a - \delta) + 2kh\mu(a + \delta),$$

the cutout factor is

$$\lambda = 1 - (a + \delta) + \frac{\delta}{\eta} \qquad \text{if } \frac{\delta}{a} \geq 2,$$

$$\lambda = 1 - (a + \delta) + [\sqrt{a^2 + 2\delta^2} - a]/\eta \quad \text{if } \frac{\delta}{a} \leq 2. \tag{25.8}$$

26. Comparison with experiment. The only known experiments on the yield loads of slabs with cutouts were carried out at the University of Washington by Vasarhelyi and Hechtman. These experiments are described in [21], and it is of some interest to compare the experimentally observed results with the theoretical results here obtained.

A total of 23 specimens were tested involving slabs without cutouts, with cutouts, and with reinforced cutouts. A variety of cutout and reinforcement shapes were considered. In each case, the slab was 36" in width, and had a gauge length of 36" so that the base slab was essentially square. All specimens were 1/4" thick, and were made of a plain-carbon semi-killed grade steel in an as rolled condition.

We shall here consider only those slabs with circular cutouts reinforced with concentric annular rings, although the methods of this report could be used to obtain a theoretical result for all the specimens tested. In order to avoid possible experimental difficulties in determining the yield stress, we shall identify the cutout factor as the ratio between the yield loads of the slab considered to the same base slab without cutout or reinforcement. Further, we shall define the yield load as the load for which a marked increase in deformation rate first occurred. In [21] this is called "general yielding". In each case the slab continued to sustain greater loads, indicating the existence of strain-hardening. Finally, we shall use the hub-base slab analysis, regardless of the actual welding process by which the reinforcement was attached.

The comparative results are given in Table 26.1. The dimensions of the slabs and reinforcements and the numbering of the specimens are taken from [21], using the notation of Fig. 25.4. Experimental results are taken from Table 4 of [21]. For two uncut slabs the general yielding load was found to be 380,000 and 390,000 pounds. Since the lower value corresponded to a higher value of the temperature than was used in any of the other experiments, we have here used 390,000 pounds as the yield load. The uniaxial cutout factor λ is thus the yield load for the slab in question divided by 390,000.

In each case we have used the "beam" approach to determine a lower bound. The lower bound for uniform edge load is determined from Eqs. 24.2 and 24.4, while the lower bound for uniform edge velocity is obtained from Eq. 25.8. Finally, the upper bound is obtained by considering sliding out of the plane (Sec. 11) and is given by

$$\lambda = 1 - (a + \delta) + \frac{\delta}{\eta} . \qquad (26.1)$$

Specimen Number	Dimensions			Lower Bounds: Uniform Load	Lower Bounds: Uniform Velocity	Experimental Value	Upper Bound
	a	δ	η				
5	$\frac{1}{4}$	1/72	1/8	0.62	0.74	0.83	0.86
6	$\frac{1}{4}$	1/72	1/4	0.62	0.74	0.83	0.79
11	$\frac{1}{4}$	1/4	1/2	0.84	0.87	0.92	1.00
12	$\frac{1}{4}$	1/8	1/2	0.64	0.74	0.85	0.88
17	$\frac{1}{4}$	15/144	1/2	0.62	0.73	0.83	0.85
18	$\frac{1}{4}$	3/72	1/4	0.62	0.74	0.87	0.88

Table 26.1
COMPARISON OF RESULTS

REFERENCES*

1. P. G. Hodge, Jr. and W. Prager, Limit design of reinforcements of cutouts in slabs, B11-2 (1951).

2. H. J. Weiss, W. Prager, and P. G. Hodge, Jr., Limit design of a full reinforcement for a circular cutout in a uniform slab, B11-5 (1951); J. Appl. Mech. 19, 397-401 (1952).

3. P. G. Hodge, Jr., Upper and lower bounds on the yield load of a square slab with a centered circular cutout, B11-7 (1952).

4. P. G. Hodge, Jr., On the plastic strains in slabs with cutouts, B11-8 (1952); J. Appl. Mech., Paper No. 52-A-22, to be published.

5. P. G. Hodge, Jr. and B. K. Froyd, The reinforcement to full strength of a thin slab with a slit, B11-10 (1953).

6. E. Levin and P. G. Hodge, Jr., The yield load of a uniform slab with a circular cutout reinforced by a bevelled ring, B11-14 (1953) (the results of this paper are included in the published version of Ref. 9).

7. P. G. Hodge, Jr., Limit design of a full reinforcement for a symmetric convex cutout in a uniform slab, B11-15 (1953).

8. P. G. Hodge, Jr., The effect of strain-hardening on an annular slab, B11-18 (1953), to be published in the J. Appl. Mech.

9. E. Levin, Symmetric reinforcements of circular cutouts, B11-17 (1953), to be published under the title On general reinforcements of circular cutouts in J. Appl. Mech.; published version will include results of Ref. 6.

10. D. C. Drucker, H. J. Greenberg, and W. Prager, The safety factor of an elastic-plastic body in plane strain, J. Appl. Mech. 18, 371-378 (1951).

* References 1 - 9 were originally issued as Technical Reports under Contract N7onr-35810 between the Office of Naval Research and Brown University, Providence, R. I., under the corresponding report numbers. If the paper has also been published, both references are given.

11. D. C. Drucker, W. Prager, and H. J. Greenberg, Extended limit design theorems for continuous media, Q. Appl. Math. 9, 381-389 (1952).

12. J. L. Synge and B. A. Griffith, Principles of Mechanics, McGraw-Hill Book Co., Inc., New York, 1949.

13. H. Tresca, Memoire sur l'ecoulement des corps solidas, Mem. pres. par. dir. sav. 18, 733-799 (1868).

14. W. Prager and P. G. Hodge, Jr., Theory of perfectly plastic solids, J. Wiley and Sons, Inc., New York, 1951.

15. J. M. English, discussion of [2], to appear in J. Appl. Mech.

16. R. T. Shield and D. C. Drucker, The application of limit analysis to punch indentation problems, to be published in J. Appl. Mech.

17. E. T. Onat and W. Prager, Limit analysis of arches, J. Mech. and Phys. of Solids, 1, 77-89 (1953).

18. E. T. Onat and W. Prager, The influence of axial forces on the collapse loads of frames, to be published in Proc. of the First Midwestern conference on Solid Mechanics, Urbana, Illinois, 1953.

19. S. Timoshenko and J. N. Goodier, Theory of elasticity, 2nd Ed., McGraw-Hill Book Co., Inc., New York, 1951.

20. R. K. Froyd, Collapse loads of slit slabs, M. S. Dissertation, Univ. of Calif., Los Angeles, 1952.

21. D. Vasarhelyi and R. A. Hechtman, Welded reinforcement of openings in structural steel members, First Progress Report, Contract NObs-50238, Univ. of Washington, Seattle, 1951.

Distribution List
for
Technical and Final Reports Issued Under
Office of Naval Research Project NR-360-364, Contract N7onr-35810

I: Administrative, Reference and Liaison Activities of ONR

Chief of Naval Research
Department of the Navy
Washington 25, D. C.
Attn: Code 438 (2)
Code 432 (1)
Code 466(via Code 108) (1)

Director, Naval Research Lab.
Washington 25, D. C.
Attn: Tech. Info. Officer (9)
Technical Library (1)
Mechanics Division (2)

Commanding Officer
Office of Naval Research
Branch Office
495 Summer Street
Boston 10, Massachusetts (2)

Commanding Officer
Office of Naval Research
Branch Office
346 Broadway
New York 13, New York (1)

Commanding Officer
Office of Naval Research
Branch Office
1000 Geary Street
San Francisco, California (1)

Commanding Officer
Office of Naval Research
Branch Office
1030 Green Street
Pasadena, California (1)

Officer in Charge
Office of Naval Research
Branch Office, London
Navy No. 100
FPO, New York, N. Y. (5)

Library of Congress
Washington 25, D. C.
Attn: Navy Research Section (2)

Commanding Officer
Office of Naval Research
Branch Office
844 N. Rush Street
Chicago 11, Illinois (1)

II: Department of Defense and other interested Government Activities

a) General

Research & Development Board
Department of Defense
Pentagon Building
Washington 25, D. C.
Attn: Library(Code 3D-1075) (1)

Armed Forces Special Weapons
Project
P. O. Box 2610
Washington, D. C.
Attn: Lt. Col. G. F. Blunda (2)

Joint Task Force 3
12 St. & Const. Ave., N.W.
(Temp. U)
Washington 25, D. C.
Attn: Major B. D. Jones (1)

b) Army

Chief of Staff
Department of the Army
Research & Development Division
Washington 25, D. C.
Attn: Chief of Res. & Dev. (1)

Office of the Chief of Engineers
Assistant Chief for Works
Department of the Army
Bldg. T-7, Gravelly Point
Washington 25, D. C.
Attn: Structural Branch
(R. L. Bloor) (1)

Engineering Research & Development
Laboratory
Fort Belvoir, Virginia
Attn: Structures Branch (1)

Army (cont.)

Office of the Chief of Engineers
Asst. Chief for Military Construction
Department of the Army
Bldg. T-3, Gravelly Point
Washington 25, D. C.
Attn: Structures Branch (M. F. Carey) (1)
Protective Construction Branch (I. O. Thornley) (1)

Office of the Chief of Engineers
Asst. Chief for Military Operations
Department of the Army
Bldg. T-7, Gravelly Point
Washington 25, D. C.
Attn: Structures Development Branch (W.F. Woollard) (1)

U.S. Army Waterways Experiment Station
P. O. Box 631
Halls Ferry Road
Vicksburg, Mississippi
Attn: Col. H. J. Skidmore (1)

The Commanding General
Sandia Base, P. O. Box 5100
Albuquerque, New Mexico
Attn: Col. Canterbury (1)

Operations Research Officer
Department of the Army
Ft. Lesley J. McNair
Washington 25, D. C.
Attn. Howard Brackney (1)

Office of Chief of Ordnance
Office of Ordnance Research
Department of the Army
The Pentagon Annex #2
Washington 25, D. C.
Attn: ORDTB-PS (1)

Ballistics Research Laboratory
Aberdeen Proving Ground
Aberdeen, Maryland
Attn: Dr. C. W. Lampson (1)

c) Navy

Chief of Naval Operations
Department of the Navy
Washington 25, D. C.
Attn: OP-31 (1)
OP-363 (1)

Chief, Bureau of Ships
Department of the Navy
Washington 25, D. C.
Attn: Director of Research (2)
Code 423 (1)
Code 442 (1)
Code 421 (1)

Director, David Taylor Model Basin
Department of the Navy
Washington 7, D. C.
Attn: Code 720, Structures Division (1)
Code 740, Hi-Speed Dynamics Div. (1)

Commanding Officer
Underwater Explosions Research Div.
Code 290
Norfolk Naval Shipyard
Portsmouth, Virginia (1)

Commander
Portsmouth Naval Shipyard
Portsmouth, N. H.
Attn: Design Division (1)

Director, Materials Laboratory
New York Naval Shipyard
Brooklyn 1, New York (1)

Chief, Bureau of Ordnance
Department of the Navy
Washington 25, D. C.
Attn: Ad-3, Technical Library (1)
Rec, P. H. Girouard (1)

Naval Ordnance Laboratory
White Oak, Maryland
RFD 1, Silver Spring, Maryland
Attn: Mechanics Division (1)
Explosive Division (1)
Mech. Evaluation Div. (1)

Commander
U.S. Naval Ordnance Test Station
Inyokern, California
Post Office - China Lake, Calif.
Attn: Scientific Officer (1)

Naval Ordnance Test Station
Underwater Ordnance Division
Pasadena, California
Attn: Structures Division (1)

Navy (cont.)

Chief, Bureau of Aeronautics
Department of the Navy
Washington 25, D.C.
Attn: TD-41, Technical Library (1)

Chief, Bureau of Ships
Department of the Navy
Washington 25, D. C.
Attn: Code P-314 (1)
Code C-313 (1)

Officer in Charge
Naval Civil Engr. Research & Evaluation Laboratory
Naval Station
Port Hueneme, California (1)

Superintendent
U.S. Naval Post Graduate School
Annapolis, Maryland (1)

d) Air Forces

Commanding General
U.S. Air Force
The Pentagon
Washington 25, D. C.
Attn: Res.& Development Div.(1)

Deputy Chief of Staff, Operations
Air Targets Division
Headquarters, U.S. Air Force
Washington 25, D. C.
Attn: AFOIN-T/PV (1)

Office of Air Research
Wright-Patterson Air Force Base
Dayton, Ohio
Attn: Chief, Applied Mechanics Group (1)

e) Other Government Agencies

U.S. Atomic Energy Commission
Division of Research
Washington, D. C. (1)

Director, National Bureau of Standards
Washington 25, D. C.
Attn: Dr. W.H. Ramberg (1)

Supplementary Distribution List

Addressee	No. of Copies Unclassified Reports	Classified Reports
Professor Lynn Beedle Fritz Engineering Laboratory Lehigh University Bethlehem, Pennsylvania	1	-
Professor R.L. Bisplinghoff Dept. of Aeronautical Engineering Massachusetts Institute of Technology Cambridge 39, Massachusetts	1	1
Professor Hans Bleich Dept. of Civil Engineering Columbia University Broadway at 117th St. New York 27, New York	1	1

Addressee	Unclassified Reports	Classified Reports
Professor B.A. Boley Dept. of Aeronautical Engineering Ohio State University Columbus, Ohio	1	-
Professor G.F. Carrier 309 Pierce Hall Harvard University Cambridge, Massachusetts	1	1
Professor R.J. Dolan Dept. of Theoretical & Applied Mechanics University of Illinois Urbana, Illinois	1	-
Professor Lloyd Donnell Department of Mechanics Illinois Institute of Technology Technology Center Chicago 16, Illinois	1	-
Professor A.C. Eringen Illinois Institute of Technology Department of Mechanics Technology Center Chicago 16, Illinois	1	-
Professor B. Fried Dept. of Mechanical Engineering Washington State College Pullman, Washington	1	-
Mr. Martin Goland Midwest Research Institute 4049 Pennsylvania Avenue Kansas City 2, Missouri	1	-
Dr. J.N. Goodier School of Engineering Stanford University Stanford, California	1	-
Professor R.M. Hermes College of Engineering University of Santa Clara Santa Clara, California	1	1
Professor R.J. Hansen Dept. of Civil & Sanitary Engineering Massachusetts Institute of Technology Cambridge 39, Massachusetts	1	1 -

Addressee	Unclassified Reports	Classified Reports
Professor M. Hetenyi Walter P. Murphy Professor Northwestern University Evanston, Illinois	1	-
Dr. N. J. Hoff, Head Department of Aeronautical Engineering & Applied Mechanics Polytechnic Institute of Brooklyn 99 Livingston Street Brooklyn 2, New York	1	1
Dr. J. H. Hollomon General Electric Research Laboratories 1 River Road Schenectady, New York	1	-
Dr. W. H. Hoppmann Department of Applied Mechanics Johns Hopkins University Baltimore, Maryland	1	1
Professor L. S. Jacobsen Department of Mechanical Engineering Stanford University Stanford, California	1	1
Professor J. Kempner Department of Aeronautical Engineering and Applied Mechanics Polytechnic Institute of Brooklyn 99 Livingston Street Brooklyn 2, New York	1	1
Professor George Lee Department of Aeronautical Engineering Renssalaer Polytechnic Institute Troy, New York	1	-
Professor Paul Lieber Department of Aeronautical Engineering Renssalaer Polytechnic Institute Troy, New York	1	1
Professor Glen Murphy, Head Department of Theoretical & Applied Mechanics Iowa State College Ames, Iowa	1	-
Professor N. M. Newmark Department of Civil Engineering University of Illinois Urbana, Illinois	1	1

Addressee	Unclassified Reports	Classified Reports
Professor Jesse Ormondroyd University of Michigan Ann Arbor, Michigan	1	-
Dr. W. Osgood Armour Research Institute Technology Center Chicago, Illinois	1	-
Dr. R.P. Petersen, Director Applied Physics Division Sandia Laboratory Albuquerque, New Mexico	1	1
Dr. A. Phillips School of Engineering Stanford University Stanford, California	1	-
Dr. W. Prager Graduate Division of Applied Mathematics Brown University Providence 12, R. I.	1	1
Dr. S. Raynor Armour Research Foundation Illinois Institute of Technology Chicago, Illinois	1	-
Professor E. Reissner Department of Mathematics Massachusetts Institute of Technology Cambridge 39, Massachusetts	1	-
Professor M.A. Sadowsky Illinois Institute of Technology Technology Center Chicago 16, Illinois	1	-
Professor V.L. Salerno Department of Aeronautical Engineering Renssalaer Polytechnic Institute Troy, New York	1	1
Professor M.G. Salvadori Department of Civil Engineering Columbia University Broadway at 117th Street New York 27, New York	1	-
Professor J.E. Stallmeyer Talbot Laboratory Department of Civil Engineering University of Illinois Urbana, Illinois	1	-

Distribution List

Addressee	Unclassified Reports	Classified Reports
Professor E. Sternberg Illinois Institute of Technology Technology Center Chicago 16, Illinois	1	-
Professor R. G. Sturm Purdue University Lafayette, Indiana	1	-
Professor F. K. Teichmann Department of Aeronautical Engineering New York University University Heights, Bronx New York, N. Y.	1	-
Professor C. T. Wang Department of Aeronautical Engineering New York University University Heights, Bronx New York, N. Y.	1	-
Project File	2	2
Project Staff	5	-
For possible future distribution by the University	10	-
To ONR Code 438, for possible future distribution	-	10